REVIEW ARTICLE

REVIEW ON A RESEARCH LINE FOR HEALING AND REGENERATION OF CARTILAGE AND MENISCUS TISSUES

G.M. PERETTI, L.J. BONASSAR[1], T.J. GILL[1], M.A. RANDOLPH[1], L. MANGIAVINI[2], and D.J. ZALESKE[1]

Faculty of Exercise Sciences,University of Milan, Italy;[1]Department of Orthopaedic Surgery,Massachusetts General Hospital, Harvard Medical School Boston, MA, USA; [2]Department of Orthopaedics and Traumatology, San Raffaele Scientific Institute, Milan, Italy

Received May 29, 2008 – Accepted January 7, 2009

This review describes a series of experiments designed to investigate the ability of isolated chondrocytes seeded onto scaffolds to produce cartilaginous matrix and heal lesions in meniscal cartilage. Devitalized cartilaginous matrices were seeded with isolated articular chondrocytes, stacked and wrapped in fibrin glue, and implanted subcutaneously in nude mice. Samples were harvested at different time points, ranging from one week to eight months and analyzed grossly, histologically, histomorphometrically and biomechanically. The efficacy of the seeded cells to generate an active tissue and bond cartilage matrices together was demonstrated. Subsequent studies were performed to apply this methodology to the repair of meniscus tissue. Articular chondrocytes were seeded onto meniscal slices and inserted *ex vivo* into bucket-handle lesions of ovine menisci. Samples were wrapped in fibrin glue and implanted in nude mice. The capacity of seeded chondrocytes to repair a lesion in the meniscal tissue was demonstrated after fourteen weeks of implantation and encouraged us to move to the application of this cell-based repair method to a pre-clinical large animal model. Autologous chondrocytes were seeded onto devitalized allogeneic meniscal slices and sutured inside a meniscal lesion. After nine weeks from implantation, gross, histological and histomorphometrical results showed bonding of the margins of the lesions in the experimental group. In conclusion, this series of experiments demonstrated the ability of seeded chondrocytes to produce active cartilaginous matrix with healing capability. The successful application of these findings to the repair of meniscal tissue is a potential new tool for meniscus repair.

Large populations of patients suffer from pain, stiffness, and loss of structure and function related to cartilage defects resulting from burns, tumors, trauma, arthritis, or other metabolic causes. Injured cartilaginous tissues have limited innate capabilities for healing and self-regeneration, and the reparative tissue that generally forms does not resemble the native cartilage in biochemical composition or biomechanical properties. Consequently, injury to cartilages in articulating joints, the cranium, and other cartilaginous tissues often results in scar formation leading to permanent loss of structure and function (1).

In joints, for example, cartilages of the meniscus and the articular surface are partially or completely isolated from the vascular environment. This lack

Key words: cartilage repair; healing; bonding; meniscus repair; chondrocytes

Mailing address: Prof. Giuseppe M. Peretti,
Faculty of Exercise Sciences,
University of Milan
Via Kramer 4/A
20129 Milan, Italy
Tel: ++390226432009 Fax: +390226432449
email: gperetti@iol.it

1973-6401 (2009)

of vascularity, combined with the extreme forces to which the articulating cartilage is subjected, probably impedes the normal wound repair processes observed in vascularized tissues like skin. Current surgical techniques for cartilage repair rely heavily on either autogenous composite tissue grafts or on the placement of artificial prosthetic implants. More recently, techniques have been introduced to re-implant autologous, cultured chondrocytes delivered to the lesion as cell suspension (2-3) or carried by biologically derived tissue membranes (4-8). Each of these techniques has often demonstrated imperfect clinical results, but also has some serious drawbacks that limit clinical utility. Harvesting autologous tissue to obtain cells can result in unwanted donor site morbidity and may cause additional complications over the long term. Furthermore, the repair tissue has not been fully evaluated in restoring normal biochemical composition and biomechanical properties. On the other hand, prosthetic metallic or plastic implants undergo migration, extrusion, and unknown long-term side affects (9-10).

During the last decade, many investigators have reported studies involving isolated chondrocytes seeded in natural or synthetic scaffolds, including collagen gel (11-14), fibrin glue (15-16), polyglycolic acid (17), polyethylene oxide gel (18), alginate gel (19), carbon fiber pads (20), and devitalized xenogeneic matrix (21). Using these methods, the transplantation of previously isolated and cultured chondrocytes into articular cartilage defects were performed in several animal models which include chick (22), rabbit (14,23), dog (24) and horse (13,25). In spite of all these efforts, however, the repair of cartilaginous tissues still remains a challenge.

Developing a minimally invasive method for the in vivo generation of new cartilage to permanently repair cartilage defects in these patient populations has been the primary goal of our laboratory. To achieve the desired result, however, one must consider both the properties of the native tissue at the site of injury and the properties of the scaffold being used to deliver the cells to generate cartilage repair tissue. Most importantly, however, the engineered cartilage must integrate into the defect and heal to the surrounding cartilage at the site of implantation. Generating engineered cartilage tissue, the integration of this neo-cartilage with native cartilage, and the ability of the cells to bond or heal cartilaginous matrices are the primary goals of the following studies.

MATERIALS AND METHODS

Experimental development of cartilaginous tissue bonding

The first fundamental step in this series of experiments was to ascertain whether isolated chondrocytes could adhere to cartilage matrix and have the ability to promote integration of separate fragments of cartilage (26). As depicted in the diagram in Fig. 1, slices of articular cartilage were harvested from lambs and devitalized by five freeze-thaw cycles. Devitalized cartilage matrix was employed to eliminate any possible contribution of chondrocytes residing in the slices, and, therefore, only test the new cartilage generated by cells seeded onto the dead matrices. Chondrocytes were isolated from cartilage of animals of the same species by collagenase digestion. The slices were then either co-cultured for three weeks in the presence (cellular density of 0.2 million/ml) or absence of chondrocytes in suspension culture in Ham F12 medium with 10% fetal bovine serum, 50 mg/ml ascorbate, 292 mg/l glutamine and antibiotics in order to allow chondrocytes to adhere to the matrices. Composites of three such slices were assembled, wrapped in fibrin glue, and implanted into nude mice for 7, 14, 21, 28, and 42 days. Bonding of the experimental matrices with viable dividing chondrocytes was achieved at 28 and 42 days as assessed by direct examination and histology. No bonding occurred in the control composites without chondrocytes (Fig. 2). In particular, bonding of the composites were examined grossly with a pair of jewelers forceps for the existence of tissue planes between the slices of cartilage matrix and the ability to separate the tissue planes by passive opening the forceps. Cell mitotic activity was tested by [^{3}H]thymidine uptake at time 0 (before implantation), 14, 28 and 42 days following implantation. Histological evaluation of samples before implantation showed presence of few layers of live chondrocytes on the surface of devitalized cartilage matrix in experimental samples, whereas no vital cells were found in control samples (Fig. 3). Moreover, examination of samples after implantation documented chondrocytes forming new cartilage matrix in the contact planes between the slices of experimental composites. This new cartilage layer increased in thickness from day 7 to day 42 with obliteration of the space between the matrices observed by day 21. The fibrin glue layer shrank progressively and disappeared by day 21 (Fig. 4 and 5). At later observation time points, erosion of the devitalized matrix could be sporadically noted with ingrowth of new cartilage (Fig. 6).

Analysis by fluorescence microscopy of samples treated with fluorescent dye solutions (live/dead kit: calcein and ethidium homodimer) confirmed that this invading tissue was composed of live cells penetrating into the devitalized cartilage matrix (data not shown). The [^{3}H]thymidine study showed a statistically significant decrease in incorporation into the experimental composites from day 0 to day 28 followed by a slight increase at day 42 (Fig. 7). From these results, we concluded that proliferating chondrocytes could achieve confluence at the interface and integration of the devitalized cartilage matrices. Although we were able to follow the adhesion process of the newly formed tissue throughout the experimental times, we were not able to measure the strength of these bonds.

The main goal of the following experiment was designed in order to investigate the ability of chondrocytes to adhere to and remodel devitalized cartilage matrix, and most importantly, to quantify the biomechanical properties of the tissue bond by tensile testing (27). Standardized articular hyaline cartilage discs (5mm X 1mm) were harvested from the articular joints of lambs and devitalized by freeze-thaw cycles. Articular chondrocytes were enzymatically isolated from cartilage pieces from animals of the same species. The devitalized cartilage discs were incubated in the presence (experimental) or absence (control) of chondrocytes in suspension culture for three weeks. After *in vitro* culture, pairs of cartilage discs were held in apposition in fibrin glue and implanted subcutaneously in nude mice for up to six weeks. Two experimental samples (with cells) and one control (without cells) were implanted in each mouse. Groups of 5 mice were sacrificed at 1, 2, 3, 4, and 6 weeks after implantation. Mechanical testing was performed on the samples after which the tissues were formalin fixed, processed, sectioned, and stained with Safranin-O. Some specimens in each group were fixed immediately upon collection for pre-test histological evaluation. The mechanical integrity of newly formed tissue was evaluated by tensile testing on a Dynastat mechanical spectrometer. Chondrocyte-matrix constructs were attached to plexiglass rods using cyanoacrylate glue and the rods were mounted in the Dynastat. Tensile displacements were applied at a rate of 10 μm/s to failure and the resultant loads were recorded. Sample displacements and loads were normalized to strain and stress by sample geometry and tensile strength, fracture strain, fracture energy, and tensile modulus were calculated from the resultant stress-strain curves (Fig. 8). The histological examination showed new cartilage matrix formed by chondrocytes adhered to devitalized matrix, leading to complete fusion of the two matrix discs by week 3. This was consistent with the previous study (Fig. 4). Starting at week 3, the newly synthesized cartilage formed buds of penetration in devitalized matrix, which became more frequent with time. Histological analysis of biomechanically tested samples showed that failure occurred at the interface between new matrix and devitalized cartilage (Fig. 9A). Moreover, post-test histological evaluation showed that the presence of these buds of penetration stabilized the interface between new tissue and matrix, with failure occurring on opposite side of these formations in 80% of the cases (Fig. 9B). Mechanical testing indicated that tensile strength (Fig. 10A), fracture strain (Fig. 10B), fracture energy (Fig. 10C) and tensile modulus (Fig. 10D) increased with time for the experimental group while control group showed no increase. By six weeks, this resulted in 10-fold increase in tensile strength ($p<.01$), 50-fold increase in fracture energy ($p<.01$), 10-fold increase in fracture strain ($p<.01$), and a 3-fold increase in tensile modulus ($p<.05$).

The results from this study confirmed that transplanted chondrocytes had the ability to adhere to devitalized cartilage and synthesize new matrix. Further, these chondrocytes had the capacity to repair and remodel the cartilage matrix in a way that increases the biomechanical properties of the tissue construct. The level of biomechanical function reported in this model was encouraging, given that all reported properties increased with time. This motivated us to perform longer-term studies, which could yield specimens with superior appearance and mechanical properties. Therefore, the experiment was repeated (28) for an extended study, but the cell and matrix source was changed from lamb to juvenile pig. Again, the chondrocyte-matrix constructs were assembled with fibrin glue, implanted in dorsal subcutaneous pockets in nude mice (Fig. 11), and assessed at 1, 2, 4, and 8 months after implantation. Histological analysis from this study also confirmed that chondrocytes grown on devitalized cartilage discs produced new matrix that was able to bond and integrate cartilage discs. Biomechanical testing (Fig. 12) demonstrated a time dependent increase in tensile strength, failure strain, failure energy, and tensile modulus to values 5-30% of normal articular cartilage by eight months *in vivo*. Importantly, the values recorded at four months were not statistically different from those collected at the latest time point, indicating that the limits of the biomechanical property values were reached after four months from implantation.

Simultaneously, we decided to further analyze the morphological appearance of the living cells at the interface between the newly formed tissue and the devitalized cartilaginous scaffold matrices (29). In fact, we believed that the chondrocytes in this area were somehow more active in the remodeling process of the cartilage matrix scaffolds and, most importantly, these cells played an important role in the bonding capacities of the newly

formed cartilaginous tissue. As in the previous protocols, articular cartilage was harvested from young sheep and seeded onto pieces of devitalized sheep cartilage. The seeded pieces were stacked in pairs and wrapped in fibrin glue, and then implanted subcutaneously in the dorsum of athymic mice. Samples were harvested after 6 weeks and examined by transmission electron microscopy (TEM) or by light microscopy. After harvesting and processing of the samples, TEM revealed that the cells distant from the interface with scaffold tissue were more rounded in shape with large nuclei that appeared similar to normal chondrocytes (Fig. 13A). On the other hand, the cells in direct apposition to the devitalized cartilage were elongated, with an enlarged cytoplasm, and a ruffled border (Fig. 13B). Quantitative morphometry of histology specimens revealed that cell area, relative amount of cytoplasm (with respect to the nuclear area), cell aspect ratio (between major axis and minor axis, indicating elongation of the cell), and relative nuclear displacement (in the periphery or in the center of the cell) were all higher in cells near the interface with the scaffold tissue, and decreased with distance from the interface. These findings of cell morphology were all considered indices of active remodeling of the scaffold at the cell–scaffold interface.

Experimental development of meniscal tissue healing

The capacity of seeded chondrocytes to bond cartilaginous matrices inspired us to seek another important application for this model—the healing of lesions in the knee meniscus. Since menisci play a crucial role in knee function (30-34), significant effort has been attempted to salvage these structures following injury. This structure is not entirely vascularized and a blood supply is found only peripherally in the outer third (35). As a result, reparative process cannot occur in lesions involving the avascular inner portion of the meniscus (36). Based on the results from our previous work, it seemed reasonable to initiate studies on the application of this bonding phenomenon to meniscal tissue. The purpose of the following study (37) was to utilize chondrocyte-seeded cartilaginous scaffolds for repairing bucket-handle type of lesions in devitalized meniscal tissue in an *in vivo* nude mouse model.

As depicted in the diagram of Fig. 14, meniscus specimens were harvested from the inner third of the menisci of lambs. Menisci were treated with five freeze-thaw cycles to devitalize the matrix. A four-millimeter bucket-handle lesion was created with a knife about two millimeters from the free margin of the avascular zone. Meniscal slices (4mm X 2mm X 0.5mm) were sectioned from the same tissue. Articular chondrocytes were isolated from cartilage from animals of the same species by overnight digestion in collagenase. The devitalized meniscal slices were incubated in the presence (cellular density of 0.2 million/ml) or absence (control) of chondrocytes in suspension culture in Ham F12 media with 10% FBS, 50 mg/ml ascorbate, and antibiotics for 21 days in order to allow chondrocytes to adhere to the slices. After *in vitro* culture, the meniscus slices with seeded chondrocytes (experimental group 1) and without chondrocytes (control group 2) were placed inside the bucket-handle lesion of the meniscus samples and sutured with 6-0 Vicryl suture (see Fig. 15 for group design). Other control groups were prepared by simply suturing the meniscal lesion (group 3) or leaving the lesion untreated (group 4). All constructs were wrapped into a fibrin glue clot, and eight meniscal samples/group were implanted into subcutaneous pouches in the backs of nude mice. The specimens were harvested at 14 weeks, examined grossly, and tested for repairing. Samples were then fixed and processed for histological analysis. Results from this study showed complete bonding of lesion margins grossly in seven out of eight experimental samples (87.5%). Conversely, no control samples were repaired (0%), and the fracture was still visible by gentle distraction of the sample (Fig. 16). Histological analysis showed complete adherence between the margins of meniscal fracture and the cell-seeded scaffold in experimental group 1 (Fig. 17A), whereas no repairs were achieved in control group specimens (Fig. 17B). Moreover, viable chondrocytes were visible at the interface of the pre-seeded slices and the meniscal lesion in group 1 specimens. The distinction of the exact boundary between the scaffold slice and the fracture line of the meniscus was recognizable only by the orientation of the fibers of the two tissues, confirming good integration of the newly formed tissue with the native tissue of the meniscal samples. Conversely, no live chondrocytes were present in all control samples—those with unseeded meniscal slices in the bucket-handle lesion (group 2) and those without slices (groups 3 and 4). In our opinion, this work represented a model in which the reparative capacity of isolated chondrocytes can be evaluated for meniscus fracture. In this nude mouse model, the tissue engineered cell-scaffold composite was able to achieve repair of a bucket-handle lesion in the avascular inner zone of the knee meniscus, a region thus far considered to have practically no healing potential.

Based on the results of this study, we hypothesize that a cell-based tissue engineered construct could be employed for treating lesions of the knee meniscus orthotopically in a large animal model (38). Considering that the pig knee adequately resembles the human knee in terms of dimensions and load supported, we chose the swine model for our investigation. Additionally, a previous study demonstrated meniscal tears in pigs do not repair spontaneously (39). The purpose of the following

work was to assess the capacity of articular chondrocytes that are seeded onto a cartilaginous scaffold to repair a longitudinal tear of the knee meniscus in swine.

The first part of the study was designed to analyze the vascularization of the Yorkshire pig meniscus. Four Yorkshire pigs were utilized for these anatomical studies. Under general anesthesia, the femoral artery was cannulated and perfused with Indian ink, while the flow from a catheter inserted in the femoral vein was aspirated. The vessels were clamped and the animals were sacrificed. The hind limb was disarticulated, fixed in 10% buffered formalin for three days. After the limbs were removed from fixative, the knee was opened and the menisci were harvested for gross analysis. The menisci were cleared by immersion in methyl salicylate and further analysis of their vascular supply was performed on a diaphanoscope. The analysis of our samples demonstrated that vascularity of the pig menisci originates from the periphery of the structure and does not involve the inner aspect (Fig. 18). No vascular supply was found in the inner third of the meniscus consistent with the vascular supply to the meniscus in humans (35). This finding gave us guidance as to where the experimental lesion should be made in our model for healing in the avascular region.

The second part of the study was designed to analyze the potential of cell-based therapy to repair a bucket handle lesion in the avascular part of the knee meniscus. From the longitudinal aspect of a cross section of devitalized pig menisci, meniscal slices (10mm X 2mm X 0.5mm) were sectioned (Fig. 19). Sixteen Yorkshire pigs were utilized for this study. Cartilage specimens were surgically harvested from the patellar groove of the left knee of the pigs belonging to the experimental group. As shown in the experimental diagram (Fig. 20), chondrocytes were isolated by enzymatic digestion and seeded by suspension culture onto the previously processed allogeneic meniscal slices. Following *in vitro* culture, a second surgery was performed using an anteromedial approach to expose the left medial meniscus of the same pig from which chondrocytes were harvested. A one-centimeter bucket-handle lesion was made at the margin of the inner third and the outer two thirds of the meniscus. The cell-seeded meniscal construct was secured in the lesion in four pigs of the experimental group (group 1). Identical lesions were made in the left medial meniscus of all other pigs. In four animals the lesion was treated with an unseeded scaffold (group 2); in four the lesion was sutured without insertion of any other material (group 3); in four the lesion was left untreated (group 4). The experimental design is shown in Fig. 21. Animals were sacrificed after nine weeks and the menisci harvested. The specimens were examined grossly, fixed in buffered formalin, processed, sectioned, and stained with hematoxylin and eosin and safranin-O for histological analysis. All histological slides were photographed at the lesion sites with a low magnification lens (25X) for histomorphometric analysis of the percentage of repair obtained in each study group.

Macroscopic evaluation indicated better repair for samples of group 1 where three out of four samples from this group revealed gross healing of the lesion (Fig. 22A). Only one sample from group 2 had approximation of the lesion margins, whereas the remaining menisci from group 2 (Fig. 22B) did not appear to be repaired grossly. No evidence of repair was also observed in all menisci from groups 3 (Fig. 22C) and 4 (Fig. 22D). The implanted meniscal scaffold itself was macroscopically noted in the site in three out of four specimens of group 1, whereas it was present in only one sample in group 2.

Histological analysis demonstrated persistence of the meniscal tear in all samples from all control groups, with a notable gap between the two lesion margins (Fig. 23). In the analysis of the specimens belonging to the experimental samples in group 1, it was clear that the seeded chondrocytes transplanted inside the lesion by the meniscal chip scaffold were able to synthesize fibro-cartilaginous matrix. In fact, this tissue was present at the boundary of the implanted scaffold and the meniscal lesion (Fig. 24A). The safranin-O staining demonstrated that this new tissue had sulfated proteoglycans (Fig. 24B). In one specimen from group 1, the histological cross-section was taken at the edge of the bucket-handle lesion where the inserted scaffold did not reach into this portion of the lesion. The cell-loaded carrier was not involved in this particular section (Fig. 25A, small image at top right corner), and the lesion was entirely filled with reparative tissue (Fig. 25A), which appeared to be constituted by neo-tissue presenting an interesting interdigitation with the native meniscus (Fig. 25B). Finally, the percentage of the repaired interface compared with the total extension of the lesion margins (% of repair) was calculated histomorphometrically as 30.17 ± 17.83 % for the specimens in experimental group 1. No adherence was noted in all samples of control groups 2, 3, and 4.

The results from this study demonstrated that a meniscal lesion involving the inner (avascular) one-third of the pig meniscus could now benefit from the bonding capabilities of the transplanted chondrocytes. We believe that these results in a large animal model validate this cell-based therapy as promising approach to repair tears in the avascular third of the meniscus, a region considered thus far to have no capacity for healing.

DISCUSSION

The healing of cartilaginous tissues in the joint is on of the most challenging clinical problems

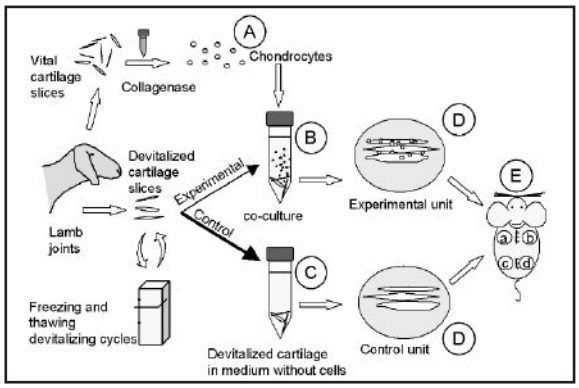

Fig. 1. *Diagram of experimental protocol for the construction of cartilaginous composites and implantation in nude mice.* **A)** *Ovine chondrocytes were isolated by enzymatic digestion from hip and shoulder lamb joints, adjusted to a concentration of 10^6 cells/ml and combined with three slices of cartilage matrix* **B)***, which were previously devitalized through several freeze-thaw cycles. The matrices and chondrocytes were co-cultured for 21 days.* **C)** *Similar devitalized matrices were kept in culture also for 21 days without viable chondrocytes.* **D)** *After culturing, three devitalized cartilage slices with chondrocytes (experimental) or three slices without chondrocytes (control) were removed from the media and joined into a composite with fibrin glue. The resulting composites were implanted into the dorsal subcutaneous tissue of athymic mice using four separate implantation sites (a, b, c, d).* **E)** *Two experimental and two control cartilage composites randomly assigned were implanted into either one of the cranial or one of the caudal sites. The composites were harvested at 7, 14, 21, 28 and 42 days after implantation. Permission has been obtained from J Orthop Res (26).*

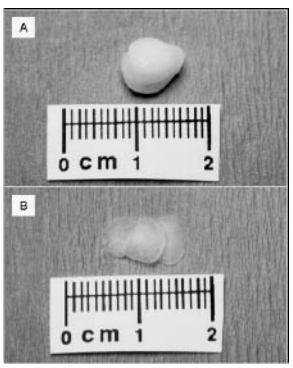

Fig. 2. *Macroscopic view of the composites 42 days following implantation.* **A)** *Experimental composite. While the original slices of matrix are discernible, the composite has united into a solid cartilaginous mass.* **B)** *Control composite. The three devitalized cartilage pieces slid apart immediately after the removal of the thin fibrous capsule, which surrounded the samples at the moment of harvesting. Permission obtained from J Orthop Res (26).*

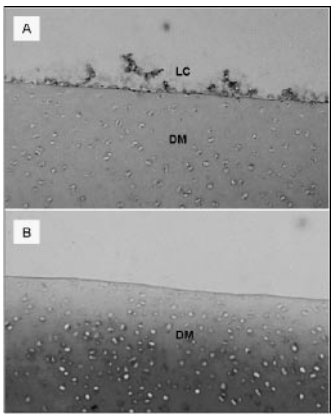

Fig. 3. *Histologic sections (safranin-O, original magnification 200X) of samples after in vitro culture and before implantation.* **A)** *Experimental sample. Few layers of live chondrocytes (LC) are present on the surface of devitalized matrix (DM).* **B)** *Control sample. No live cells are present in this section. Some nuclear debris from dead cells remains in the devitalized matrix. Permission obtained from J Orthop Res (26).*

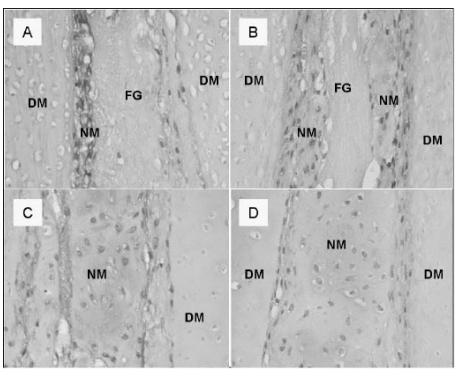

Fig. 4. *Histologic sections (safranin-O, original magnification 200X) of composites after implantation.* **A)** *Experimental composite, 7 days following implantation. Two devitalized matrices (DM) are seen on either side. Viable chondrocytes forming new matrix (NM) are seen on their surfaces. The fibrin glue (FG) forms a relatively thick layer between the contact surfaces.* **B)** *Experimental composite, 14 days following implantation. The two layers of viable chondrocytes have increased in thickness and the fibrin glue layer has decreased.* **C)** *Experimental composite, 21 days following implantation. The contact space between the devitalized matrices has now been completely filled with newly formed matrix. The fibrin glue has been largely absorbed.* **D)** *Experimental composite, 28 days following implantation. There is now complete confluence of the viable chondrocytes forming new matrix between the two devitalized matrices. Permission obtained from J Orthop Res (26).*

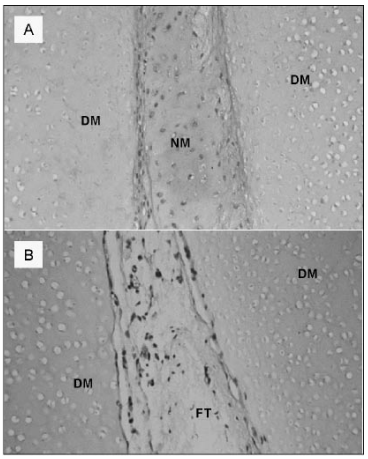

Fig. 5. *Histologic sections (safranin-O, original magnification 200X) of composites after implantation.* **A)** *Experimental composite, 42 days following implantation (200X). Newly formed cartilaginous tissue (NM) has formed, bonding the devitalized cartilage matrices (DM).* **B)** *Control composite, 42 days following implantation. Fibrous tissue (FT) is observed between the devitalized matrices. This tissue stained only with the fast green counter-stain and not safranin-O. Moreover, as observed by gross analysis, it was not able to achieve bonding between the native cartilage slices. No viable chondrocytes are present. Permission obtained from J Orthop Res (26).*

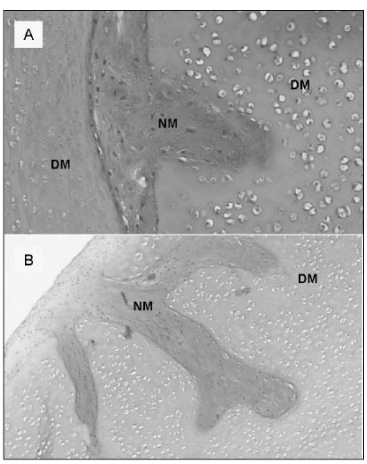

Fig. 6. *Histologic sections (safranin-O) of composites 42 days after implantation.* **A)** *A bud of new cartilage matrix (NM) is seen penetrating the devitalized matrix (original magnification 200X).* **B)** *Another bud of new cartilage with branches is seen penetrating the devitalized matrix (DM) (original magnification 100X). Permission obtained from J Orthop Res (26).*

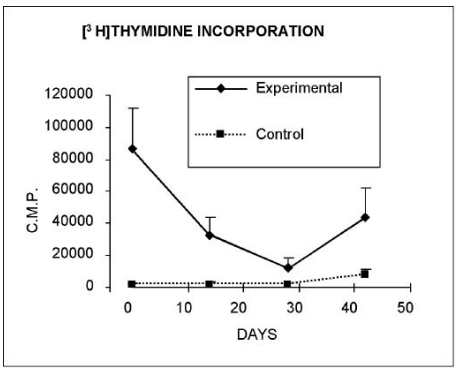

Fig. 7. *Graph of (^{3}H)thymidine incorporation into the composites at 0, 14, 28 and 42 days following implantation. The incorporation into the experimental composites decreased from 0 to 28 days with an increase at 42 days. The incorporation into the control composites was not significantly different from baseline at any time point. The differences between the experimental and control groups were significant ($p<0.05$) at each observation period. C.P.M. = Counts per minute. Permission obtained from J Orthop Res (26).*

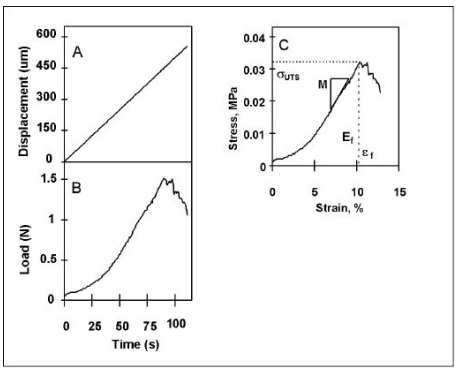

Fig. 8. *Representative example of applied tensile displacement* **(A)** *and measured tensile load* **(B)** *from an experimental construct seeded with chondrocytes and implanted in vivo. A stress-strain curve* **(C)** *was generated from this data by normalizing displacement data to measured sample thickness and load data to sample area. From this curve, ultimate tensile strength (σ_{UTS}) and fracture strain (ε_f) were determined by inspection or when the measured load was observed to be < 0.05 N, dynamic tensile modulus (M) was calculated from slope of the linear portion of the curve, and fracture energy (E_f) was calculated as the area under the curve. Permission has been obtained from Tissue Eng (27).*

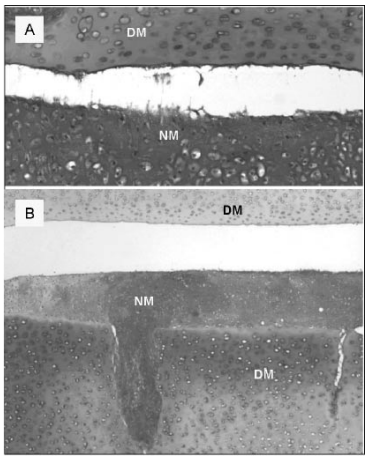

Fig. 9. *Histologic sections of samples after biomechanical testing (safranin-O staining).* **A)** *Experimental sample, tested 28 days following implantation (original magnification 200X). Failure occurred at the interface between the newly formed matrix (NM) and the devitalized cartilage matrix (DM).* **B)** *Experimental sample, tested 42 days following implantation (original magnification 100X). When chondrocytes penetrated devitalized tissue, fracture occurred at the opposing interface in 80% of the sections sampled. Permission has been obtained from Tissue Eng (27).*

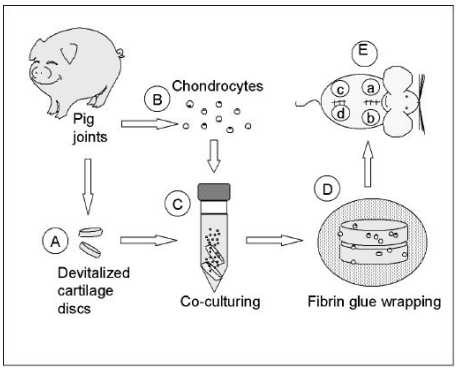

Fig. 11. *Diagram showing the experimental protocol.* **(A)** *Hyaline articular cartilage discs were harvested from the articular joints of pigs and devitalized by multiple freeze-thaw cycles* **(B)**. *Chondrocytes were enzymatically isolated from cartilage from animals of the same species by collagenase digestion* **(C)**. *Devitalized cartilage discs were incubated in the presence of chondrocytes in suspension culture for 21 days in order to allow chondrocytes to adhere to matrix* **(D)**. *After in vitro culture, pairs of cartilage discs were held in apposition in fibrin glue* **(E)** *and implanted subcutaneously in nude mice for up to eight months. Permission obtained from J Biomed Mater Res (28).*

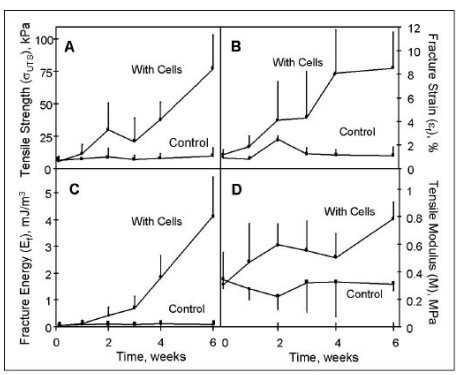

Fig. 10. *Time course of changes in tensile strength* **(A)**, *fracture strain* **(B)**, *fracture energy* **(C)** *and tensile modulus* **(D)** *over 6 weeks in vivo for constructs seeded with chondrocytes or unseeded controls. All data are shown as mean ± SD. Permission was obtained from Tissue Eng (27).*

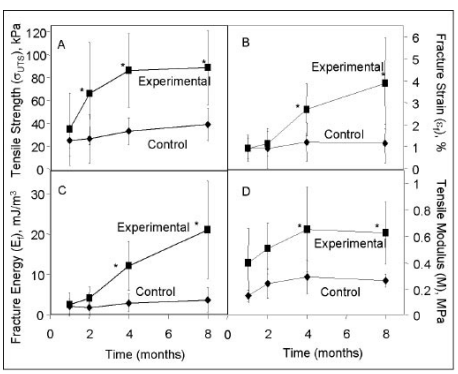

Fig. 12. *Time course of changes in tensile strength* **(A)**, *failure strain* **(B)**, *failure energy* **(C)** *and tensile modulus* **(D)** *over eight months in vivo for constructs seeded with chondrocytes or unseeded controls. All data are shown as mean ± SD, with the n=5 for experimental and control samples. In each figure * denotes the appropriate p value for significance of difference between the experimental group and the control at that time point, as determined by two-factor ANOVA and post-hoc Tukey test. Permission obtained from J Biomed Mater Res (28).*

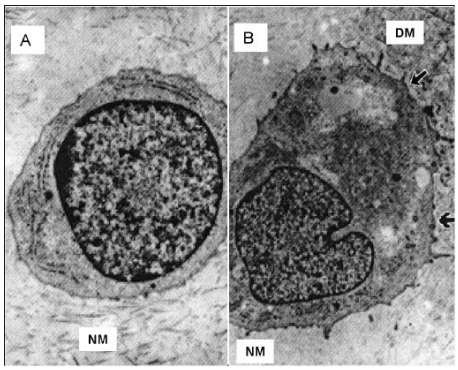

Fig. 13. A) *Transmission electron microscopy of a chondrocyte far from the interface and surrounded by newly synthesized matrix (NM).* **B)** *Transmission electron microscopy of a chondrocyte at the interface between newly synthesized matrix (NM) and the devitalized matrix (DM) used as a scaffold. Chondrocytes bordering the DM had ruffled borders (arrows) characteristic of remodeling activity. Original magnification:* **A)** *31900X;* **B)** *31400X. Permission obtained from Tissue Eng (29).*

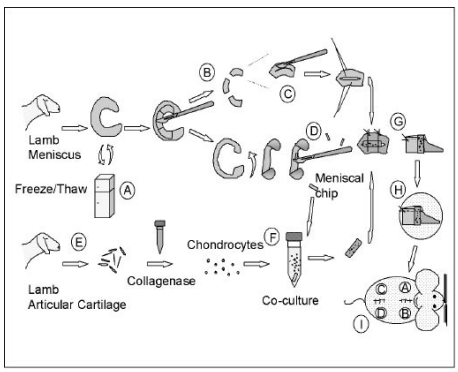

Fig. 14. *Experimental protocol for making the scaffolds, the meniscal constructs and for their transplantation to nude mice.* **(A)** *Entire menisci were harvested from lamb knees and devitalized by repetitive freezing and thawing* **(B)**, *three sections of the inner part were obtained with a scalpel* **(C)** *and a four-millimeter bucket-handle incision was made within the avascular zone* **(D)**. *From other menisci, chips were cut from the inner third. Articular cartilage was harvested from knees and shoulders of unrelated lambs* **(E)** *and enzymatically digested to suspend the chondrocytes* **(F)**. *The isolated cells were co-cultured with the previously made meniscal chips* **(G)**. *Such chips with seeded chondrocytes were sutured inside the bucket-handle incision. The samples were wrapped in fibrin glue* **(H)** *and transplanted to dorsal pouches in nude mice at four different sites* **(I)**. *Permission obtained from J Orthop Res (37).*

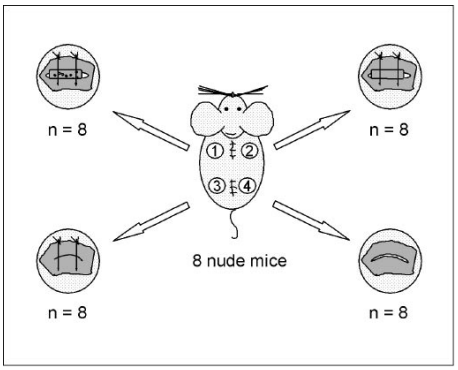

Fig. 15. *Study group design. Four different groups were established. One specimen from each group was transplanted to one of four dorsal pouches on a single nude mouse. Eight nude mice were used for a total of eight samples per each study group. In experimental group 1, a meniscal chip with seeded chondrocytes was sutured inside the bucket-handle incision of the devitalized meniscal block. In control group 2, a meniscal chip without chondrocytes was sutured inside the incision. In control group 3, the meniscal incision was simply sutured, whereas in control group 4, the meniscal incision was left untreated. Permission obtained from J Orthop Res (37).*

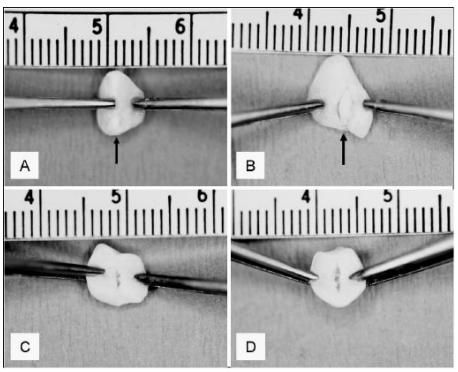

Fig. 16. *Macroscopic analysis of samples upon retrieval from nude mice. The experimental sample of group 1* **(A)** *shows good repair, with the pre-seeded chip in the middle of the bucket-handle lesion, now bridging the edges of the meniscal incision (arrow). No separation of the fracture edges is evident with traction by the two forceps. On the other hand, none of the control samples revealed any attempt at repair of the meniscal incision* **(B)**. *In a sample of group 2, the non pre-seeded chip is still visible (arrow) not attached to either side of the meniscal incision after gentle traction* **(C)**. *In a sample of group 3, treated only with suture* **(D)**, *and in a sample of group 4, where the lesion was left untreated, the meniscal incision alone is evident without any attempt at repair. Permission obtained from J Orthop Res (37).*

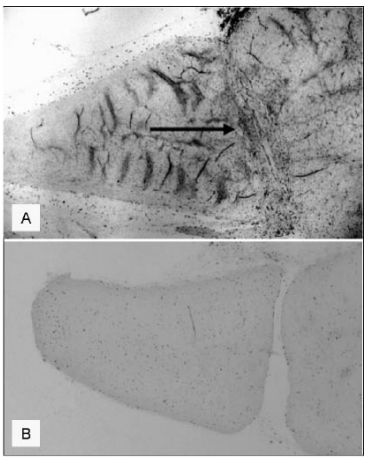

Fig. 17. *Photomicrographs of specimens from experimental group 1 and from control group 4 (toluidine blue, original magnification 20X).* **A)**, *In experimental samples the meniscal chip is located in the middle of the bucket-handle lesion (arrow) allowing bonding of the two edges of the incision through the newly formed tissue, that was synthesized by the viable chondrocytes.* **B)** *Analysis of the control sample showed no repair of the incision, as shown in this histological slide of a group 4 specimen. Permission obtained from J Orthop Res (37).*

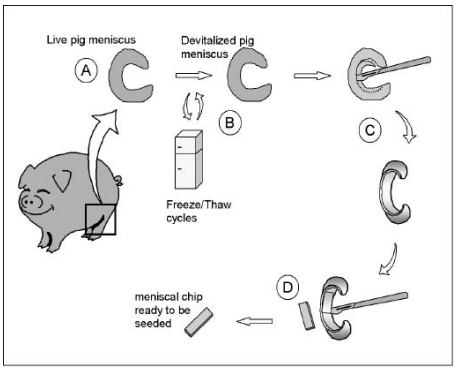

Fig. 19. *Experimental protocol for the preparation of the allogeneic meniscal scaffold.* **A)** *Menisci were harvested from knees of pigs and* **B)** *devitalized by freeze-thaw cycles.* **C)** *The inner portion of each meniscus was removed and from the inner portion of the longitudinal aspect of the outer meniscal sections,* **D)** *slices were cut and standardized as flat chips measuring approximately 4 millimeters in width, 10 millimeters in length, and 0.5 millimeters in thickness. Such an implant was ready to be seeded with isolated chondrocytes to form the reparative implant. Permission obtained from Am J Sports Med (38).*

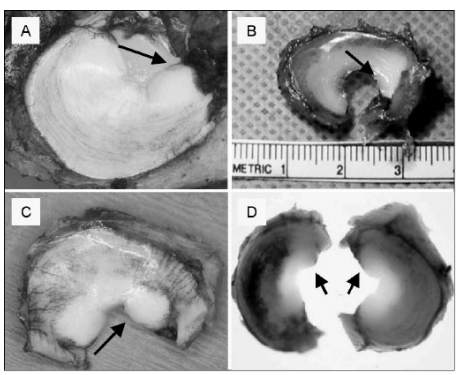

Fig. 18. *India ink perfusion study; all samples were perfused with India ink.* **A)** *A medial meniscus after being fixed in formalin, and before being harvested from the native site;* **B)** *a meniscus, explanted and cleared with methyl salicylate, which demonstrated an involvement of the vascularity of the outer third of the structure;* **C)** *another meniscus observed from its inferior surface;* **D)** *two menisci, belonging to the same knee, analyzed under the diaphanoscope. The arrows indicate the anterior horn of the menisci. Permission obtained from Am J Sports Med (38).*

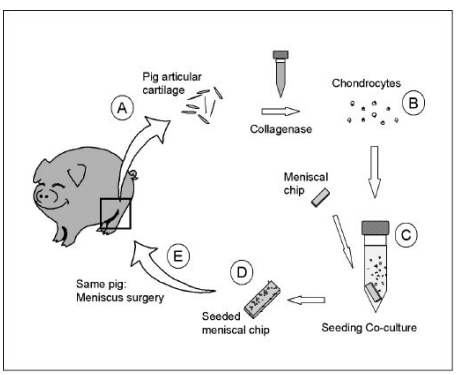

Fig. 20. *Experimental design.* **A)** *Articular cartilage slices were surgically harvested in sterile condition and* **B)** *chondrocytes were enzymatically isolated.* **C-D)** *Chondrocytes were cultured in the presence of the allogeneic meniscal slices in order to be seeded onto their surface.* **E)** *The obtained seeded meniscal chips were surgically implanted in a meniscal bucket-handle lesion performed in the same pig, from which the articular chondrocytes were isolated. Permission obtained from Am J Sports Med (38).*

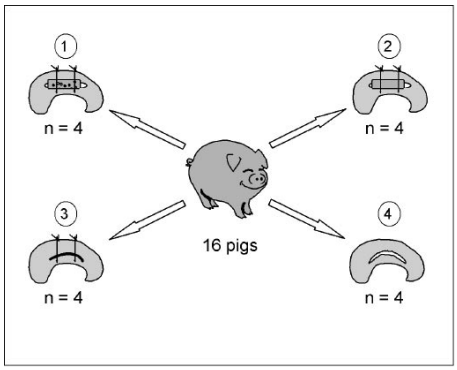

Fig. 21. *Study group design. Sixteen pigs were divided in four groups of four animals each. In experimental group 1, the bucket-handle meniscal lesion was treated by the implantation of the allogeneic meniscal slice, seeded with autologous chondrocytes. In control group 2, the lesion was treated with the implantation of an unseeded meniscus slide. In control group 3, the meniscal lesion was simply sutured, whereas in control group 4, the meniscal lesion was left untreated. Permission was obtained from Am J Sports Med (38).*

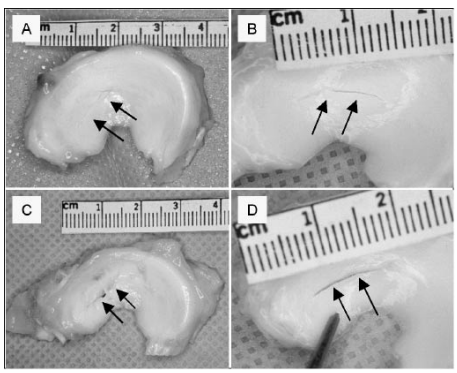

Fig. 22. *Macroscopic analysis of samples upon harvesting from the animals.* **(A** *The experimental meniscus sample of group 1 appears to present good gross healing between the implanted meniscal scaffold and the bucket-handle lesion margins.* **(B)** *On the other hand, no signs of repair are present in the samples from group 2,* **C)** *from group 3, and* **D)** *from group 4. The arrows show where the original lesion was created. Permission was obtained from Am J Sports Med (38).*

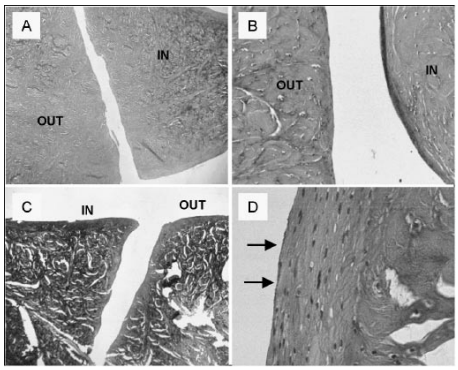

Fig. 23. *Histological analysis (hematoxylin and eosin, transverse section through the longitudinal tear) of specimens belonging to control groups 2, 3, and 4. In all images the lesion is still present.* **A)** *Specimen belonging to group 2 (original magnification 25X), where the meniscus was treated with an unseeded meniscal scaffold, which was not found at the time of explant;* **B)** *specimen belonging to group 3 (original magnification 100X), treated only with suture;* **C)** *specimen belonging to group 4 (original magnification 25X), where lesion was left untreated. At higher magnification (***D)** *taken from specimen in image B, original magnification 400X, an analysis of the lesion margins demonstrated an increased cellularity with fibroblast-like cells (arrows). IN: inner part of the meniscus. OUT: outer part of the meniscus. Permission was obtained from Am J Sports Med (38).*

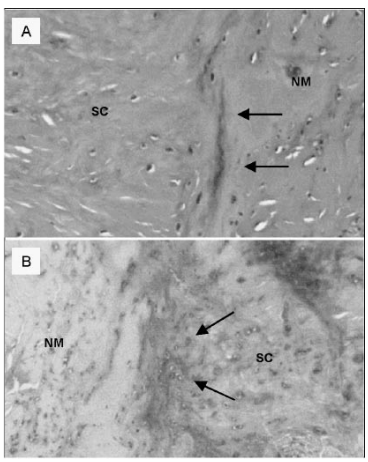

Fig. 24. *Histological analysis (***A)** *hematoxylin and eosin;* **B)** *safranin-O, original magnification 100X of a group 1 specimen, treated with the seeded meniscal scaffold (transverse section through the longitudinal tear).* **A)** *the boundary between the native meniscus (right) and the seeded scaffold (left) is visible (arrows).* **B)** *The safranin-O staining shows new matrix production, with highly intensive stain at the boundary (arrows) between the seeded scaffold (right) and the native meniscus (left). SC: meniscal scaffold. NM: native meniscus. Permission was obtained from Am J Sports Med (38).*

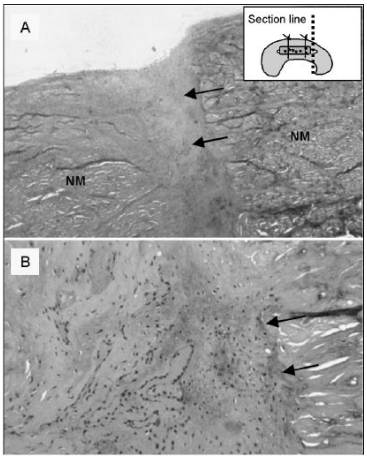

Fig. 25. *Histological analysis (hematoxylin and eosin) of a group 1 specimen, treated with the seeded meniscal scaffold. This section was made perpendicular to the long axis of the lesion. The histological cut was taken at the edge of the bucket-handle lesion, not involving the cell-carrier scaffold, as shown in the insert at the top right corner of image* **A).** *At 25X magnification, filling was noted in the gap between the lesion margins by fibrotic-like tissue (arrows).* **B)** *Interdigitations between the native meniscus and the reparative tissue were seen at 100X magnification. The arrows indicate the limit between the outer part of the meniscus and the reparative tissue. Permission obtained from Am J Sports Med (38)*

confronting orthopedic surgeons and basic science researchers. Articular cartilage and the inner zone of the meniscus do not spontaneously regenerate and heal when injured (1,36). When a reparative process occurs, it does not resemble the morphology, the composition and, most importantly, the biomechanical properties of the native tissue. For these reasons, investigators have started to pursue different pathways to tackle cartilage regeneration and healing. In our opinion, cell-based therapy is a promising approach to achieve these goals. Cells can be modulated in order to duplicate the original phenotype of the injured biological structure and also can produce an extracellular matrix with the capacity to bond and eventually heal the native tissue. It is these aspects of cell therapy and their ability to bond and heal cartilage that have been the subject of our studies.

Previous studies from other researchers have analyzed the integration of entire cartilage blocks when put in apposition *in vitro* (40). In their work the main objective was to determine the relationship between the integration of the cartilage blocks and the deposition of newly synthesized collagen by the cells native to the tissue. The same research group also analyzed the adhesive capacity of isolated chondrocytes seeded onto cartilage matrices *in vitro* (41). The main goal of this other study was to determine the effect of the duration of *in vitro* seeding time on the ability of chondrocytes to resist detachment from cartilage when subjected to mechanical perturbation.

The experiments performed from our group, on the other hand, looked into the integration of the engineered cartilage, synthesized *in vivo* by chondrocytes seeded onto cartilaginous matrices. We have deeply analyzed the phenomena occurring at the interface between the newly formed tissue and the native cartilage, demonstrating for the fist time the presence of interdigitations penetrating from the engineered cartilage into the native cartilage. We have shown how this phenomenon reinforces the biomechanical adhesion between these two tissues.

After having demonstrated and quantified the bonding properties of engineered cartilage produced by the seeded chondrocytes, we have applied this model to repairing of meniscal lesions in the heterotopic subcutaneous environment of athymic mice. Finally, we have proven the potential for this method to repair orthotopically placed meniscal lesions in a swine model. We believe the results achieved in these experimental series represent a logical sequence from fundamental understanding of chondrocyte interactions with scaffolds to a relevant pre-clinical model. We now believe the cartilaginous lesions, and meniscal tears in particular, can be successfully repaired with a cell-based therapy. Further studies are now under investigation, analyzing different cell sources and scaffold materials to translate this pre-clinical model into clinical application.

REFERENCES

1. Mankin HJ. The response of articular cartilage to mechanical injury. J Bone Joint Surg 1982; 64A: 460-6.
2. Brittberg M, Lindahl A, Nilsson A, Ohlsson C,

Isaksson O, Peterson L. Treatment of deep cartilage defects in the knee with autologous chondrocyte transplantation. N Engl J Med 1994; 331:889-95.

3. Steinwachs M, Kreuz PC. Autologous chondrocyte implantation in chondral defects of the knee with a type I/III collagen membrane: a prospective study with a 3-year follow-up. Arthroscopy 2007; 23(4): 381-7.
4. Marcacci M, Zaffagnini S, Kon E, Visani A, Iacono F, Loreti I. Arthroscopic autologous chondrocyte transplantation: technical note. Knee Surg Sports Traumatol Arthrosc 2002;10(3):154-9.
5. Ronga M, Grassi FA, Bulgheroni P. Arthroscopic autologous chondrocyte implantation for the treatment of a chondral defect in the tibial plateau of the knee. Arthroscopy 2004; 20(1):79-84.
6. Cherubino P, Grassi FA, Bulgheroni P, Ronga M. Autologous chondrocyte implantation using a bilayer collagen membrane: a preliminary report. J Orthop Surg (Hong Kong) 2003; 11(1):10-5.
7. Grigolo B, Roseti L, De Franceschi L, Piacentini A, Cattini L, Manfredini M, Faccini R, Facchini A. Molecular and immunohistological characterization of human cartilage two years following autologous cell transplantation. J Bone Joint Surg Am 2005; 87(1):46-57.
8. Erggelet C, Sittinger M, Lahm A. The arthroscopic implantation of autologous chondrocytes for the treatment of full-thickness cartilage defects of the knee joint. Arthroscopy 2003; 19(1):108-10.
9. Rubin, JP, Yaremchuk MJ. Complications and toxicities of implantable biomaterials used in facial reconstructive and aesthetic surgery: a comprehensive review of the literature. Plast Reconstr Surg 1997; 100(5):1336-53
10. Gupta SK, Chu A, Ranawat AS, Slamin J, Ranawat CS. Osteolysis after total knee arthroplasty. J Arthroplasty 2007; 22(6):787-99.
11. Foster BK, Hansen AL, Gibson GJ, Hopwood JJ, Binns GF, Wiebkin OW. Reimplantation of growth plate chondrocytes into growth plate defects in sheep. J Orthop Res 1990; 8(4):555-64.
12. Nixon AJ, Sams AE, Lust G, Grande D, Mohammed HO. Temporal matrix synthesis and histologic features of a chondrocyte-laden porous collagen cartilage analogue. Am J Vet Res 1993; 54(2):349-56.
13. Sams AE, Minor RR, Wootton JA, Mohammed H, Nixon AJ. Local and remote matrix responses to chondrocyte-laden collagen scaffold implantation in extensive articular cartilage defects. Osteoarthritis Cartilage 1995; 3(1):61-70.
14. Wakitani S, Kimura T, Hirooka A, Ochi T, Yoneda M, Yasui N, Owaki H, Ono K. Repair of rabbit articular surfaces with allograft chondrocytes embedded in collagen gel. J Bone Joint Surg Br 1989; 71(1):74-80.
15. Homminga GN, Buma P, Koot HW, van der Kraan PM, van den Berg WB. Chondrocyte behavior in fibrin glue in vitro. Acta Orthop Scand 1993; 64(4): 441-5.
16. Peretti GM, Randolph MA, Villa MT, Buragas MS, Yaremchuk MJ. Cell-based tissue-engineered allogeneic implant for cartilage repair. Tissue Eng 2000; 6(5):567-76.
17. Vacanti CA, Kim W, Schloo B, Upton J, Vacanti JP. Joint resurfacing with cartilage grown in situ from cell-polymer structures. Am J Sports Med 1994; 22(4):485-8.
18. Sims CD, Butler PE, Casanova R, Lee BT, Randolph MA, Lee WP, Vacanti CA, Yaremchuk MJ. Injectable cartilage using polyethylene oxide polymer substrates. Plast Reconstr Surg 1996; 98(5):843-50.
19. van Susante JL, Buma P, van Osch GJ, Versleyen D, van der Kraan PM, van der Berg WB, Homminga GN. Culture of chondrocytes in alginate and collagen carrier gels. Acta Orthop Scand 1995; 66(6):549-56.
20. Brittberg M, Nilsson A, Lindahl A, Ohlsson C, Peterson L. Rabbit articular cartilage defects treated with autologous cultured chondrocytes. Clin Orthop Relat Res 1996; 326:270-83.
21. Caruso EM, Lewandrowski KU, Ohlendorf C, Tomford WW, Zaleske DJ. Repopulation of laser-perforated chondroepiphyseal matrix with xenogeneic chondrocytes. An experimental model. J Orthop Res 1996; 14(1):102-7.
22. Itay S, Abramovici A, Nevo Z. Use of cultured embryonal chick epiphyseal chondrocytes as grafts for defects in chick articular cartilage. Clin Orthop Relat Res 1987; 220:284-303.
23. Grande DA, Pitman MI, Peterson L, Menche D, Klein M. The repair of experimentally produced

defects in rabbit articular cartilage by autologous chondrocyte transplantation. J Orthop Res 1989; 7(2):208-18.

24. Shortkroff S, Barone L, Hsu HP, Wrenn C, Gagne T, Chi T, Breinan H, Minas T, Sledge CB, Tubo R, Spector M. Healing of chondral and osteochondral defects in a canine model: the role of cultured chondrocytes in regeneration of articular cartilage. Biomaterials 1996; 17(2):147-54.
25. Hendrickson DA, Nixon AJ, Grande DA, Todhunter RJ, Minor RM, Erb H, Lust G. Chondrocyte-fibrin matrix transplants for resurfacing extensive articular cartilage defects. J Orthop Res 1994; 12(4):485-97.
26. Peretti GM, Randolph MA, Caruso EM, Rossetti F, Zaleske DJ. Bonding of cartilaginous matrices with cultured chondrocytes: an experimental model. J Orthop Res 1998; 16(1):89-95.
27. Peretti GM, Bonassar LJ, Caruso EM, Randolph MA, Zaleske DJ. Biomechanical analysis of a cell-based model for articular cartilage repair. Tissue Eng 1999; 5(4):317-26.
28. Peretti GM, Zaporojan V, Spangenberg KM, Randolph MA, Fellers J, Bonassar LJ. Cell-based bonding of articular cartilage: an extended study. J Biomed Mater Res 2003; 64A(3):517-24.
29. Spangenberg KM, Peretti GM, Trahan CA, Randolph MA, Bonassar LJ Histomorphometric analysis of a cell-based model of cartilage repair. Tissue Eng 2002; 8(5):839-46.
30. King D. The function of semilunar cartilages. J Bone Joint Surg 1936;18:1069–76.
31. Krause WR, Pope HM, Johnson RJ, Wilder DG. Mechanical changes in the knee after meniscectomy. J Bone Joint Surg Am 1976; 58:599–604.
32. Hargreaves DJ, Seedhom BB. On the "bucket-handle" tear: Partial or total meniscectomy? A quantitative study (abstract). J Bone Joint Surg 1979; 61:381.
33. Ahmed AM, Burke DL. In vitro measurement of static pressure distribution in synovial joints: Part I. Tibial surface of the knee. J Biomech Eng 1983; 105: 216–25.
34. Levy IM, Torzilli PA, Gould JD, Warren RF. The effect of lateral meniscectomy on motion of the knee. J Bone Joint Surg Am 1989; 71:401–6.
35. Arnoczky SP, Warren RF. Microvasculature of the human meniscus. Am J Sports Med 1982; 10(2):90-5.
36. Arnoczky SP, Warren RF. The microvasculature of the meniscus and its response to injury: An experimental study in the dog. Am J Sports Med 1983;11:131–41.
37. Peretti GM, Caruso EM, Randolph MA, Zaleske DJ. Meniscal Fracture Repair using Engineered Tissue. Journal Orthop Res 2001;19(2):278-85.
38. Peretti GM, Gill TJ, Xu JW, Randolph MA, Morse KR, Zaleske DJ. Cell-based therapy for meniscal repair: a large animal study. Am J Sports Med 2004; 32(1):146-58.
39. Ghadially FN, Wedge JH, Lalonde JM. Experimental methods of repairing injured menisci. J Bone Joint Surg 1986; 68B:106-10.
40. DiMicco MA, Waters SN, Akeson WH, Sah RL. Integrative articular cartilage repair: dependence on developmental stage and collagen metabolism. Osteoarthritis Cartilage 2002; 10(3):218-25.
41. Schinagl RM, Kurtis MS, Ellis KD, Chien S, Sah RL. Effect of seeding duration on the strength of chondrocyte adhesion to articular cartilage. J Orthop Res 1999; 17(1):121-9.

REVIEW ARTICLE

SURGERY OF POSTERIOR CRUCIATE LIGAMENT INJURY

C-H. CHEN

Department of Orthopaedic Surgery, Chang Gung Memorial Hospital, Keelung
Chang Gung University College of Medicine, Taiwan

Received September 15, 2008 – Accepted February13, 2009

Successful posterior cruciate ligament (PCL) reconstruction is challenging because of its complex structure, it requires difficult reconstruction techniques and has an inconsistent long term clinical outcome. Factors that affect the surgical results in restoring PCL function include difficulty to duplicate PCL anatomy, concomitant ligament injury, difficulty in accurate tunnel placement, tunnel erosion or migration, high internal graft stress, wide variation in broad femoral insertion footprint, and progressive graft elongation. The outcome of conservative treatment of isolated PCL injuries is generally acceptable with residual mild or moderate laxity. However, more severe straight posterior laxity or combined ligament injury patterns may result in a worse prognosis without adequate surgery. Clinical results of PCL reconstruction are variable and often unpredictable because of the complexity of the injury. It is generally agreed that surgical reconstruction is indicated for symptomatic severe posterior knee instability and multiple ligament injuries. Accepted surgical techniques for treatment of PCL tears include primary repair for PCL avulsion fracture, open or arthroscopic reconstruction using the transtibial or tibial inlay technique and the one or double bundle method. Controversy continues over the choice of graft tissue, single or double bundle reconstruction, location of tunnel placement, knee position when securing the graft, and graft fixation techniques.

The incidence of PCL injuries occurs in approximately 3.4 to 20 percent of all knee ligament injuries (1). Isolated partial or complete PCL tears have typically been treated conservatively producing satisfactory short-term results but controversial long term outcomes. In complete PCL tear with associated posterolateral lesion, nonoperative treatment has been unreliable due to inadequate ligament healing and associated posterolateral instability. Long-term follow-up studies have shown a high incidence of progressive osteoarthritis and poor knee function (2). Surgical results of PCL reconstruction are variable and often unpredictable. Recent studies on PCL anatomy and biomechanics have led to a better understanding of the biomechanical properties of PCL reconstructions (3-9). For better functional recovery after PCL injury, surgical reconstruction is indicated for symptomatic severe posterior knee instability and multiple ligament injuries. When considering treatment for PCL injury, the following factors should be considered: pain or instability, instability level, acute or chronic injury, MRI findings, isolated or combined injury, and active or inactive life style.

Controversy continues over the choice of graft tissue, one or double bundle reconstruction, tunnel placement, knee position when securing the graft, and the fixation technique (10). The single-bundle technique was developed to reconstruct the anterolateral PCL bundle because of its larger size and greater biomechanical properties when compared with the posteromedial bundle. In

Key words: posterior cruciate ligament, reconstruction, tendon graft

Mailing address: Prof. Chih-Hwa Chen
Department of Orthopaedic Surgery,
Chang Gung Memorial Hospital
222, Mai-Chin Road,
204 Keelung, Taiwan
Tel: ++886 2 24313131 ext. 2625 Fax: ++886 2 24332655
e-mail: afachen@doctor.com

1973-6401 (2009)

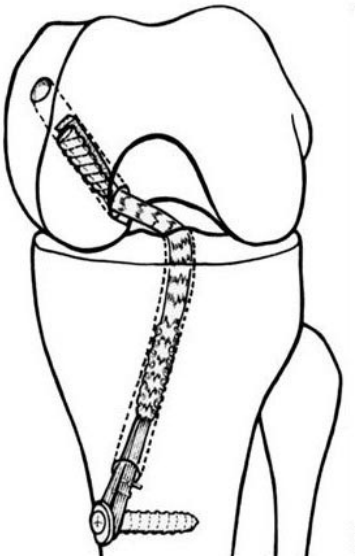

Fig. 1. *Quadriceps tendon autograft for single-bundle PCL reconstruction.*

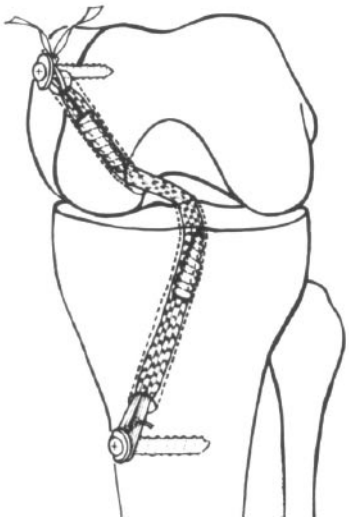

Fig. 3. *Hamstring tendon autograft for single-bundle PCL reconstruction.*

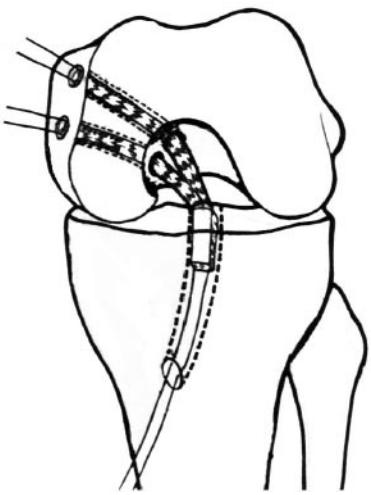

Fig. 2. *Quadriceps tendon autograft for double-bundle PCL reconstruction.*

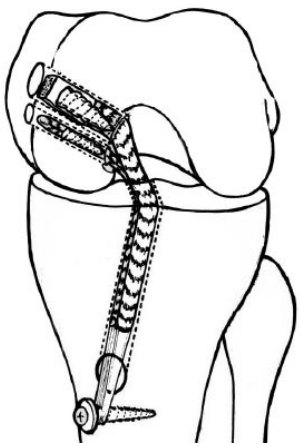

Fig. 4. *Quadriceps tendon and hamstring tendon grafts for double-bundled PCL reconstruction.*

addition, the anterolateral bundle of the PCL has the greatest tension at 90° flexion, which is the most functional position to resist posterior tibial translation (11). A biomechanical study to evaluate a single-bundle versus a double-bundle posterior cruciate ligament reconstruction has shown that double-bundle reconstructions can more closely restore the biomechanics of the intact knee than can the single-bundle reconstruction throughout the range of knee flexion. Only the double-bundle graft could restore normal knee laxity across the full range of flexion (12-15).

A variety of techniques for PCL reconstruction have been proposed including autograft, allograft, artificial ligament, graft with prosthetic augmentation, and extra-articular reconstruction (16). Bone-patellar tendon-bone autograft is typically preferred for its graft-healing potential. The Achilles tendon

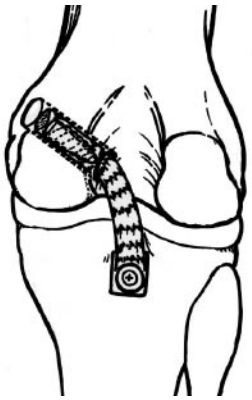

Fig. 5. *Quadriceps tendon autograft for single-bundle PCL reconstruction with tibial inlay technique.*

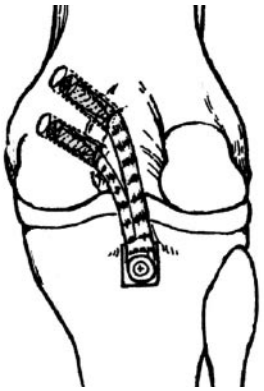

Fig. 6. *Quadriceps tendon autograft for double-bundle PCL reconstruction with tibial inlay technique.*

allograft has been favored due to its lack of donor site problems. The hamstring tendon graft has been more popular in recent years. The hamstring tendon graft with semitendinosus and gracilis tendons is technically easier, safer, and more reproducible. Hamstring tendon morbidity at harvesting is very low and presents a minimal residual flexor and extensor strength deficit. Quadriceps tendon autograft has the advantage of being easily available, requires a relatively easier arthroscopic technique, and is of a suitable size. Gross anatomy has revealed that the quadriceps tendon is thicker, longer, and wider than the patellar tendon. For double bundle fixation, there are several different graft choices including Achilles tendon allograft-semitendinosus autograft, double tendon strand form quadriceps tendon graft, semitendinosus-gracilis, double strands anterior tibialis tendon allograft, and double-bundle Y-shaped hamstring tendon graft (17-22). A biomechanical study has been done to evaluate and compare the fixation strength of three common grafts, the bone-patellar tendon-bone graft, the quadruple tendon graft and the Achilles tendon graft in PCL reconstruction (23). All three had a weaker initial fixation strength and stiffness than normal PCL. In the maximal failure load, the four-strand tendon group was significantly greater than the other two grafts but had the greatest translation. Graft failure occurred mainly at the tendon-bone junction and tendon-suture sites. The Patellar tendon group had significantly less translation during continued loading.

Injuries to the posterolateral structures of the knee are challenging to treat (24-26). When acute grade 3 posterolateral injuries are combined with PCL injuries, all structures should be addressed at the time of surgery. Due to their presence, the lateral collateral ligament (LCL), the popliteus, and popliteofibular ligament, should be preferred for the repair of the posterolateral structures of the knee (27-31). The popliteus tendon was observed to be the primary restraint to external rotation and the LCL the primary restraint to varus opening. Injury of the LCL and popliteus tendon created increased external rotation and varus rotation at all angles of knee flexion. Severe acute injuries generally require surgical repair at an early stage. Combined injuries should be treated with repair or reconstruction of both the posterolateral complex ligaments and PCL. Many reconstructive procedures have been described for chronic posterolateral instability and no general consensus exists. A variety of grafts, including split Achilles tendon allograft, patellar tendon bone-tendon-bone autograft or allografts, quadriceps tendon graft, or hamstring tendon graft, have been described for reconstruction of the posterolateral structures (32).

Surgical indication

The surgical indications for PCL reconstruction include acute severe PCL injury with instability, associated with multiple ligament injuries, and symptomatic chronic posterior failure (11). For patients with Grade 3 PCL injuries without significant posterolateral instability, PCL reconstruction could

be performed. For patients with combined PCL injury and posterolateral instability, simultaneous PCL and PL reconstruction should be performed. PCL rupture can be identified by the positive posterior drawer test, the posterior sag sign and MRI. Posterolateral instability can be diagnosed with external tibial rotation at 30 and 90 degrees, external rotation with the thigh foot angle test, the posterolateral external rotation test, the reverse pivot-shift test, the external rotation recurvatum test and the posterolateral drawer test. Each patient should be fully informed of the disease, the surgical procedures, and the postoperative rehabilitation program. Arthroscopic surgery should not be performed for acute injuries until the knee has achieved an almost full range of motion (ROM) with minimal pain and effusion. Accepted surgical techniques for treatment of PCL tears include primary repair for PCL avulsion fracture, open or arthroscopic reconstruction using the transtibial or tibial inlay technique and the one or double bundle method. For patients with concomitant posterolateral instability, a semitendinosus tendon autograft from contralateral limb or tendon allograft is used to reconstruct the popliteofibular ligament and fibular collateral ligament (33,34).

Rehabilitation programs

The initial goal in postoperative management of PCL reconstruction is to decrease pain, inflammation and swelling, to re-establish quadriceps control, and to restore a normal gait. Postoperatively, the knee is immobilized in full extension for the first week. Full weight-bearing is allowed as tolerated by the patient. Quadriceps isometric exercises, straight-leg raises and a passive ROM should be initiated as early as possible. During the first 4 weeks following surgery, protected ROM from 0^0 to 60^0 is maintained, and a series of closed kinetic-chain exercises are started. At 6 weeks, the brace is unlocked to establish a normal gait and passive ROM. At 8 weeks, the active ROM should progress to complete flexion and extension, and aggressive hamstring-strengthening exercises should be initiated. Quadriceps and hamstring muscle strength are trained according to a home rehabilitation program and according to the graft used. Patients usually return to normal daily activity after 3 months, and return to light sports activity by 6 months. Resumption of full pre-injury sports activities can be undertaken between 9 and 12 months following reconstruction. For the patients with combined PCL and PL reconstruction, the full extension brace is applied for 3 weeks for non weight bearing immediately after operation. Progressive range of motion occurs during weeks 4 through 6. Progressive weight bearing starts at the end of the 6th week. Progressive closed-chain kinetic strength training and continued motion exercises are performed. The brace is discarded after 10 weeks. Return to sports and heavy labor activity is recommended after 9 months when sufficient muscle strength and range of motion has recovered.

Surgical techniques

Tibial side techniques

The results of PCL reconstruction using the transtibial tunnel technique have been inconsistent and have achieved variable outcomes at long-term follow-up. Some authors have reported excellent results using a single-bundle graft and a transtibial tunnel technique (35-38). However, others have had difficulty duplicating these promising results (39-41). There were some recognized weaknesses and limitations in these clinical studies of PCL reconstruction. The series were mixed acute and chronic cases. The surgical outcome analysis included isolated and combined reconstructions and also acute and chronic cases that may have influenced the preoperative scores and stability test results.

The tibial inlay technique for PCL reconstruction has been developed to decrease the disadvantage in the transtibial technique (15, 42-43). The tibial inlay technique can approach the PCL insertion site directly and achieve anatomic fixation avoiding the killer-turn and graft thinning or elongation, hence leading to better biomechanics, and graft healing. However, it is a technically demanding procedure with many challenges, including patient positioning, incision balancing, proximity to the neurovascular structures, graft selection, and tibial graft fixation (20, 44-45). Furthermore, the tibial inlay technique requires the removal of all remaining posterior cruciate ligament tissue. In many patients, there are substantial posterior cruciate ligament and meniscofemoral ligament attachments that can be preserved and used during the arthroscopic reconstruction. Usually, it is not the procedure of choice for primary PCL

reconstruction. This technique does have a role in certain primary PCL reconstruction and revision procedures in which the transtibial tunnel is found to be poorly positioned (46-49).

Graft choice

The optimal graft choice remains controversial. The patellar tendon-bone autograft is a commonly used graft because of its graft-healing potential. However, this graft presents some problems when using the transtibial technique and the graft donor site may suffer postoperative anterior knee pain. The Achilles tendon allograft appears to be a popular PCL substitute as there usually are no donor site problems. However, allograft tissues are not widely available in many countries and the risk of disease-transmission remains uncertain.

The quadriceps tendon autograft has the advantage of being patient-available, requiring the easier arthroscopic technique, of a suitable size and strength, making it an acceptable choice for PCL reconstruction (50,51). The mean cross-sectional area measurements of a 10 mm wide quadriceps tendon averaged 64.4 ± 8.4 mm^2, which is significantly larger than the mean measurements of the patellar tendon, which measured 36.8±5.7 mm. The mean lengths of quadriceps tendons average 87.0 ± 9.7 mm and 85.2 ± 8.4 mm for right and left knee in comparison to the mean lengths of the patellar tendons measured 51.6 ± 6.9 mm and 52.2 ± 4.8 mm. These anatomical studies reveal that the quadriceps tendon is thicker, longer, and wider than the patellar tendon. In biomechanical studies, structural tensile property analysis shows that the ultimate tensile failure load for unconditioned quadriceps tendon-bone complexes is at 2173 ± 618 N compared to 1953 ± 325 N for bone-patellar tendon-bone complexes. The ultimate tensile failure load of the quadriceps tendon is 1.36 times that of a patellar tendon graft of comparable-width (52). Data from anatomical and biomechanical analyses support the use of the quadriceps tendon-patella construct for ligament reconstruction.

The hamstring tendon graft has become popular for PCL reconstruction in recent years. However, a single-strand semitendinosus tendon seems to be insufficient for PCL reconstruction. The maximum tensile load of a single-strand semitendinosus tendon is inferior to that of the ACL (1216 N to 1725 N, respectively) (53). The cross-sectional area of a single-strand semitendinosus tendon tends to be much smaller than that of a central 10 mm patellar tendon from the same donor (13.6 mm^2 and 36.9 mm^2, respectively). For ligament reconstruction, a 4-strand graft of semitendinosus and gracilis tendons is generally adequate with a suitable graft size. The ultimate failure load and stiffness measured in the 4 strands tendon group was the highest among three commonly used grafts. Although the quadruple tendons graft had greater translation during continuous loading it provided the strongest primary fixation strength (23).

Fixation techniques

For the fixation of the hamstring tendon graft in PCL reconstruction, bioabsorbable screws, sutures to screw, and Mersilene tapes to screw have been used (40, 54-56). However, the sutures-tendon junction is a weak point when loading. Sutures slipping out of the tendons are the most common failure described. It is better to avoid posterior loading on the graft prior to tendon-bone integration in the early stage of rehabilitation. When using tendon grafts for PCL reconstruction, a double fixation at both the femoral and tibial sides may be an effective method for augmentation of initial fixation stability. We think that additional fixation near the bone tunnel with interference screws combined with external suspension fixation will achieve more rigid and adequate graft fixation in the early postoperative stage and avoid progressive graft elongation (57).

Our techniques

Quadriceps tendon autograft for single-bundle PCL reconstruction

A quadriceps tendon graft consisted of a 20x10x8 mm bone plug of upper patellar bone with an 80x10x6 mm of central quadriceps tendon (58,59). The quadriceps tendon autograft has the advantage of being self-available, requires a relatively easier arthroscopic technique, and has a suitable size, making it an acceptable choice for PCL reconstruction. At a minimum of 3 years of follow-up, 83% patients achieved good or excellent results on the Lysholm knee rating, fifty-five percent of the patients could return to moderate or strenuous activity; 86% had a ligament laxity

of less than 5 mm.; 83% were rated as normal or nearly normal according to the International Knee Documentation Committee (IKDC) guidelines. A statistically significant difference exists in the thigh girth difference, extensor strength, and flexor strength before and after reconstruction. A one-incision endoscopic technique could be used for PCL reconstruction with quadriceps tendon-patellar bone autograft (60). At the femoral side, the bone plug is fixed by an interference screw. At the tibial side, the tendon portion is fixed by a suture to a screw on the anterior cortex and an interference bioscrew in the posterior tibial tunnel opening. The 1-incision technique provides a simple reconstruction method for PCL insufficiency without a second incision at the medial femoral condyle (Fig. 1).

Quadriceps tendon autograft for double-bundle PCL reconstruction

Quadriceps tendon autograft could be applied for double-bundled reconstruction of PCL (61). The quadriceps tendon portion was longitudinally split into two separate tendons for anterolateral (AL) and posteromedial (PM) bundles. AL and PM tunnels at the femoral condyle were created to reproduce the double-bundle structure of the PCL. The bone plug is situated at the tibial tunnel and fixed by a titanium interference screw. Each of the bundles of the tendon graft is rigidly fixed at the femoral tunnel with a bioabsorbable screw (Fig. 2).

Hamstring tendon autograft for single-bundle PCL reconstruction

PCL reconstruction techniques using quadruple hamstring tendon autograft with a double-fixation technique has been developed (57,62). A hamstring tendon graft is composed of a quadruple-stranded semitendinosus tendon and gracilis tendon 10 cm in length. The semitendinosus and gracilis tendon graft is adequate in graft size, technically easier to perform and more reproducible. At the minimal 4-year follow-up, the mean Lysholm score was 54 (40-65) and 91 (65-100) points ($p<0.01$) before and after surgery; 58% patients could return to moderate or strenuous activity; the average posterior displacement measured with KT-1000 was 11.69+/-2.01 mm preoperatively and 3.45+/-2.04 mm postoperatively; 81% of the patients demonstrated less than grade 1 ligament laxity and 81% of the patients were rated as normal or nearly normal based on IKDC scores. Arthroscopic reconstruction for PCL with the four-strand hamstring tendon graft produced satisfactory results (Fig. 3). A clinical study has compared the outcomes of PCL reconstruction using quadriceps tendon autograft and the quadruple hamstring tendon autograft (63). The IKDC rating showed no significant difference between the 2 groups in terms of activity level, ligament laxity, and final rating. Comparable satisfactory results between the 2 surgical groups were shown at a minimal 2-year follow-up.

Quadriceps tendon and hamstring tendon grafts for double-bundled PCL reconstruction

We have proposed a novel arthroscopic technique for double-bundle reconstruction of the PCL using quadriceps and hamstring tendon autografts (64). A quadriceps tendon-patellar bone autograft is used to reconstruct the major anterolateral bundle. A double-stranded semitendinosus tendon is used to reconstruct the posteromedial bundle. An anatomic reconstruction can be achieved by using these 2 autografts (Fig. 4).

Quadriceps tendon autograft for single-bundle PCL reconstruction with tibial inlay technique

An arthroscopic-assisted inlay technique for PCL reconstruction using quadriceps tendon autograft has been developed (65). The bone plug is fixed at the original PCL insertion site to the tibia and the free tendon is fixed with the Bioscrew and screw to the femoral condyle. When comparing with the BPTB graft, the quadriceps tendon autograft is an acceptable alternative for single-bundle PCL reconstruction (Fig. 5).

Quadriceps tendon autograft for double-bundle PCL reconstruction with tibial inlay technique

We have presented an inlay technique for arthroscopic PCL reconstruction with a double-bundled quadriceps tendon-patellar bone autograft (66). The tendon portion of the quadriceps tendon graft is split into two, the larger part for reconstruction of the anterolateral bundle and the smaller part for posteromedial bundle. The bone plug is fixated at original PCL insertion site at posterior tibia and 2 free tendon parts is fixated with Bioscrew and screw within two tunnels at femoral condyle. The double-

bundle graft appears to restore normal knee stability across the full range of flexion (Fig. 6).

Etiology analysis for PCL surgery failures

Failed PCL Surgery Syndrome includes the associated clinical symptoms and signs that occurred after PCL surgery. We postulated a classification for clinical assessments and subsequent treatments. Type 1 is posterior instability. Type 2 is posterolateral instability. Type 3 is combined posterior and PL instability. Type 4 is combined posterior and anterior instability. Type 5 is malalignment or osteoarthritis without instability. Type 6 is knee pain or knee stiffness without instability. In our series, 17% of the patients had type 1 (P instability), 32% had type 2 (PL instability), 23% had type 3 (P + PL instability), 9% had type 4 (P+A instability), 7% had type 5 (OA), and 12% had type 6 (pain/stiffness). The common etiologies of surgical failure were inadequate posterolateral stability, improper tunnel positioning, re-injury, inadequate correction of ACL insufficiency, and inadequate avulsion fracture fixation. The treatment of these cases of failure included PCL revision surgery, PCL-PL reconstruction, PCL-ACL reconstruction, re-fixation of avulsion fragment, and salvage arthroscopic treatment depending on the etiology of the failure.

Clinical outcome of PCL surgery

Variables that affect the results of surgery to restore PCL function include combined associated ligaments injury; difficulty to duplicate PCL precisely; wide variation in broad femoral insertion footprint; difficulty in accurately placing the transtibial tunnel; tunnel erosion or migration and high internal graft stresses and graft elongation with the transtibial technique. The outcome of conservative treatment of isolated PCL injuries with mild or moderate laxity is generally acceptable. However, more severe straight posterior laxity or combined injury patterns lead to a worse prognosis (39,67-68). Arthroscopic reconstruction for PCL can achieve satisfactory results for most patients if adequate surgical principles and techniques are followed.

When using the hamstring tendon graft for PCL reconstruction, postoperative limitation in ROM may be a problem. The impaired range of motion may be due to anterior knee tightness or discomfort of the popliteal fossa. Rigid reconstruction performed simultaneously for posterior and posterolateral structures may defer the final flexion. Hamstring muscle rehabilitation may be an issue in flexor strength recovery. Thigh muscle atrophy and incomplete thigh muscle strength recovery seem inevitable after PCL injury especially in those patients who are not competitive athletes and therefore are not motivated to follow strenuous muscle training. A more aggressive muscle training program should always be emphasized to better recover function.

From the outcome analyses in our series, the average Lysholm knee scores were 86-89 points at final assessment. For return to sports activity evaluated with the IKDC score, 55-59 % of the patients could return to strenuous or moderate activities after reconstruction. For subjective knee function, 85-86% of the patients rated their reconstructed knee as normal or nearly normal. For ligament laxity, 56-58% revealed grade 1 ligament laxity when measured with KT-1000 arthrometer tests; 9 to 15 % of the patients had grade 2 knee posterior laxity and functional tests showed that 81-85% recovered 90% of the normal knee function. In the IKDC final rating, 81-82% of the patients rated as nearly normal or normal. Significant improvement in posterior laxity can be achieved with our techniques.

CONCLUSION

In recent years, the significant progress made in the fields of anatomy, biomechanics and arthroscopic surgical techniques in PCL injury have in part resolved the controversial issues regarding the choice of graft, the tunnel location, the transtibial or tibial inlay technique, the one or two bundle reconstruction, the knee position when securing the graft, and the fixation techniques. With adequate surgical principles and techniques, PCL reconstruction can achieve satisfactory results for patients with symptomatic posterior knee instability and multiple ligament injuries.

REFERENCES

1. Miyasaka KC, Daniel DM, Stone ML. The incidence of knee ligament injuries in the general population.

Am J Knee Surg 1991;4:3-8.
2. Dandy DJ, Pusey RJ. The long-term results of unrepaired tears of the posterior cruciate ligament. J Bone Joint Surg Br 1982;64:92-4.
3. Markolf KL, McAllister DR, Young CR, McWilliams J, Oakes DA. Biomechanical effects of medial-lateral tibial tunnel placement in posterior cruciate ligament reconstruction. J Orthop Res 2003;21:177-82.
4. McAllister DR, Markolf KL, Oakes DA, Young CR, McWilliams J. A biomechanical comparison of tibial inlay and tibial tunnel posterior cruciate ligament reconstruction techniques: graft pretension and knee laxity. Am J Sports Med 2002;30:312-7.
5. Morgan CD, Kalman VR, Grawl DM. The anatomic origin of the posterior cruciate ligament: where is it? Reference landmarks for PCL reconstruction. Arthroscopy 1997;13:325-31.
6. Girgis FG, Marshall JL, Al Monajem ARS. The cruciate ligaments of the knee joint: anatomical, functional and experimental analysis. Clin Orthop 1975;106:216-31.
7. Galloway MT, Grood ES, Mehalik JN, Levy M, Saddler SC, Noyes FR. Posterior cruciate ligament reconstruction. An in vitro study of femoral and tibial graft placement. Am J Sports Med 1996;24:437-45.
8. Markolf KL, Slauterbeck JR, Armstrong KL, Shapiro MS, Finerman GA. A biomechanical study of replacement of the posterior cruciate ligament with a graft. Part 1: Isometry, pre-tension of the graft, and anterior-posterior laxity. J Bone Joint Surg Am 1997;79:375-80.
9. Xerogeanes JW, Livesay GA, Carlin GJ, Smith BA, Kusayama T, Kashiwaguchi S, Woo SL. The human posterior cruciate ligament complex: an interdisciplinary study. Ligament morphology and biomechanical evaluation. Am J Sports Med 1995;23:736-45.
10. Covey DC, Sapega AA. Current concepts review: injury to the posterior cruciate ligament injuries. Am J Sports Med 1993;21:132-6.
11. Harner CD, Hoher J. Evaluation and treatment of posterior cruciate ligament injuries. Am J Sports Med 1998;26:471-82.
12. Race A, Amis AA. The mechanical properties of the two bundles of the human posterior cruciate ligament. J Biomech 1994;27:13-24.
13. Race A, Amis AA. PCL reconstruction. In vitro biomechanical comparison of isometric versus single and double-bundled 'anatomic' grafts. J Bone Joint Surg Br 1998;80:173-9.
14. Harner CD, Janaushek MA, Kanamori A, Yagi M, Vogrin TM, Woo SL. Biomechanical analysis of a double-bundle posterior cruciate ligament reconstruction. Am J Sports Med 2000;28:144-51.
15. Bergfeld JA, Graham SM, Parker RD, Valdevit AD, Kambic HE. A biomechanical comparison of posterior cruciate ligament reconstructions using single- and double-bundle tibial inlay techniques. Am J Sports Med 2005;33:976-81.
16. Chhabra A, Kline AJ, Harner CD. Single-bundle versus double-bundle posterior cruciate ligament reconstruction: scientific rationale and surgical technique. Instr Course Lect 2006;55:497-507.
17. Stahelin AC, Sudkamp NP, Weiler A. Anatomic double-bundle posterior cruciate ligament reconstruction using hamstring tendons. Arthroscopy 2001;17:88-97.
18. Richards RS 2nd, Moorman CT 3rd. Use of autograft quadriceps tendon for double-bundle posterior cruciate ligament reconstruction. Arthroscopy 2003, 19:906-15.
19. Kim SJ, Park IS, Cheon YM, Ryu SW. Double-bundle technique: endoscopic posterior cruciate ligament reconstruction using tibialis posterior allograft. Arthroscopy 2004;20:1090-4.
20. Kim SJ, Park IS. Arthroscopic reconstruction of the posterior cruciate ligament using tibial-inlay and double-bundle technique. Arthroscopy 2005;21: 1271.
21. Yoon KH, Bae DK, Song SJ, Lim CT. Arthroscopic double-bundle augmentation of posterior cruciate ligament using split Achilles allograft. Arthroscopy 2005;21:1436-42.
22. Makino A, Aponte Tinao L, Ayerza MA, Pascual Garrido C, Costa Paz M, Muscolo DL. Anatomic double-bundle posterior cruciate ligament reconstruction using double-double tunnel with tibial anterior and posterior fresh-frozen allograft. Arthroscopy 2006;22:684.1-5.
23. Chen CH, Chou SW, Chen WJ, Shih CH. Fixation strength of three different grafts types used in posterior cruciate ligament reconstruction. Knee

Surg Sports Traumatol Arthrosc 2004;12: 371-5.
24. Baker CL, Norwood LA, Hughston JC. Acute posterolateral rotatory instability of the knee. J Bone Joint Surg Am 1983:65:614-8.
25. Baker CL, Norwood LA, Hughston JC. Acute combined posterior cruciate and posterolateral instability of the knee. Am J Sports Med 1984:12: 204-18.
26. Hughston JC. Jacohson KE. Chronic posterolateral rotatory instability of the knee. J Bone Joint Surg Am 1985:67:351-9.
27. Ferrari DA, Ferrari JD. Coumas J. Posterolateral instability of the knee. J Bone Joint Surg Br 1994:76: 187-92.
28. Veltri DM. Deng XH, Torzilli PA, Warren RF, Maynard MJ. The role of the cruciate and posterolateral ligaments in stability of the knee: A biomechanical study. Am J Sports Med 1995;23:436-43.
29. Terry CC, LaPrade RE. The posterolateral aspect of the knee. Anatomy and surgical approach. Am J Sports Med 1996:24:732-9.
30. LaPrade RE. Terry CC. Injuries to the posterolateral aspect of the knee: Association of anatomic injury patterns ~with clinical instability. Am J Sports Med 1997:25:433-8.
31. LaPrade RF. Resig S, Wentorf F, Lewis JL. The effects of grade III posterolateral knee complex injuries on anterior cruciate ligament graft force. A biomechanical analysis. Am J Sports Med 1999:27: 469-75.
32. Noyes ER. Barber-Westin SD. Surgical reconstruction of severe chronic posterolateral complex injuries of the knee using allograft tissues. Am J Sports Med 1995:23:2-12.
33. Fanelli GC, Giannotti BE, Edson CJ. Arthroscopically assisted combined posterior cruciate ligament/ posterior lateral complex reconstruction. Arthroscopy 1996;12: 521-30.
34. Freeman RT, Duri ZA, Dowd GS. Combined chronic posterior cruciate and posterolateral corner ligamentous injuries: a comparison of posterior cruciate ligament reconstruction with and without reconstruction of the posterolateral corner. Knee 2002;9:309-12.
35. Clancy WG Jr, Pandya RD (1994) Posterior cruciate ligament reconstruction with patellar tendon autograft. Clin Sports Med 1994;13:561-70.
36. Fanelli GC, Edson CJ. Arthroscopically assisted combined anterior and posterior cruciate ligament reconstruction in the multiple ligament injured knee: 2- to 10-year follow-up. Arthroscopy 2002;18:703-14.
37. Bianchi M. Acute tears of the PCL: clinical study and results of operative treatment in 27 cases. Am J Sports Med 1983;11:308-14.
38. Aglietti P, Buzzi R, Lazzara. Posterior cruciate ligament reconstruction with the quadriceps tendon in chronic injuries. Knee Surg Sports Traumatol Arthrosc 2002;10:266-73.
39. Lipscomb AB Jr, Anderson AF, Norwig ED, Hovis WD, Brown DL. Isolated PCL reconstruction: long-term results. Am J Sports Med 1993;21:490-6.
40. Trickey EL. Injuries to the posterior cruciate ligament: diagnosis and treatment of early injuries and reconstruction of late instability. Clin Orthop 1980;147:76-81.
41. Wang CJ, Chen HS, Huang TW, Yuan LJ. Outcome of surgical reconstruction for posterior cruciate and posterolateral instabilities of the knee. Injury 2002;33:815-21.
42. Berg EE. Posterior cruciate ligament tibial inlay reconstruction. Arthroscopy 1995;11:69-76.
43. Miller MD, Olszewski AD. Posterior inlay technique for PCL reconstruction. Am J Knee Surg 1995;8: 145-54.
44. Markolf KLZ, McAllister DR. Cyclic loading of posterior cruciate ligament replacements fixed with tibial tunnel and tibial inlay methods. J Bone Joint Surg Am 2002;84: 518-24.
45. Miller MD, Kline AJ, Gonzales J, Beach WR. Vascular risk associated with a posterior approach for posterior cruciate ligament reconstruction using the tibial inlay technique. J Knee Surg 2002;15:137-40.
46. McAllister DR, Markolf KL, Oakes DA, Young CR, McWilliams J. A biomechanical comparison of tibial inlay and tibial tunnel posterior cruciate ligament reconstruction techniques: graft pretension and knee laxity. Am J Sports Med 2002;30: 312-7.
47. Kim SJ, Choi CH, Kim HS. Arthroscopic posterior cruciate ligament tibial inlay reconstruction.

Arthroscopy. 2004;20:149-54.
48. Seon JK, Song EK. Reconstruction of isolated posterior cruciate ligament injuries: a clinical comparison of the transtibial and tibial inlay techniques. Arthroscopy 2006;22:27-32.
49. Mariani PP, Margheritini F. Full arthroscopic inlay reconstruction of posterior cruciate ligament. Knee Surg Sports Traumatol Arthrosc 2006;14:1038-44.
50. Staubli HU, Schatzmann L, Brunner P, Rincon L, Nolte LP. Quadriceps tendon and patellar ligament: cryosectional anatomy and structural properties in young adults. Knee Surg Sports Traumatol Arthrosc 1996;4:100-10.
51. Staubli HU, Jakob RP. Central quadriceps tendon for anterior cruciate ligament reconstruction. Part I: morphometric and biochemical evaluation. Am J Sports Med 1997;25:725-7.
52. Fulkerson JP, Langeland R. An alternative cruciate reconstruction graft: the central quadriceps tendon. Arthroscopy 1995;11:252-4.
53. Noyes FR, Butler DL, Grood ES. Biomechanical analysis of human ligament grafts used in knee-ligament repairs and reconstructions. J Bone Joint Surg Am 1984; 66: 344-52.
54. Houe T, Jorgensen U. Arthroscopic posterior cruciate ligament reconstruction: one- vs. two-tunnel technique. Scand J Med Sci Sports 2004;14:107-11.
55. Lill H, Glasmacher S, Korner J, Rose T, Verheyden P, Josten C. Arthroscopic-assisted simultaneous reconstruction of the posterior cruciate ligament and the lateral collateral ligament using hamstrings and absorbable screws. Arthroscopy 2001;17:892-7.
56. Pinczewski LA, Thuresson P, Otto D, Nyquist F. Arthroscopic posterior cruciate ligament reconstruction using four-strand hamstring tendon graft and interference screws. Arthroscopy 1997;13: 661-5.
57. Chen CH, Chen WJ, Shih CH. Arthroscopic Reconstruction of the posterior cruciate ligament with quadruple hamstring tendon graft a double fixation method. J Trauma 2002;52: 938-45.
58. Chen CH, Chen WJ, Shih CH, Chou SW. Arthroscopic posterior cruciate ligament reconstruction with quadriceps tendon autograft - Minimal 3 years follow-up. Am J Sport Med 2004;32: 361-8.
59. Chen CH, Chen WJ, Shih CH. Arthroscopic posterior cruciate ligament reconstruction with quadriceps tendon-patellar bone autograft. Arch Orthop Trauma Surg. 1999;119:86-8.
60. Chen CH, Chen WJ, Shih CH. One-incision endoscopic technique for posterior cruciate ligament reconstruction with quadriceps tendon-patellar bone autograft. Arthroscopy 2001;17:329-32.
61. Chen CH, Chen WJ, Shih CH. Arthroscopic double-bundled posterior cruciate ligament reconstruction with quadriceps tendon-patellar bone autograft. Arthroscopy 2000;16:780-2.
62. Chen CH, Chuang TY, Wang KC, Chen WJ, Shih CH. Arthroscopic posterior cruciate ligament reconstruction with hamstring tendon autograft: results with a minimum 4-year follow-up. Knee Surg Sports Traumatol Arthrosc 2006;e-Pub
63. Chen CH, Chen WJ, Shih CH. Arthroscopic posterior cruciate ligament reconstruction Comparison of quadriceps tendon autograft and hamstring tendon autograft Arthroscopy 2002;18:603-12.
64. Chen CH, Chen WJ, Shih CH. Double-bundle posterior cruciate ligament reconstruction with quadriceps and semitendinosus tendon grafts. Arthroscopy 2003;19:1023-6.
65. Chuang TY, Chen CH, Chou SW, Chen YJ, Chen WJ. Tibial inlay technique with quadriceps tendon-bone autograft for posterior cruciate ligament reconstruction. Arthroscopy 2004;20:331-5.
66. Chuang TY, Ho WP, Chen CH, Liao YS, Chen WJ. Double-bundle posterior cruciate ligament reconstruction using inlay technique with quadriceps tendon-bone autograft. Arthroscopy 2004;20:e23-8.
67. Torg JS, Barton TM, Pavlov H, Stine R. Natural history of the posterior cruciate ligament deficient knee. Clin Orthop 1989;246:208-16.
68. Veltri DM, Warren RF. Isolated and combined posterior cruciate ligament injuries. J Am Acad Ortho Surg 1993;1:67-75.

EDITORIAL

ROLE OF CYTOKINES IN THE PATHOGENESIS OF BONE RESORPTION

Y. SHAIK, A. ANOGIANAKI[1], G.S. KATSANOS[2], M.L. CASTELLANI[2], S. FRYDAS[3], J. VECCHIET[4], S. TETÈ[5], C. CIAMPOLI[5], V. SALINI[6], D. DE AMICIS[6], M. FULCHERI[7], C. ORSO[6], R. POLLICE[8], T.C. THEOHARIDES[9], R. DOYLE[10] and P. CONTI[2]

Dept. Medicine, Section of Infectious Diseases, Boston University School of Medicine, Boston, MA, USA; [1]Department of Physiology, Faculty of Medicine, Aristotle University of Thessaloniki, Greece; [2]Immunology Division, Medical School, University of Chieti-Pescara, Chieti, Italy; [3]Parasitology and Parasitic Diseases Department, Aristotle University of Thessaloniki, Greece; [4]Clinical of Infectious Diseases, Medical School, University of Chieti-Pescara, Chieti, Italy; [5]Dental School, University of Chieti-Pescara, Chieti, Italy;[6]Orthopedic Division, University of Chieti-Pescara, Chieti, Italy; [7]Psychology Unit, University of Chieti-Pescara, Chieti, Italy; [8]Department of Experimental Medicine, University of L'Aquila, Italy; [9]Department of Pharmacology and Experimental Therapeutics, Tufts University School of Medicine, Tufts-New England Medical Center, Boston, MA, USA; [10]Psychiatry Division, Massachusetts General Hospital, Harvard Medical School, Boston, MA, USA

Received April 11, 2008 – Accepted January 8, 2009

Bone resorption is a process modified by cytokines that is involved in the pathophysiology of several diseases, including rheumatoid arthritis, human middle ear cholesteatoma and chronic sinusitis which present a significantly large number of IL-1, IL-8 and TNF-alpha positive cells. Interleukin-1 (IL-1) is a preliminary inflammatory cytokine which stimulates the expression of genes associated with inflammation. Tumor necrosis factor (TNF) is also an inflammatory cytokine closely related to IL-1, although the structure and the receptors for IL-1 and TNF are clearly distinct. IL-1 and TNF provoke fever, inflammation, and tissue destruction. IL-1 and TNF are monokines produced by monocytes/macrophages following the activation of soluble factors and contact with the stimulated TH1 lymphocytes. The contact between lymphocytes and macrophages is regulated by ligands and counterligands such as beta-2 integrins, CD4-CD4L, and CD69.

Bone is continuously destroyed and reformed to maintain a constant homeostatic volume. Osteogeneic cells, osteoclasts and osteoblasts, are responsible for resorbing bone during physiologic remodeling (1-9). Osteoblasts and osteoclasts are specialized cells responsible for bone formation and resorption, respectively. Osteoclasts, which are giant multinucleated cells, are present only in bone and have the capacity to resorb mineralized tissues (10). They are derived from hematopoeitic progenitors of the monocyte/macrophage lineage. Osteoblasts are bone marrow-derived stromal cells involved in

Key words: Bone resorption, interleukins, inflammation, cytokines

Mailing address: Prof. Pio Conti,
Department of Oncology and Neuroscience,
University of Chieti-Pescara,
Via dei Vestini,
66100 Chieti, Italy
Tel: ++39 0871 355 4805 Fax: ++39 0871 355 4804
e-mail: pconti@unich.it

1973-6401 (2009)

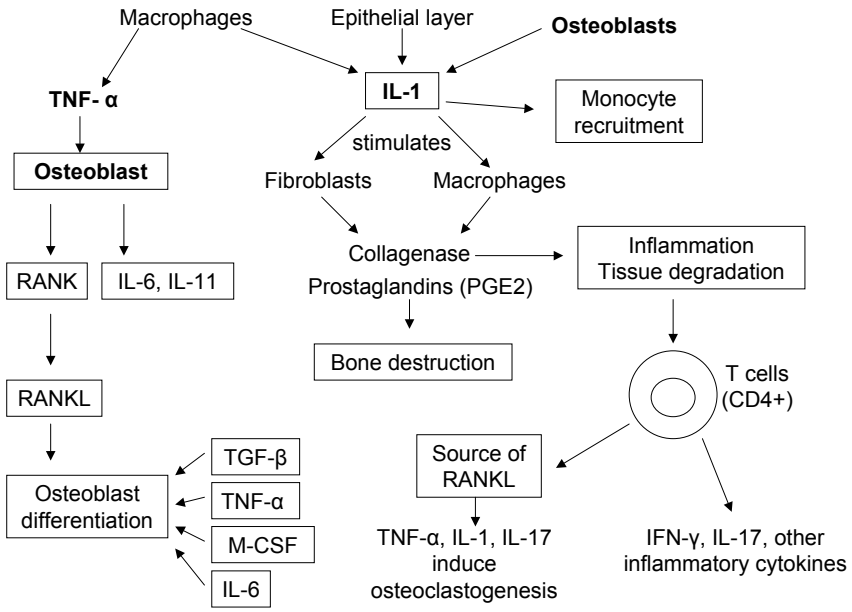

osteoclastogenesis through a mechanism involving cell to cell contact with osteoclast progenitors.

The erosion progression through the course of inflammatory diseases is generally correlated with the severity of the disease. The use of antagonists to IL-1 and TNF-alpha in experimental bone destruction has demonstrated a cause-and-effect relationship between the activity of these cytokines and the spread of an inflammatory front to deeper areas in the connective tissue, loss of connective tissue attachment, osteoclast formation, and the loss of alveolar bone (11-13). New evidence indicates that osteoclasts are key mediators of human middle ear cholesteatoma and bone morphogenetic proteins play critical roles in osteoblast differentiation (14). Inflammatory cytokines such as TNF-alpha and IL-1 directly regulate osteoclast differentiation and function (Fig. 1). TNF-alpha and IL-1 are the most potent osteoclastogenic cytokines produced in inflammation and are pivotal in the pathogenesis of this disease (15). Production of TNF-alpha and IL-1 is largely CD4+ T-cell dependent and are mostly the result of INF-gamma secretion. Inflammed tissue T cells secret IFN-gamma, IL-17 and other inflammatory cytokines interacting with macrophages, fibroblasts, and osteoclasts (16-17). This T cell activation provides an abundant source of receptor activator of NF-kappaB ligand (RANKL). RANK and its ligand RANKL have well established regulatory effects on bone metabolism (18). Osteoclast precursors that express RANK, a receptor for RANKL, recognize RANKL through the cell-cell interaction and differentiate into mature osteoclasts. The ligand RANKL binds to its receptor RANK to induce bone resorption. RANKL is a transmembrane protein expressed in various cell types and particularly in osteoblasts and activated T-cells (19). RANKL secretion by activated T-cells induces osteoclastogenesis, a mechanism enhanced by various cytokines such as IL-1, TNF, IL-6, and IL-17, which promote inflammation and bone resorption (20-21). Recently, it has been reported that the two anti-inflammatory cytokines, IL-4 and IL-10, can inhibit this system (22). Moreover, TNF-alpha and IL-1 target stromal-osteoblastic cells to induce IL-6 and IL-11. In the presence of levels of RANKL, TNF-alpha acts directly to stimulate osteoclast differentiation of macrophages and amyloid progenitor cells. IL-1 and TNF, acting together with RANKL, can promote osteoclast recruitment, activation and osteolysis in inflammatory states (23). Treatment of osteoblasts with bone resorption factor upregulates the expression of RANKL mRNA. In contrast, TNF-alpha stimulates osteoclast differentiation in the presence of m-CSF through a mechanism independent of the RANKL system (24).

Moreover, TGF-beta strikingly enhances osteoclast activation induced by RANKL. Transforming growth factor-beta (TGF-beta) superfamily members and IFN-gamma have also been shown to be important regulators in osteoblastogenesis (25). Inflammatory diseases involving bone resorption are driven, in part, by interactions between T cells and macrophages by pro-inflammatory cytokines that these cells produce. Treatment with biological agents now have the potential to retard or possibly prevent the function of these cytokines and subsequent morbidity in many patients. Three anti-TNF-alpha compounds are currently available, but only etanercept (Enbrel) has been approved in the United States. Etanercept is a fully human soluble fusion protein of the p75 TNF receptor and the human FcIgG1; while infliximab (Remicade) is a chimeric humanized monoclonal IgG1 antibody, and adalimumab (Humira) is a fully humanized monoclonal antibody. The anti-TNF-alpha agents are generally well tolerated and their safety profile deserves consideration. However, the real role of the anti-inflammatory agents in inflammatory diseases involving bone resorption remains to be determined.

REFERENCES

1. Kim HJ, Zhao H, Kitaura H, Bhattacharyya S, Brewer JA, Muglia LJ, Patrick Ross F, Teitelbaum SL. Glucocorticoids and the osteoclast. Ann NY Acad Sci 2007; 116:335-9.
2. Castellani ML, Bhattacharya K, Tagen M, et al.Anti-chemokine therapy for inflammatory diseases. Int J Immunopathol Pharmacol 2007; 20:447-54.
3. Ringe JD, Body JJ. A review of bone pain relief with ibandronate and other bisphosphonates in disorders of increased bone turnover. Clin Exp Rheumatol 2007; 25:766-74.
4. Pannone G, Sanguedolce F, De Maria S, et al. Cyclooxygenase isozymes in oral squamous cell carcinoma: a real-time RT-PCR study with clinic pathological correlations. Int J Immunopathol Pharmacol 2007; 20:317-24.
5. di Lorenzo L, Vacca A, Corfiati M, Lovreglio P, Soleo L. Evaluation of tumor necrosis factor-alpha and granulocyte colony-stimulating factor serum levels in lead-exposed smoker workers. Int J Immunopathol Pharmacol 2007; 20:239-47.
6. Inoue K, Takano H, Oda T, Yanagisawa R, Tamura H, Ohno N, Adachi Y, Ishibashi K, Yoshikawa T. Candida soluble cell wall β-D-glucan induces lung inflammation in mice. Int J Immunopathol Pharmacol 2007; 20:499-507.
7. Nwadinigwe CU, Anyaehie UE. Effects of cyclooxygenase inhibitors on bone and cartilage metabolism--a review. Niger J Med 2007; 16(4):290-4.
8. Tian XY, Zhang Q, Zhao R, Setterberg RB, Zeng QQ, Ma YF, Jee WSS. Continuous infusion of PGE(2) is catabolic with a negative bone balance on both cancellous and cortical bone in rats. J Musculoskelet Neuronal Interact 2007; 7:372-81.
9. Zaidi M, Blair HC, Iqbal J, Zhu LL, Kumar TR, Zallone A, Sun L. Proresorptive actions of FSH and bone loss. Ann NY Acad Sci 2007; 1116:376-82.
10. Karsdal MA, Neutzsky-Wulff AV, Dziegiel MH, Christiansen C, Henriksen K. Osteoclasts secrete non-bone derived signals that induce bone formation. Biochem Biophys Res Commun 2008; 366:483-8.
11. Esteve FR, Roodman GD. Pathophysiology of myeloma bone disease. Best Pract Res Clin Haematol 2007; 20:613-24.
12. Accardo-Palumbo A, Ferrante A, Ciccia F, Cadelo M, Giardina AR, Impastato R, Triolo G. Pentoxifylline inhibits Vγ9/Vδ2 T lymphycyte activation of patients with active Behçet's disease *in vitro*. Int J Immunopathol Pharmacol 2007; 20:601-6.
13. Magloire H, Joffre A, Hartmann DJ. Localization and synthesis of type III collagen and fibronectin in human reparative dentine. Immunoperoxidase and immunogold staining. Histochemistry 1988; 88:141-9.
14. Bodini A, D'Orazio C, Peroni DG, Corradi M, Zerman L, Folesani G, Assael BM, Boner AL, Piacentini GL. IL-8 and pH values in exhaled condensate after antibiotics in cystic fibrosis children. Int J Immunopathol Pharmacol 2007; 20: 467-72.
15. Feliciani C, Ruocco E, Zampetti A, Toto P, Amerio Pa, Tulli A, Amerio P, Ruocco V. Tannic acid induces *in vitro* acantholysis of keratinocytes via IL-1α and TNF-α. Int J Immunopathol Pharmacol 2007; 20: 289-300.

16. Deepak P, Kumar S, Acharya A. IL-13 neutralization modulates function of type II polarized macrophages *in vivo* in a murine T-cell lymphoma. Eur J Inflamm 2007; 5:37-45.
17. Cadoni S, Ruffelli M, Fusari S, de Pità O. Oral allergic syndrome and recombinant allergens rBet v 1 and rBet v 2. Eur J Inflamm 2007; 5:21-5.
18. Rodriguez-Bores L, Barahona-Garrido J, Yamamoto-Furusho JK. Basic and clinical aspects of osteoporosis in inflammatory bowel disease. World J Gastroenterol 2007; 13:6156-65.
19. Zhu W, Mantione KJ, Kream RM, Cadet P, Stefano GB. Cholinergic regulation of morphine release from human white blood cells: evidence for a novel nicotinic receptor via pharmacological and microarray analysis. Int J Immunopathol Pharmacol 2007; 30:229-38.
20. Shim JY, Han Y, Ahn JY, Yun YS, Song JY. Chemoprotective and adjuvant effects of immunomodulator ginsan in cyclophosphamide-treated normal and tumor bearing mice. Int J Immunopathol Pharmacol 2007; 20:487-98.
21. Bocchietto E, Paolucci C, Breda D, Sabbioni E, Burastero SE. Human monocytoid THP-1 cell line versus monocyte-derived human immature dendritic cells as *in vitro* models for predicting the sensitising potential of chemicals. Int J Immunopathol Pharmacol 2007; 20:259-66.
22. Falasca K, Ucciferri C, Iezzi A, Manzoli A, Mancino P, Pizzigallo E, Conti P, Vecchiet J. Metabolic syndrome and cardiovascular risk in HIV-infected patients with lipodystrophy. Int J Immunopathol Pharmacol 2007; 20:519-28.
23. De Franco S, Chiocchetti A, Ferretti M, et al. Defective function of the Fas apoptotic pathway in Type 1 diabetes mellitus correlates with age at onset. Int J Immunopathol Pharmacol 2007; 20:567-75.
24. Cuzzocrea S, Genovese T, Mazzon E, Esposito E, Muià C, Abdelrahman M, Di Paola R, Bramanti P, Thiemermann C. Glycogen synthase kinase-3β inhibition attenuates the development of bleomycin-induced lung injury. Int J Immunopathol Pharmacol 2007; 20:619-30.
25. Ahangari G, Chavoshzadeh Z, Lari Z, Ramyar A, Farhoudi A. Novel mutation detection of an inflammatory molecule Elastase II gene encoding neutrophil Elastase in Kostmann syndrome. Eur J Inflamm 2007; 5:65-71.

CLINICAL STUDY

KNEE JOINT STIFFNESS AND PROPRIOCEPTION DURING PREGNANCY

T. BÁNYAI, Á. HAGA, L. GERA, B. G. MOLNÁR[1], K. TÓTH[2], and E. NAGY

Department of Traumatology and Hand Surgery, SZTE University Teaching Hospital, Kecskemét; [1] Department of Obstetrics and Gynaecology, SZTE University, Szeged; [2]Department of Orthopaedics, SZTE University, Szeged, Hungary

Received January 28, 2008- Accepted January 8, 2009

The study performed in the Department of Orthopaedics and Department of Obstetrics and Gynaecology in Szeged regarding the physiologic changes occurring during pregnancy which influence the tension of the knee, the proprioception and balance is presented. Twenty two pregnant and eighteen non pregnant female volunteers took part in the study, measurements of arthrometry, stabilometry and position of knee joints were performed. These data are the second part of a research series to analyze the cruciate ligament tears, which are more frequent in females from a hormonal point of view than in males, and to establish the appropriate prevention measures. The detected increased weakness of the knee and the weaker proprioceptive perception of the anterior-posterior direction could explain the higher risk of injury of the anterior cruciate ligament.

Women performing the same sport as men suffer 4-8 times more frequently anterior cruciate ligament (ACL) rupture (1). More etiologic factors (extrinsic and intrinsic) are responsible for the difference. Extrinsic factors (anatomical differences, relatively higher sport activity, skill level) are relatively easier to modify like the intrinsic factors (hormone level, maximal oxygen consumption, VO_2 max, lactate response, bodyweight, plasma volume, Hgb concentration., heart rate, ventilation). Researchers suspect that oestrogen and relaxin as intrinsic factors have profound effects on women's neuromuscular systems (2) and the mechanics of soft tissue such as ligaments and tendons (3-5). More studies suggest that the hormonal factor plays an important role in the elevated ACL injury risk (6-7).

In 2005 with the study group of the Let People Move Biomechanical Laboratory in Perugia we analyzed the hormonal factor of the possible reasons (8). Between the phases of the menstrual cycle we found no significant difference in ACL stiffness and proprioception (like most other studies) (9-12). Some other studies suggested a correlation (1,13-14).

In the second phase of the study at the Medical University of Szeged, Hungary we analyzed the biomechanical properties of pregnant women because they have significantly higher sexual hormone levels.

The purpose of this study was to find relationships between the higher sexual hormone levels and knee joint laxity and proprioception.

MATERIALS AND METHODS

Volunteers

22 pregnant (average age:30.4 years, average BMI before pregnancy: 22.5, during the study 27.3) and 18 non pregnant women (average age: 33.3 years, average BMI: 21.4). The pregnant women regularly visited the

Key words: biomechanics, females, knee joint physiology, menstrual cycle physiology, proprioception physiology

Mailing address:
Dr. Tamás Bányai,
7. Szimferopol Tér,
6000 Kecskemét, Hungary
Tel: ++36303499775
Fax: ++3676516710
e-mail: medcore@t-email.hu

1973-6401 (2009)

Department of Obstetrics and Gynaecology of the Medical University in Szeged. They volunteered for the study after a personal interview. The non pregnant group was selected from the employees of the Department of Orthopaedics. In both groups there was no professional sports activity, the pregnant women took part in normal prenatal exercising, the non pregnant women did not take oral contraceptives. The dominant leg was decided with the ball kicking test. In all cases the right leg was dominant. The pregnant women were experiencing a normal pregnancy between the 13th and 40th week. We registered the actual state of the pregnancy from their medical records. We divided the pregnant women into two groups (1. 13-28th week; 2. 28-40th week).

Measuring ACL stiffness

We performed KT2000 (Medmetrics Corp, San Diego, CA, USA) arthrometry (three times 15,20,30 pounds forces and maximal femoral-tibial displacements while the knee

was placed in 30° of flexion as the subject lay supine on a bench.) We recorded the anterior-posterior displacements in millimetres. All measurements were completed by the same person.

Measuring proprioception

Stabilometry

Active and passive balance control with opened and closed eyes, detected sway path, splitted into anterior-posterior and lateral axes. The stabilometer (ZWE PII, Hungary) was connected to a computer, the participants made different balance-exercises with the help of the figures on the display:

1.Standing normally, fixing one point on the wall (20s)

2. Standing with eyes closed (20s)

3. Holding a square-figure in the centre of the screen (20s)

4. Moving a figure (mouse) to given locations (candies on a Christmas tree) within 20s

5. Moving and holding the figure in a point (within 20s)

6. Putting a pencil figure in a square (within 20s)

The computer analysed the data using the Fourier analysis.

Joint position sense

We analysed knee joint kinaesthesia during 30°, 60°, 90° knee flexion, as the patient lay supine on a bench. We measured the differences between the sensed and real knee position 3 times. We registered the positions with a goniometer.

Exclusion criteria

Operated knee, knee instability, former pregnancy, oral contraceptives

Statistical analysis

3-way ANOVA, Bonferroni test (SigmaStat), Fourier analysis (Statistica)

RESULTS

The KT-2000 arthrometer measured significant differences between the elongations of ACL in the pregnant and control groups. ($p<0.05$).

There was a significant difference between the elongations of the right and left side in both groups ($p <0.05$).

The non pregnant group sensed significantly better the joint positions with the dominant leg ($p<0.05$).

There was a significant difference between the dominant and non dominant leg during pregnancy ($p<0.05$).

With open eyes the pregnant women had significantly less total sway, with closed eyes there was no significant difference (Fig. 1). During the second part of the pregnancy this difference is higher (Fig. 2). Splitting the sway path into AP and lateral axes in the pregnant women with closed eyes there was a significantly greater instability in the anterior-posterior axis (Fig. 3).

When the second pregnant group closed their eyes they showed significantly increased instability in the anterior-posterior axis (Fig. 4).

DISCUSSION

According to the results and the well known fact that pregnant women's knees have increased laxity, we measured weaker joint position sense on the dominant leg.

With their eyes open the pregnant women had significantly less total sway, with their eyes closed there was no significant difference.

Splitting into AP and lateral axes the pregnant women with closed eyes presented a significantly increased instability in the anterior-posterior axis. By the second half of the pregnancy when women closed their eyes there was a significantly increased instability in the anterior-posterior axis.

The increased weakness of the knee and the weaker proprioceptive perception to the anterior-posterior

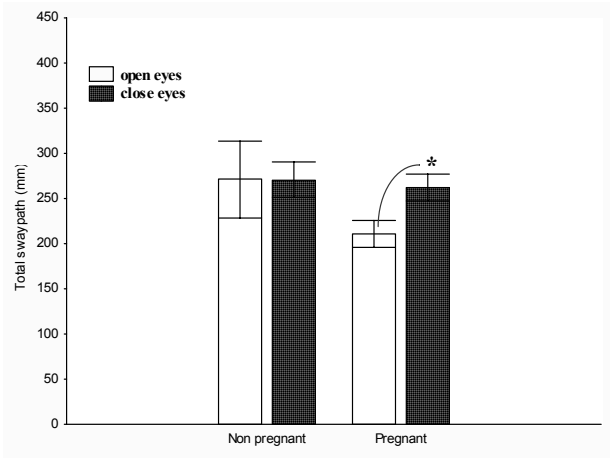

Fig. 1. *The sway path differences between pregnant and non pregnant women during stabilometry.*

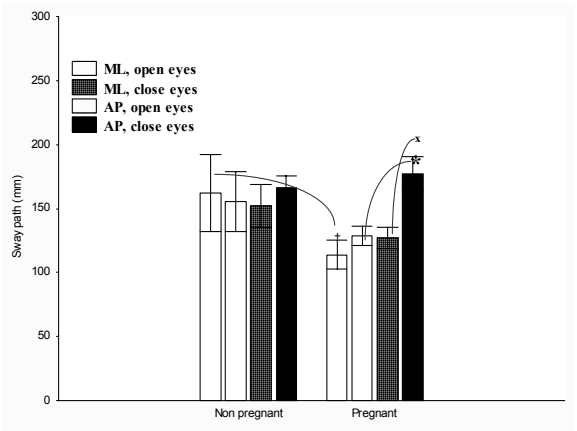

Fig. 3. *Sway path differences splitted into antero-posterior and lateral directions. (x,*,+: significant differences)*

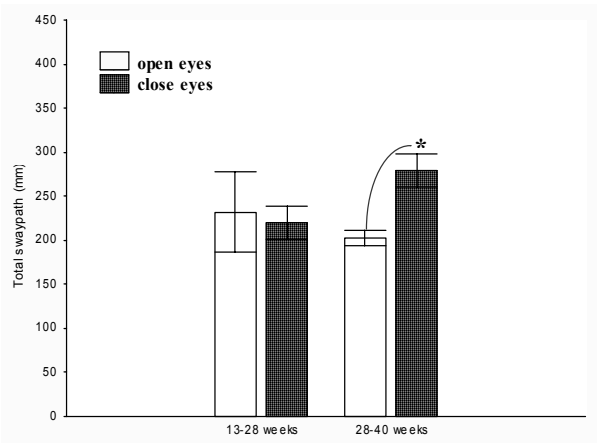

Fig. 2. *Sway path differences between the two periods of the pregnacy.*

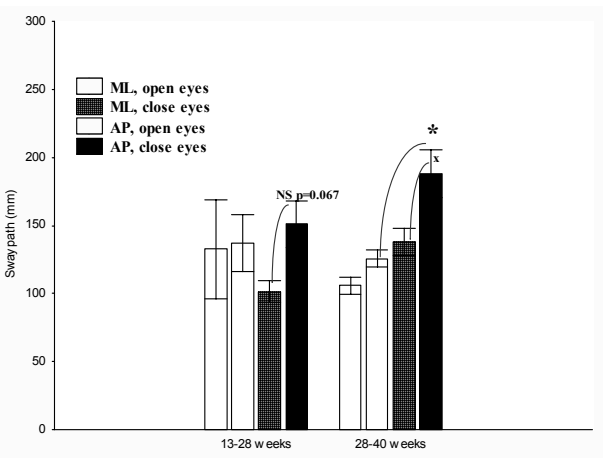

Fig. 4. *Sway path differences splitted into antero-posterior and lateral directions between the periods of pregnancy. (x,*,+: significant differences)*

direction may explain the higher injury risk of the anterior cruciate ligament. It could be advantageous to give more specific advice for body training during pregnancy. Some kinds of movements composed of more anterior-posterior kinetic components (stairs) can be more risky. During the second half of the pregnancy the hormonal influence is increased, the risk of injury is higher and more attention is needed. We shall perform further studies (the effects of oral contraceptives) to clarify the hormonal influence as a risk factor for injury during female sport activity.

ACKNOWLEDGEMENTS

The authors would like to thank Prof. Giuliano Cerulli and the staff of the Let People Move Biomechanical Laboratory in Perugia for showing us more biomechanical measuring methods and Prof. Béla Molnár G. from the University Department of Obstetrics and Gynaecology in Szeged for inviting

pregnant volunteers to participate in the study.

REFERENCES

1. Wojtys EM, Huston LJ, Boynton MD, Spindler KP, Lindenfeld TN. The effect of the menstrual cycle on anterior cruciate ligament injuries in women as determined by hormone levels. Am J Sports Med 2002;30(2):182-188.
2. Aydog ST, Hascelik Z, Demirel HA, Tetik O, Aydog E, Doral MN. The effects of menstrual cycle on the knee joint position sense: preliminary study. Knee Surg Sports Traumatol Arthrosc 2005; 13(8):649-53.
3. Braun SV, Beynnon BD, Johnson RJ, Sargent ME, Bernstein IM. Serum hormone levels at the time of ACL injury. MDACL Study Group March 2002.
4. Liu SH, Al-Shaikh RA, Panossian V. Primary immunlocalisation of oestrogen and progesterone target cells in the human ACL. J Orthop Res 1996; 14:526-33.
5. Yu WD, Panossian V, Hatch JD, Liu SH, Finerman GA. Combined effects of estrogen and progesterone on the anterior cruciate ligament. Clin Orthop 2001; 383:268–81.
6. Slauterbeck JR, Fuzie SF, Smith MP, Clark RJ, Xu K, Starch DW, Hardy DM. The menstrual cycle, sex hormones, and anterior cruciate ligament injury. J Athl Train 2002;37:275–8.
7. Slauterbeck JR, Pankratz K, Xu KT, Bozeman SC, Hardy DM. Canine ovariohysterectomy and orchiectomy increases the prevalence of ACL injury. Clin Orthop Relat Res 2004;429:301–5.
8. T. Bányai, G. Cerulli, M. Lorenzini, A. Liti, A. Archilletti. Effects of female's hormonal changes on joint laxity, neuromuscular balance during the menstrual cycle. 9th International Conference in Orthopaedics, Biomechanics and Sports Rehabilitation, Assisi, Abstract Volume 2005;278-9
9. Beynnon BD, Bernstein IM, Belisle A, Brattbakk B, Devanny P, Risinger R, Durant D. The effect of estradiol and progesterone on knee and ankle joint laxity. Am J Sports Med 2005;33:1298-304.
10. Carcia CR, Shultz SJ, Granata KP, Gansneder BM, Perrin DH. Knee ligament behaviour following a controlled loading protocol does not differ by menstrual cycle day. Clin Biomech (Bristol, Avon) 2004;19:1048–54.
11. Eiling E, Bryant ĆAL, Petersen Ć W, Murphy ĆA, Hohmann ĆE. Effects of menstrual-cycle hormone fluctuations on musculotendinous stiffness and knee joint laxity. Knee Surg Sports Traumatol Arthrosc 2007;15:126–32.
12. Janse de Jonge XA, Boot CR, Thom JM, Ruell PA, Thompson MW. The influence of menstrual cycle phase on skeletal muscle contractile characteristics in humans. J Physiol 2001;530(Pt 1):161-6.
13. Fridén C. Neuromuscular performance and balance during the menstrual cycle. 8th International Conference of Orthopaedics, Biomechanics, Sport's Rehabilitation 2004
14. Fridén C, Hirschberg AL, Saartok T, Backstrom T, Leanderson J, Renstrom P. The influence of premenstrual symptoms on postural balance and kinaesthesia during the menstrual cycle. Gynecol Endocrinol 2003; 17(6):433-9.

DISTAL TIBIAL-FIBULAR FRACTURES: TREATMENT WITH FIBULAR FIXATION AND LOCKED INTRAMEDULLARY NAILING

R. BUZZI, F. A. BERTINI[1], F. CECCHI[2] and F. GIRON

Orthopaedic Clinic, University of Florence, Firenze; [1]Orthopaedic Department, Ospedale Misericordia e Dolce, Prato; [2]Fondazione Don Carlo Gnocchi, Institute for Recovery and Care with Scientific Character, Firenze, Italy

Received August 6, 2008 – Accepted January 13, 2009

Locked intramedullary nailing of distal tibial-fibular fractures involves a risk of malalignment due to the lack of intimate contact between the nail and the endosteum. The purpose of this study was to evaluate the results of a technique based on fibular fixation and locked intramedullary nailing. We prospectively studied a consecutive series of 14 distal tibial-fibular fractures operated by a single surgeon. There were 12 (86%) males and 2 (14%) females with an average age of 48.7 years. Nine (64%) fractures were closed and 5 (36%) were open. Tibial fracture according to the AO classification was 42-A in 3 (21%) and 42-B in 11 (79%). Minimally displaced posterior or medial malleolar fractures were present in 2 (14%) cases. Open reduction and internal fixation of the fibula was performed first and followed by locked intramedullary nailing of the tibia. Distal locking was performed with 2 screws in 11 cases (79%) and 3 screws in 3 cases (21%). The patients were reviewed with an average follow-up of 27 months (range 13-61). An anatomic alignment of the fracture was achieved 12 (86%) cases. Two cases (14%) had a procurvatum within 5°. There were no soft tissue complications around the lateral approach. There was one (7%) delayed union and one (7%) nonunion which healed after nail removal and plating. According to the Johner and Wruhs criteria there were 7 (50%) excellent, 5 (36%) good, one (7%) fair and one (7%) poor result. The fair result was due to ankle stiffness and pain after an open injury. The poor result was due to the above mentioned nonunion. Preliminary fibular fixation significantly contributes to realignment of distal tibial-fibular fractures through the intact tibiofibular ligaments. Locked intramedullary nailing successfully stabilizes the tibial fracture without adding to the soft tissue trauma.

Fractures of the distal third of the leg are characterized by the frequent injury to the delicate soft tissue envelope. Effective treatment aims at stable fixation without additional soft tissue damage.

Cast treatment requires a prolonged immobilization and is prone to loss of reduction and decreased ankle motion (1). Frequent radiographs are required during the early healing phase and cast wedging may be necessary. External fixation using monoaxial, hybrid, or Ilizarov type fixators is often complicated by pin track infections, delayed union, malalignment and loss of ankle motion (2-4). Traditional open reduction and internal fixation of

Key words: tibial-fibular fracture, osteosynthesis, intramedullary nailing

Mailing address:
Dr. Roberto Buzzi,
Clinica Ortopedica dell'Università di Firenze.
Largo P.Palagi 1,
5013, Firenze, Italy
Tel: ++39 349 6372854 Fax: ++39 055 4224063
email: rbuzzi@unifi.it

1973-6401 (2009)

distal tibial-fibular fractures requires an extensive exposure with possible devascularization of bone, wound dehiscence and infection (5-6). To overcome these problems minimally invasive plating techniques have been developped. Subcutaneous insertion of the plate (7-8) may be helpful in reducing complications, but it is technically demanding and its use is still not widespread.

Locked intramedullary nailing (IMN) is widely used in the treatment of displaced tibial-fibular fractures including those with soft tissue and open injuries (9-15). Fractures of the middle third of the diaphysis are easely aligned with this technique because of the intimate contact between the nail and the endosteum. However difficulties increase when the fracture is located close to the proximal or distal metaphysis. Fractures of the proximal third of the tibial shaft treated with IMN are notoriously prone to malalignment, delayed union and nonunion (16-17). Nailing of fractures of the distal third of the tibia bears some risk of instability and malalignment, more frequently in valgus (Fig. 1), due to widening of the medullary canal distal to the istmus. Fibular fixation has been suggested to decrease the incidence of malalignment and to improve stability of these fractures (18-19). However there is a lack of information about the effectiveness of this method and its complications.

The purpose of this study is to evaluate the results of fibular fixation and IMN in a consecutive series of 14 distal tibial-fibular fractures.

MATERIALS AND METHODS

In the period between 01/2002 and 05/2007 fourteen patients with a distal tibial-fibular fracture were operated by a single surgeon (RB) using fibular fixation and locked IMN. Their data were prospectively collected.

There were twelve (86%) males and two (14%) females, with an average age of 48.7 years (range 19-69). Ten (71%) fractures involved the right leg and four (29%) the left. In one patient the injured limb was affected by the sequelae of a poliomyelitis with equinus foot deformity. Twelve (86%) fractures were caused by a high energy trauma: five (36%) patients were involved in a motorcycle accident, 5 (36%) were automobile-pedestrians accidents, one (7%) patient was involved in a car accident and one (7%) patient was victim of an assault with a cane. Two (14%) fractures were due to low energy trauma during a fall to the ground level. Associated muscoloskeletal injuries were present in six (43%) patients and included one ipsilateral open patella fracture, one facial fracture, one C2 and one L2 vertebral body fractures, one open forefoot injury and one extensive soft tissue injury to the opposite leg.

Nine (64%) fractures were closed. The soft tissue injury was classified (20) grade I in one fracture and grade II in eight fractures. Five (36%) fractures were open, and were classified (21-22) grade II in 3 cases and IIIA and grade IIIB in one case each. There were no neurologic injuries or fully developped compartment syndromes. One occlusion of the tibialis anterior artery at the fracture level was diagnosed by ultrasonography evaluation.

All fractures were in the distal third of the leg. Tibial fracture type according to the AO classification (23) was 42-A2 in one (7%) case, A3 in 2 (14%), B1 in one (7%), B2 in two (14%) and B3 in 8 (57%). Fibular fracture classification was A3 in 5 (36%) cases, B2 in 3 (21%), B3 in 4 (29%), C2 and C3 in one case (7%) each. All the fibular fractures were in the distal third of the bone close to the tibial fracture level. One (7%) patient had an associated posterior malleolar fracture, and one (7%) patient had an associated posterior and medial malleolar fractures.

Antitromboembolic prophilaxis with low molecular weight heparin was started at admission and continued up to full recovery of mobility. Antibiotic profilaxis was administered preoperatively (on admission in open injuries) and continued for 48 hours. We used cephazoline in closed fractures and we added tobramicine in grade III open fractures. Open fractures underwent debridment, lavage and osteosynthesis within 8 hours. Closed fracture were operated 2-12 days after the injury (5.8 days on average).

Fibular fixation was performed first using a lateral approach in front of the peroneal muscles. In 13 (93%) cases plate fixation was employed with a 1/3 tubular plate (10 cases), a LCP 3.5 mm (2 cases) or a LC-DCP 3.5 mm plate (1 case) (Synthes, Oberdorf, Switzerland). In one case (7%) with a transverse fracture of the fibula we employed a retrograde intramedullary Kirschner wire. At the end of the operation the lateral skin incision was sutured in 13 (93%) cases. In one patient (7%) with moderate swelling and skin tension the plate was covered by advancing the peroneal muscles. A split-thickness skin graft was placed over the muscle. Osteosinthesis of the posterior and medial malleoli was achieved with lag screws.

The tibial nailing was performed through a medial parapatellar approach in 10 (71%) cases, through a lateral parapatellar approach in 3 (21%) and through the defect offered by an open patellar fracture in one (7%) case. A proximal tibial entry hole was produced in line with

the medullary canal. Reduction of the tibial fracture was improveded using manual traction, the femoral distractor (Synthes, Oberdorf, Switzerland) or with the percutaneous application of pointed clamps. The reamer guide wire was advanced into the tibia until it reached the subcondral bone of the tibial plafond. Attention was paid to achieve a central position of the tip of the guide wire in the distal tibia as visualized in the anteroposterior and lateral views. The canal was reamed in all the cases. An U.T.N., C.T.N. or Expert tibial nail (Synthes, Oberdorf, Switzerland) was used in 9 cases (64%) and a T2 nail (Stryker, Mahwah NJ, USA) in 5 (36%). Distal locking was performed with 2 screws in 11 cases (79%). In 3 cases (21%) a third screw was added. Proximal locking was static in 8 cases (57%) and dynamic in 6 (43%), according to the stability of the fracture.

Postoperatively a posterior plaster splint was applied to prevent the development of an equinus contracture. The soft tissue defect in open fractures was treated with delayed primary closure in 3 (21%) cases, with a split thickness skin graft and a soleus rotational muscle flap in one case each (7%). Two patients, one with a open and one with a closed fracture, underwent an autologous bone graft from the iliac crest 6 weeks postoperatively to treat a bone defect. Both achieved uneventful union. One open fracture underwent dinamization 3 months postoperatively and healed uneventfully.

Mobilization of the foot, ankle and knee were started early in the postoperative period. Touch-down weight bearing was allowed as soon as the soft tissues could tolerate the dependent position. Progressive weight bearing was encouraged after the first 6 weeks according to callus formation.

There were no intraoperative or postoperative complications in this series. All the patients were personally followed at 6-8 week intervals until fracture healing.

The results at follow-up were classified according to the Johner and Wruhs four-level scale [24]. Parameters evaluated included nonunion, osteitis, amputation, neurovascular disturbances, deformity, knee, ankle and subtalar joint mobility, pain, gait and activity level. Preinjury and follow-up activity levels were evaluated according to Tegner (25). Patients were asked to rate their satisfaction with the results of surgery as completely satisfied, partially satisfied, unsatisfied and totally unsatisfied.

Anterior-posterior and lateral radiographs were obtained at postoperative and follow-up visits. The tibial fracture was considered united when there was evidence of bony trabeculae crossing the fracture in three of the four zones around the nail and the patient walked without pain at the fracture site. Malignement was defined as more than 5 degrees of angular deviation in the frontal and/or in the sagittal plane. Rotational malalignement was evaluated clinically by means of the thigh-foot angle.

RESULTS

The patients were personally reviewed with clinical and radiological evaluation with an average follow-up of 27.1 months (range 13-61)

Time to union was 7.1 months on average (range 3-14). Twelve fractures (86%) healed within 8 months. One fracture (7%) healed in 12 months and was classified as delayed union. One fracture (7%) progressed to nonunion and required nail removal and plate fixation 9 months postoperatively. All fibular fractures showed evidence of union at follow up.

Two patients (14%) complained of knee pain in the operated limb. One patient sustained an open fracture of the patella. The second patient complained of mild knee pain while walking downhill. No patient reported pain at the fracture site.

The activity level according to Tegner rated 5.7 points on average (range 2-9) before the injury and 4.6 points (range 0-8) at follow-up. Seven (50%) patients recovered their preinjury activity level and 5 (36%) patients lost 1 point. The patient with the associated open patellar fracture lost 6 points due to the knee injury with residual patellofemoral pain and crepitation. One patient with an open injury lost three points.

Thirteen (93%) patients were completely satisfied with the outcome of surgery while one (7%) was satisfied with reservations.

Thirteen (93%) patients returned to the preinjury work within 6.2 months on average (range 2-13 months). One patient (7%) did not return to work because af ankle pain and stiffness.

Soft tissues were healed and stable in all patients. Eleven (79%) patients recovered a complete range of motion at the knee and at the ankle. The patient with associated patellar fracture lost 10° of knee flexion, 10° of ankle plantar flexion and 20% of pronosupination. A second patient lost 20° of knee flexion, 20° of ankle dorsiflexion, 10°of plantar flexion and 40% of subtalar motion. A third patient with an open fracture and a complex forefoot injury lost 5° of ankle dorsiflexion and 20% of subtalar motion.

Fig. 1. ***A)*** *Anteroposterior radiograph of a distal tibial-fibular fracture.* ***B)*** *Following treatment with locked intramedullary nailing union with valgus malalignment is evident.*

Fig. 2. ***A and B)*** *Anteroposterior and lateral radiographs of a distal tibial-fibular fracture in a 34 year old man following an automobile accident.* ***C)*** *Intraoperative image shows that anatomic reduction of the tibia was possible after fibular fixation and pointed clamp application.* ***D and E)*** *Anteroposterior and lateral radiographs at follow-up.*

Evaluation of alignment on follow-up radiographs showed no cases of malalignement of the tibia in the frontal plane and two (14%) cases of procurvatum within 5°. There were no cases of leg length discrepancy or rotational malalignment.

The final result according to Johner and Wruhs (24) was excellent in 7 (50%) cases, good in 5 (36%), fair and poor in one (7%) case each. The fair result was due to ankle stiffness and pain following an open injury. The poor result was due to the previously mentioned nonunion. At the final follow-up after reoperation the patient with nonunion was healed and scored excellent.

DISCUSSION

Locked IMN is a widely used techinique for treating both closed and open diaphyseal fractures of the tibia. However its use in distal third tibial-fibular fractures is more challenging and controversial (26-31). Concerns include a less than perfect alignment of the fracture, the insufficient stability of fracture fixation, the risk of propagation of the fracture into the ankle joint, and delayed union or nonunion with breakage of the nail and locking screws.

In this series of 14 distal tibial-fibular fractures

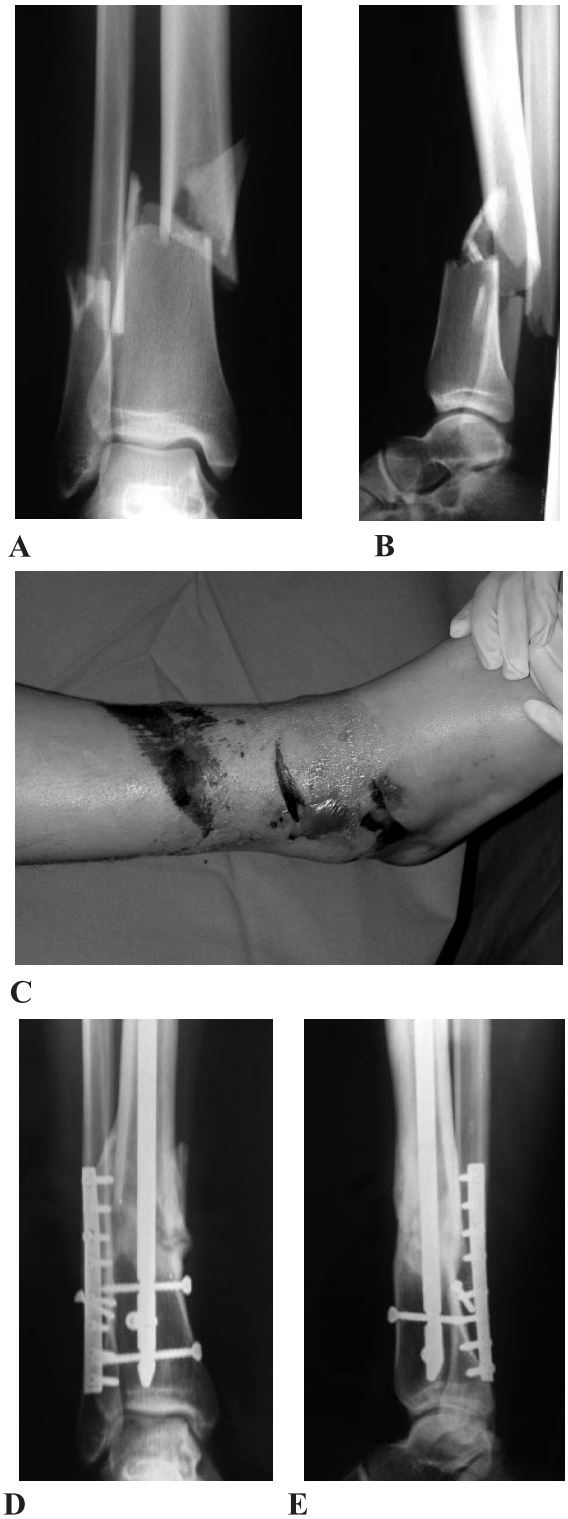

Fig. 3. ***A and B)*** *Anteroposterior and lateral radiographs of a distal tibial-fibular fracture in a 20 year old male with comminution and displacement.* ***C)*** *Significant grade 2 soft tissue injury is evident.* ***D and E)*** *Two-year follow-up radiographs show good healing with minor procurvatum.*

preliminary fibular fixation and IMN were an effective and convenient technique. An anatomic alignment was achieved in 12 (86%) cases and it was within 5° in 2 (14%). There were no cases of loss of alignment during the postoperative period. A nonunion developped in one (7%) fracture and was successfully treated with nail removal and plating.

This series is admittently small. However the patients were uniformly treated by a single surgeon and the data were prospectively collected.

The soft tissue coverage around the distal tibia is delicate and the consequences of unjudicious handling of soft tissues are well known. In this respect, IMN of distal tibio-fibular fractures has the advantage of full respect of the soft tissues. Intramedullary nailing is also advantageous to treat segmental tibial fractures and fractures with a proximal extension. A recognized disadvantage of tibial nailing is the possible occurrence of anterior knee pain (32-34).

The prerequisite to consider IMN of a distal metaphyseal fracture of the tibia is the ability to reduce the fracture and mantain the reduction until the nail insertion and locking is completed. The introduction of the implant will not assist in reducing the fracture due to the lack of contact between the thin nail and the large metaphysis. Several techniques of fracture reduction have been suggested, including percutaneous clamps, insertion of Schanz pins as joysticks, the use of the femoral distractor, the temporary application of a small fragment plate with unicortical screws (in open fractures), the use of blocking screws (35), and open reduction and plate fixation of the fibula (18-19). Often more than one method is employed to achieve an anatomical alignement (Fig. 2).

The use of fibular plating was described by Ruëdi and Allgower (36) as the first step in surgical reconstruction of pilon fractures. The application to distal metaphyseal tibial fractures is an extension of this original observation. The tibiofibular ligaments are frequently spared in distal metaphyseal tibial fractures. Therefore fibular reduction and fixation assists in tibial fracture reduction.

The lateral approach to the malleolus and distal fibula is straightforward. Reduction and fixation of the fibula has to be precise to allow exact realignment of the tibia. In the presence of a complex fracture

of the fibula anatomic reconstrucion of length and rotation may be time consuming. Healing of the surgical incision over the fibula was uneventful in every case. When swelling prevents a primary skin suture, the peroneal muscles can be advanced over the plate and covered with a split-thickness skin graft.

We did not observe any case of loss of alignement in the healing phase, although touch-down weight bearing and mobilization were allowed early. Fibular plating may have contributed to this favourable outcome. Fibular fixation has been shown to increase the stiffness of a diaphyseal tibial defect stabilized with external fixation (37). Weber et al (38) confirmed that plating of the fibula can decrease motion across a diaphyseal tibial defect stabilized with an external fixator; but when a more rigid intramedullary locked nail was used, fibular plate did not contribute to further stability. Kumar et al (39) found that fibular plate fixation increased the rotational stability of distal tibial fractures compared with that provided by IMN alone, but the difference lost significance as the applied torque was increased.

New nail designs have multiplanar locking screws close to the tip of the nail. They are useful to stabilize short metaphyseal segments. The use of a minimum of two distal screws, one in the frontal and one in the sagittal plane, is recommended. Three screws, 2 in the frontal and 1 in the sagittal plane should be used if possible. Locking screws of adequate diameter and strength are necessary to prevent screw breackage, since high stresses are expected in distal fractures.

It is well recognized that tibial fractures with an intact fibula have a tibiofibular length discrepancy which may lead to delayed union, malunion or non union (40). Theoretically, plating the fibular fracture and nailing the tibial fracture may lead to similar problems. Fibular plating restores the length and alignment but may prevent impaction at the tibial fracture site enhancing the development of delayed union or nonunion In this series we observed only one (7%) case of nonunion which required further surgery.

In conclusion we feel that fibular fixation and IMN of distal tibial-fibular fractures is a valid technique which prevents malalignment and respects the soft tissue envelope (Fig. 3). Preliminary fibular fixation can also be helpful before minimally invasive plating of the tibia or application of an external fixator.

REFERENCES

1. Sarmiento A, Gersten LM, Sobol PA et al. Tibial shaft fractures treated with functional braces. Experience with 780 fractures. J Bone Joint Surg 1989;71B: 602-9
2. Bonar SK, Marsh JL. Unilateral external fixation for severe pilon fractures. Foot Ankle 1993;14: 57-64.
3. Anglen JO. Early outcome of hybrid external fixation for fracture of the distal tibia. J Orthop Trauma 1999; 13: 92-7
4. Tucker HL, Kendra JC, Kinnebrew TE. Management of unstable open and closed tibial fractures using the Ilizarov method. Clin Orthop 1992;280:125-35.
5. Teeny SM, Wiss DA. Open reduction and internal fixation of tibial plafond fractures. Variables contributing to poor results and complications. Clin Orthop Relat Res 1993;292:108-17.
6. Wyrsch B, McFerran MA, McAndrew M et al. Operative treatment of fractures of the tibial plafond. A randomized, prospective study. J Bone Joint Surg 1996;78A:1646-57.
7. Helfet DL, Shonnard PY, Levine D et al. Minimally invasive plate osteosynthesis of distal fractures of the tibia. Injury 1997; 28 (suppl.1):A 42-8
8. Oh CW, Kyung HS, Park JH et al. Distal tibia metaphyseal fractures treated by percutaneous plate osteosynthesis. Clin Orthop Rel Res 2003;408:286-91.
9. Keating JF, O'Brien PJ, Blachut PA et al. Locking intramedullary nailing with and without reaming for open fractures of the tibial shaft. A prospective, randomized study. J Bone Joint Surg 1997;79A:334-41.
10. Blachut PA, O'Brien PJ, Meek RN et al. Interlocking intramedullary nailing with and without reaming for the treatment of closed fractures of the tibial shaft. A prospective randomized study. J Bone Joint Surg 1997;79A:640-6.
11. Krettek C, Schandelmaier P, Tscherne H. Nonreamed interlocking nailing of closed tibial fractures with severe soft tissue injury. Clin Orthop 1995;315:34-47.
12. Court-Brown CM, Christie J, McQueen MM. Closed intramedullary tibial nailing. Its use in closed and

type I open fractures. J Bone Joint Surg 1990; 72B: 605-11.
13. Court-Brown CM, McQueen MM, Quaba AA et al. Locked intramedullary nailing of open tibial fractures. J Bone Joint Surg 1991;73B:959-64
14. Whittle AP, Russel TA, Taylor JC et al. Treatment of open fractures of the tibial shaft with the use of interlocking nailing without reaming. J Bone Joint Surg 1992;74A:1162-71
15. Bonatus T, Olson SA, Lee S et al. Nonreamed locking intramedullary nailing for open fractures of the tibia. Clin Orthop 1997;339:58-64
16. Freedman EL, Johnson EE. Radiographic analysis of tibial fracture malalignment following intramedullary nailing. Clin Orthop 1995;315:25-33.
17. Lang GJ, Cohen BE, Bosse MJ et al. Proximal third tibial shaft fractures. Should they be nailed? Clin Orthop 1995;315:64-74.
18. Schweighofer F, Fellinger M, Wildburger R. Combined tibial and ankle joint fractures. Unfallchirurg 1992;95(1):47-9.
19. White RR, Babikian GM. Tibia Shaft. In AO principles of fracture management. T. P. Ruedi, W. M. Murphy, eds. Thieme, Stuttgard, 2000; p 519-36.
20. Oestern HJ, Tscherne H. Pathophysiology and classification of soft tissue injuries associated with fractures. In Fractures with soft tissue injuries. H. Tscherne, L. Golzen. Springer-Verlag, Berlin, 1994; p 1-9.
21. Gustilo RB, Anderson JT. Prevention of infection in the treatment of one thousend and twenty-five open fractures of long bones: retrospective and prospective analyses. J Bone Joint Surg 1976;58A (4):453-8.
22. Gustilo RN, Mendoza RM, Williams DN. Problems in the management of type III (severe) open fractures: a new classification of type III open fractures. J Trauma 1984;24(8):742-6.
23. Muller ME, Nazarian M, Koch P et al. Eds. The comprehensive classification of fractures of long bones. Springer-Verlag, Berlin, 1990.
24. Johner R, Wruhs O. Classification of tibial shaft fractures and correlation with the results of rigid internal fixation. Clin Orthop 1983;178:7-25.
25. Tegner Y, Lysholm J. Rating systems in the evaluation of knee ligament injuries. Clin Orthop Relat Res Sep 1985;198:43-9.
26. Konrath G, Moed BR, Watson JT et al. Intramedullary nailing of unstable diaphyseal fractures of the tibia with distal intrarticular involvement. J Orthop Trauma 1997;11:200-5.
27. Mosheiff R, Safran O, Segal D et al. The unreamed tibial nail in the treatment of distal metaphyseal fractures. Injury 1999;30:83-90.
28. Robinson CM, McLauchlan GJ, McLean JP et al. Distal metaphyseal fractures of the tibia with minimal involvement of the ankle. Classification and treatment by locked intramedullary nailing. J Bone Joint Surg 1995;77B:781-7.
29. Tyllianakis M, Megas P, Giannikas D et al. Interlocking intramedullary nailing in distal tibial fractures. Orthopedics 2000;23:805-8.
30. Im GI, Tae SK. Distal metaphyseal fractures of tibia: a prospective randomized trial of closed reduction and intramedullary nail versus open reduction and plate and screws fixation. J Trauma 2005;59 (5): 1219-23.
31. Nork SE, Schwartz AK, Agel G, et al. Intramedullary nailing of distal metaphyseal tibial fractures. J Bone Joint Surg 2005;87A;1213-21.
32. Court-Brown CM, Gustilo T, Shaw AD. Knee pain after intramedullary tibial nailing: its incidence, etiology and outcome. J Orthop Trauma 1997;11: 103-5.
33. Toivanen JA, Vaisto O, Kannus P et al. Anterior knee pain after intramedullary nailing of fractures of the tibial shaft. A prospective randomized study comparing two different nail-insertion techniques. J Bone Joint Surg 2002;84A:580-5.
34. Keating JF, Orfaly R, O'Brien PJ. Knee pain after tibial nailing. J Orthop Trauma 1997;11:10-3.
35. Krettek C., Stephan C, Schandelmaier P The use of Poller screws as blocking screws in stabilizing tibial fractures treated with small diameter intramedullary nails. J Bone Joint Surg Br 1999; 1(6): 963-8.
36. Ruedi T, Allgower M. Fractures of the lower end of the tibia into the ankle joint. Injury 1969;1:92-9.
37 Morrison KM, Ebraheim NA, Southworth SR et al. Plating of the fibula. Its potential value as an adjunct to external fixation of the tibia. Clin Orthop 1991; 266:209-13.
38. Weber TG, Harrington RM, Henley B, et al. The role of fibular fixation in combined fractures of the tibia

and fibula: a biomechanical investigation. J Orthop Trauma 1997;11(3):206-11.
39. Kumar A, Charlebois SJ, Cain EL, et al. Effect of fibular plate fixation on rotational stability of simulated distal tibial fractures treated with intramedullary nailing. J Bone Joint Surg 2003; 85A: 604-8.
40. Teitz CC, Carter DR, Frankel VH. Problems associated with tibial fractures with intact fibulae. J Bone Joint Surg 1980;62A(5):770-6.

THE EFFECT OF CAM FEMOROACETABULAR IMPINGEMENT ON HIP MAXIMAL DYNAMIC RANGE OF MOTION

M. J. KENNEDY, M. LAMONTAGNE[1] and P. E. BEAULÉ [2]

School of Human Kinetics, [1] Department of Mechanical Engineering, [2]Division of Orthopaedic Surgery, University of Ottawa, Canada

Received August 29, 2008 – Accepted November 17, 2008

Cam femoroacetabular impingement (FAI) is caused by decreased concavity of the femoral head-neck junction which results in a jamming of the proximal femur into the acetabulum within normal range of motion (ROM). This condition is known to decrease hip ROM, but only passive hip mobility has been quantitatively studied. It is important to determine the effect of cam FAI on self-generated dynamic ROM in order to ascertain its influence on hip functionality. This study quantified the affect of cam FAI on total dynamic hip ROM in each plane, and on peak angular displacement in flexion, extension, adduction, abduction and internal and external rotation with the hip flexed at 90º. A cam impingement group (n = 17) was compared to a matched control group (n = 14) using between-group one-way ANOVAs. The FAI group had a decreased flexed internal rotation, external rotation and total transverse ROM, as well as decreased hip abduction and total sagittal ROM compared to the matched control group.

Femoroacetabular impingement (FAI) is a relatively new clinical diagnosis (1), which is gaining recognition in the medical community as a cause of hip pain in young adults (2-3). Due to the fact that FAI is a relatively new diagnosis, a limited number of studies have been undertaken to define the multifaceted effects of this condition, contributing to its difficulty to diagnose with certainty (3). However, the database on FAI is rapidly growing due to its current popularity in research (1). One reason for the increased attention generated by FAI is its potential as a cause of idiopathic hip osteoarthritis (OA) (4-9). This relationship with coxa arthritis has increased the urgency to develop surgical strategies to correct FAI before the onset of hip OA (10-17). However, it is also imperative to increase our understanding of how FAI affects hip function in order to increase the diagnostic criteria for this evasive condition and to develop conservative treatments, especially with the lack of long-term surgical results (1).

FAI is defined by an anatomical morphology of the acetabulum and/or the proximal femur which causes abnormal contact at the hip joint. Pincer impingement is related to overcoverage of the acetabulum as with acetabular retroversion and coxa profunda. Cam impingement is caused by decreased concavity of the femoral head-neck junction, most commonly in the anterosuperior region (12-13, 18-19). Pincer impingement is caused by a linear abutment of the acetabular labrum with the proximal femur (20). Decreased femoral head-neck concavity causes a jamming of the femoral head into the acetabulum at the limits of range of motion (ROM) during assisted flexion and internal rotation (20-21). The pain generated by cam impingement is thought to occur after the onset of cartilage damage, caused by "outside-in" damage of the acetabular labral-chondral junction (18). Because of the different

Key words: Biomechanics, Kinematics, Femoroacetabular Impingment, Hip, Range of Motion

Mailing address: Prof. Mario Lamontagne,
University of Ottawa,
School of Human Kinetics,
K1N 6N5 Ottawa, On, Canada
Tel: ++1 613 562 5800, ext. 4258
Fax: ++1 613 562 5149
e-mail: mlamon@uottawa.ca

1973-6401 (2009)

proposed pathomechanism between cam and pincer FAI, it was necessary to only focus on one type of impingement to avoid having more than one independent variable. This study only assesses the dynamic ROM of cam FAI.

Depending on the location of bone deformation, FAI patients with cam impingement show a decreased passive hip ROM as compared to healthy controls in flexion (19, 22), abduction (19), internal rotation with hip flexed at 90º (19, 22-23) and external rotation with hip flexed at 90º (19). Similar results were also found in two computer-simulated ROM studies based on the CT scans (24-25) of participants with FAI, and matched controls, with FAI patients having decreased simulated hip flexion, abduction and internal rotation. Other studies show a low passive ROM in patients with cam FAI, without comparing to a control group (17, 26-27). Finally Philippon et al. (28) found that unilateral FAI patients had decreased passive hip flexion, abduction, adduction, internal rotation and external rotation compared to their contralateral leg. However, there are limitations to these studies. There was no mention of the measuring device used to quantify passive ROM in any of the aforementioned non-simulated studies except for the study by Philippon et al (28). Furthermore, the computer-simulated ROM studies only accounted for bone on bone contact, greatly exaggerating hip mobility, and neglecting the influence of all soft tissues on hip mobility. Finally, these studies only assessed the influence of hip impingement on the simulated, passive or assisted, as opposed to the self-generated dynamic movement of the hip.

In order to predict which activities to avoid in developing a conservative treatment it is imperative to determine how FAI affects the functional mobility of the hip. There are some activities known to cause hip pain in people with FAI such as: squatting or prolonged sitting, stair climbing, excessive walking and athletic activities requiring a large ROM (3-4, 6, 20, 29). However, in order to predict other exacerbating activities it is necessary to decipher which hip movements are limited, and to quantify the maximum attainable ROM. Furthermore, determining the effect of FAI on self-generated dynamic hip ROM may aid in the diagnosis of this elusive condition.

The purpose of this study was to determine the effect of cam FAI on maximal total hip ROM in each plane, and on peak hip flexion, extension, adduction, abduction, and internal and external rotation with the hip flexed at 90º. According to the dominant trends in passive ROM limitations (19, 22-25) it is hypothesized that cam FAI will have decreased self-generated dynamic flexion, internal rotation, and abduction, with no other dynamic hip ROM variables being significantly different.

MATERIALS AND METHODS

Participants

Two groups of participants were recruited: a group of patients diagnosed with cam hip impingement, and a matched control group. The FAI participants were recruited after having a positive impingement test, visible cam morphology on anteroposterior (A/P) and Dunn view radiographs (6, 26, 30-31). The alpha angle defined by Notzli (23) was measured on each hip with a value greater than 50.5 degrees diagnostic of *Cam* type FAI. All matched control participants had no history of serious lower limb injury or surgery, and had spherical femoral heads which were assessed by an A/P radiograph (31). Participants from both groups were excluded if hip OA was visible on the x-rays or if they had substantial hip joint space narrowing.

A total of 37 participants volunteered in this study. Eighteen participants diagnosed with cam FAI, and 19 age, gender and BMI matched control participants. The sample size was determined using a power analysis based on pilot data from the first 10 volunteers (five FAI and five control participants) to determine the effect size, and used peak internal rotation with the hip flexed at 90º as the key dependent variable. A total sample size of 26 was calculated using G*POWER version 3 (Faul, F. & Erdfelder, E., Bonn, Germany) (32) with an alpha value set at 0.05, and a minimal power set at 80%. This calculated sample size was the minimum required participants to achieve desired power based on our pilot data of maximal dynamic internal rotation, however; since we were looking for other variables as well, a larger sample size was chosen to maximize the statistical power of the study. Before participating in the study, which was approved by the Ottawa Hospital Research Ethics Board, and the University of Ottawa Health Sciences and Science Research Ethics Board, all participants signed an informed written consent. Five of the original control participants were excluded. It was determined that three of them had at least one aspherical femoral head based on an A/P radiograph, and the other two could not have the necessary screening x-rays. Furthermore, one

participant of the FAI group had to be excluded due to the presence of hip OA. Consequently, the remaining samples consisted of 14 control participants and 17 FAI participants (Table I). Even with the diminished sample size, we still had more participants than the power analysis required. All FAI participants had *Cam* type deformities with only one symptomatic hip. All participants filled out a Western Ontario McMaster Osteoarthritis Index (33) (WOMAC) questionnaire to control for hip pain, function and stiffness.

MATERIALS

Three-dimensional kinematics of dynamic ROM was collected using seven VICON MX-13 cameras (VICON, Los Angeles, CA USA) at 200 Hz with retro-reflective markers placed on anatomical landmarks according to a modified Helen-Hayes marker-set (34). A support frame was constructed to give stability to the participants during dynamic hip ROM trials**.**

Procedure

Participants were asked to put on a skin-tight suit and performed a stretching warm-up routine. After the stretching warm-up, participants completed a sit and reach flexibility test, had retro-reflective markers placed on anatomical landmarks, and underwent anthropometric measurements. Thereafter participants performed a series of maximal dynamic hip ROM trials. Participants stood upright holding onto a support frame while they maximally swung their leg back and forth five times in each plane at a self selected speed. Hip ROM movements consisted of maximal dynamic flexion and extension, adduction (with the mobile leg in front of the support leg) and abduction, and internal and external rotation (while flexed at 90 degrees) (Fig. 1). Movements in each plane were completed 5 times for each participant.

Data Analysis

Lower limb 3-D kinematics were calculated according to the methods explained by Kadaba et al. (34-35) and Davis et al. (36), using VICON Workstation (VICON, Los Angeles, CA USA) processing software. Hip joint angles were based on local Euler coordinate systems as defined by the aforementioned studies. Joint and segment angles were zeroed based on each participant's neutral position as determined by a standing static trial where feet were parallel and facing anteriorly approximately shoulder width apart. However, for the flexed internal and external rotation trials, the transverse hip angle was zeroed based on its transverse angle when the hip was flexed to 90° and the midline of the tibia was orthogonal to the line connecting the left and right anterior superior iliac spines of the pelvis when viewed down the axis of the femur (Fig. 2).

The kinematic variables measured in the dynamic ROM trials consisted of the peak angular displacements and total ROM of the hip in each plane. Peak angular displacement was defined as the largest hip angle achieved in flexion, extension, abduction, adduction, and internal and external rotation. The maximum range was calculated based on the addition of the two opposite maximums in each plane. Of the five dynamic ROM trials for each participant, the three largest peak angular displacements and corresponding ranges were averaged to determine maximum angles and total range in each plane. This was done to ensure that the maximal values were not attenuated by a few poor trials. These were then ensemble averaged for both groups and compared.

Statistical Analysis

One-way between-subjects ANOVAs ($\alpha = 0.05$) were run for all dependent variables in order to ascertain significant differences between the control group and the FAI group**.** The dependent variables tested between groups were: total sagittal ROM, total frontal ROM, total transverse ROM (with the hip flexed at 90º), peak flexion, peak extension, peak adduction, peak abduction, flexed internal rotation and flexed external rotation. The dependent variables that were significantly different between the two groups had additional ANCOVAs ($\alpha = 0.05$) run with flexibility as a covariate. Flexibility was determined by the sit-and-reach test score, and was added as a covariate to minimize the influence of muscular flexibility on dynamic ROM.

RESULTS

The FAI group had significantly lower peak hip internal rotation ($p = 0.005$) peak hip external

Table I. *Participant characteristics. Mean ± standard deviation.*

Condition	Number of Participants	Age (years)	BMI (kg/m^2)	WOMAC	Flexibility
Control	14 (8 males)	34.2 ± 9.5	23.0 ± 2.3	99.9 ± 0.3	27.2 ± 9.8
Cam FAI	17 (10 males)	35.5 ± 10.6	23.0 ± 2.3	77.3 ± 15.6	21.1 ± 7.5

Table II *Average values from the dynamic ROM significant findings. Mean ± standard deviation.*

Dependent Variable	Group	Mean Value (± SD)	F-Value	P-Value
Peak Flexion	Control	113.9 ± 9.4	1.467	0.236
	Cam FAI	109.8 ± 9.6		
Peak Extension	Control	26.6 ± 5.1	4.050	0.054
	Cam FAI	21.2 ± 9.0		
Total Sagittal ROM	Control	140.5 ± 9.0	5.163	0.031
	Cam FAI	130.9 ± 13.5		
Peak Abduction	Control	47.5 ± 5.7	10.773	0.003
	Cam FAI	38.3 ± 9.1		
Peak Adduction	Control	23.2 ± 7.5	0.235	0.632
	Cam FAI	24.4 ± 5.9		
Total Frontal ROM	Control	70.7 ± 12.2	3.307	0.079
	Cam FAI	62.7 ± 12.3		
Peak Internal Rotation (at 90º of hip flexion)	Control	12.4 ± 4.8	9.438	0.005
	Cam FAI	7.9 ± 3.4		
Peak External Rotation (at 90º of hip flexion)	Control	26.0 ± 7.0	7.722	0.009
	Cam FAI	20.3 ± 4.5		
Total Transverse ROM (at 90º of hip flexion)	Control	38.5 ± 9.7	12.077	0.002
	Cam FAI	28.2 ± 6.7		

rotation ($p = 0.009$) and total transverse hip ROM ($p = 0.002$) with 90º of hip flexion (Fig. 3), significantly lower peak hip abduction ($p = 0.003$) (Fig. 4), and significantly lower total sagittal hip ROM ($p = 0.031$) (Fig. 5) than the control group. None of the other dynamic ROM variables were significantly different. However, there was a trend for the FAI group to display a lower peak hip extension ($p = 0.054$), and lower total hip frontal ROM ($p = 0.079$) compared to the control group. Refer to Table II for the mean values of each finding.

DISCUSSION

Dynamic ROM

It has been well documented that cam FAI causes a decrease in passive hip ROM (17, 19, 22, 26-28), and produces bony limitations within the normal range of motion (24-25). Furthermore, it is not uncommon for patients to notice limited hip motion even before the onset of pain (22), indicating a loss of functional mobility. The limited mobility and joint damage characteristic of cam FAI is caused by premature abutment of the femoral head-neck junction with the acetabular rim, and is more dependent on extreme hip mobility than on axial loading (4, 19-20). Since the jamming of the abnormal femoral head-neck junction into the acetabulum that causes joint damage occurs during self-generated dynamic hip movements (3-4, 6, 20, 29), it is important to measure the extent to which active dynamic ROM is affected by FAI. This information will allow for a deeper understanding of cam impingement, and is essential for predicting which movements will exacerbate the condition in developing conservative treatments and could add to diagnosis criteria for this

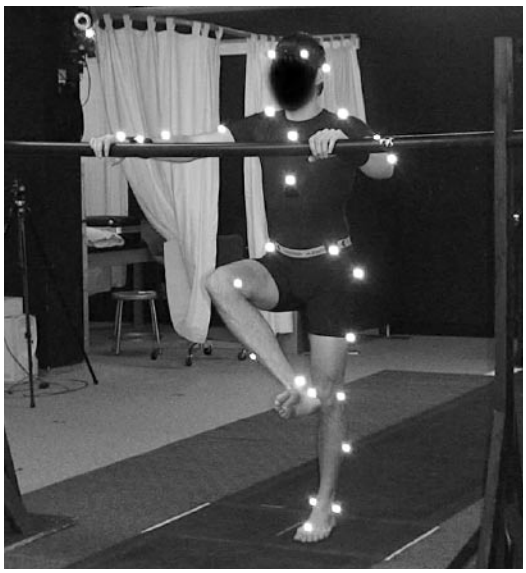

Fig. 1. *Instrumented participant performing dynamic ROM trial (external rotation at 90º of hip flexion) while holding on to support frame.*

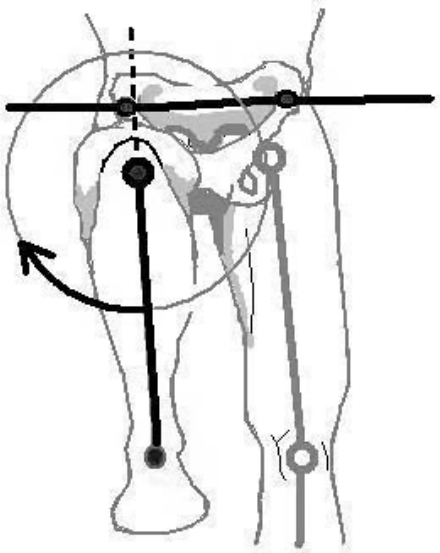

Fig. 2. *The definition of neutral transverse hip angle with the hip flexed to 90º, with the arrow the positive direction (internal rotation).*

evasive condition.

The results from our study on the impact of FAI on hip mobility have supported our hypotheses that this patient group would have decreased maximal dynamic self-generated internal rotation and abduction, but have refuted the hypothesis that the FAI group would have decreased maximal dynamic hip flexion. Moreover, there was also significant attenuation in maximal hip dynamic mobility in flexed external rotation, total hip transverse ROM and total hip sagittal ROM in the FAI group compared to the healthy matched control.

There are some limitations inherent to joint kinematic studies which may limit their accuracy and sensitivity. These limitations are caused by the use of generic calculations, marker misplacements(37) and skin or clothing artefacts (38-39). However, precautions were used to minimize the potential errors caused by these limitations. All marker placements were performed by the same researcher (MK) to minimize variability in placement locations. All angles were zeroed based on neutral static trials which removed any artificial neutral angles caused by marker misplacements. Finally, markers were either placed on the skin or tight spandex clothing to minimize clothing artefacts.

We found that there were similarities between the effect of FAI on passive hip ROM and dynamic hip ROM. The literature on passive hip ROM in participants with FAI indicated decreased maximal internal rotation at 90º of hip flexion (19, 22-25) and abduction (19, 24-25, 28) compared to a matched control, both of which were supported by our dynamic mobility results. Both of these findings correspond well to the proposed pathomechanism of cam FAI which states that impingement results from the jamming of the abnormal ridge of the femoral head-neck junction into the anterosuperior aspect of the acetabulum (20-21). Flexed internal rotation (4, 19, 28) and abduction (24-25, 40) rotate the anterosuperior femoral head-neck junction towards the anterosuperior aspects of the acetabulum. Therefore, both dynamic flexed internal rotation and abduction of the hip are likely restricted by the proximal femur jamming into the acetabulum.

Conversely, reduced passive hip external rotation in FAI participants has conflicting findings in the literature. In contrast to our hypotheses, our results showed that FAI participants had reduced self-generated dynamic external rotation compared to the control group. In accordance with our results, Ito et al. (19) found a significant decrease in passive hip external rotation with the hip flexed at 90º in patients with FAI compared to healthy controls (p

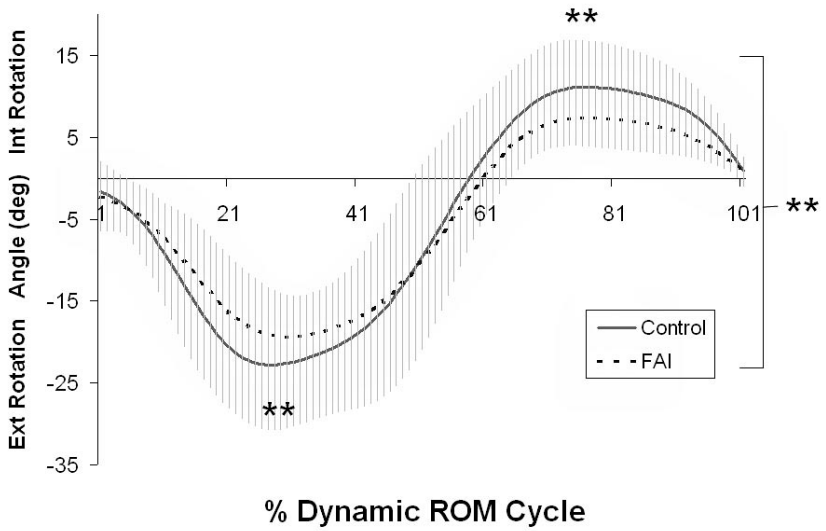

Fig. 3. *Mean maximal dynamic ROM in transverse plane at 90° of hip flexion (± standard deviation) for the symptomatic hip of cam FAI group, and for the averaged left and right hips of the matched control. Significant differences were found between the control and FAI group for peak internal rotation (p = 0.005), for peak external rotation (p = 0.009), and for total transverse ROM (p = 0.002).'*': p < 0.05'**': p < 0.01.*

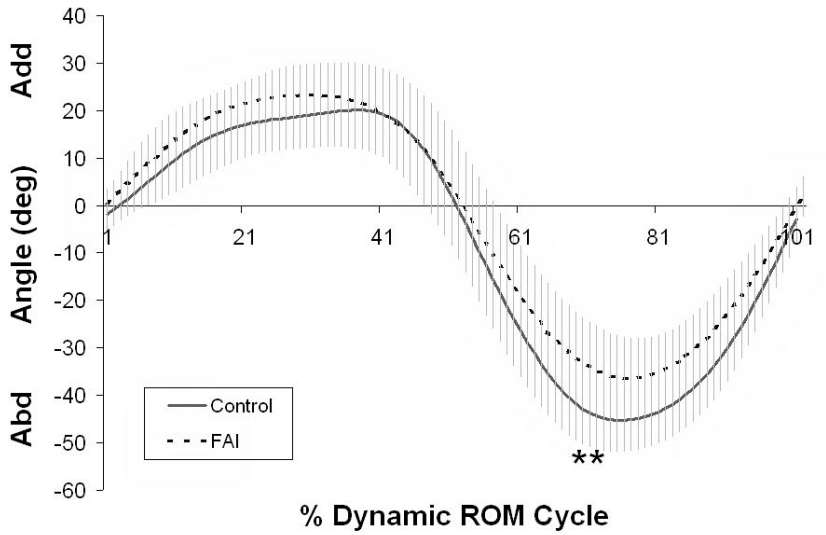

Fig. 4. *Mean maximal dynamic ROM in the frontal plane (± standard deviation). A significant differences was found between the control and FAI group for peak abduction (p = 0.003).*'*' : p < 0.05 '**' : p < 0.01.

= 0.02). Another study by Phillipon et al. (28) found a decrease in passive external rotation with a fully extended hip in the symptomatic leg of unilateral FAI participants as compared to the contralateral leg. Despite the hip being in a different orientation with a straight legged rotation as compared to a flexed rotation, the movement is similar enough to be relevant to this study. Contrary to these findings, computer simulated hip ROM studies on the effect of FAI on hip mobility showed no significant differences between the FAI and control groups (24-25). It should be noted that the aforementioned computer simulated studies examined only bony anatomy and neglected all soft tissues. This resulted in an exaggeration of hip mobility, with the predicted mobility in some planes being outside reasonable

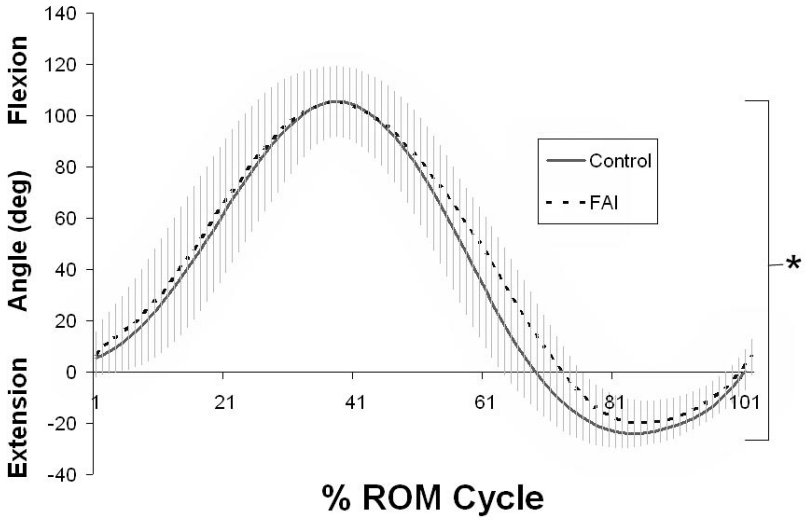

Fig. 5. *Mean maximal dynamic ROM in the sagittal plane (± standard deviation). A significant difference was found between the control and FAI group for total sagittal ROM ($p = 0.031$). '*': $p < 0.05$ '**': $p < 0.01$.*

values. For example, the predicted maximum hip external rotation in 90º of flexion was 80-100º (24-25) compared to the results from live analysis in the literature of 20-30º (19, 26) which are consistent with our results. The evident influence of soft tissue in hip external rotation makes these computer simulated studies, which neglected all soft tissue, irrelevant to our dynamic external rotation results, leaving only supportive passive external rotation findings in the literature. Previous studies have not tested for the effect of FAI on total transverse ROM. However, it can be assumed that since previous research has documented decreased passive internal (19, 22-25) and external rotation at 90º of hip flexion (19) in participants with FAI, there would be decreased total hip passive ROM. This also supports our findings on dynamic hip transverse ROM.

Although there is support of our reduction of dynamic flexed external rotation results in the passive hip ROM literature(19, 28), this finding does not fit the abovementioned pathomechanism for cam FAI (20-21). External rotation rotates the anteroposterior femoral head-neck ridge away from the acetabular labrum (40, 41), which also occurs while the hip is flexed as indicated by the huge flexed external rotation predicted without the presence of soft tissue in the computer simulated studies (24-25). This suggests that the soft-tissue of the hip likely contributes to the limited external rotation in the FAI group rather than just the bony structures and labrum. It is possible that the bulge on the anterosuperior head-neck junction in cam FAI causes increased tension on the iliofemoral ligament – which crosses the anterosuperior femoral neck, and limits external rotation (40) – during flexed external rotation. This could contribute to the restricted hip mobility, however this is purely speculation and beyond the scope of this study.

Not all of our dynamic hip mobility findings were supported by the passive ROM literature. Most literature reported attenuated passive hip flexion in FAI patients (19, 22, 24-25), yet our results showed no significant differences between the two groups in dynamic hip flexion ($p = 0.236$). The FAI group did have a slight decrease in hip flexion, but by only four degrees. The relatively high variability in peak hip flexion with a standard deviation of approximately nine degrees, coupled with a modest sample size, rendered the small difference between groups not significant. The convex anterosuperior head-neck junction is moved towards the anterosuperior acetabular labrum during hip flexion (4, 19, 28). Based on the proposed pathomechanism of cam FAI, (20-21) one would expect cam FAI to have decreased hip flexion. A potential explanation is that self-generated dynamic hip flexion cannot

achieve true peak hip flexion without external assistance (40). The added applied pressure from a clinician in passive ROM trials may be required to push the hip to the point where bony limitation occurs, and therefore may be required in order to elicit differences in hip flexion between the FAI and control groups. This explanation is supported by the fact that our control group's peak mean flexion was only 113.9º compared to approximately 120-130º of flexion in the control groups of other studies (19, 24-25, 28), indicating that the level of assisted hip flexion substantially exceeds self-generated peak hip flexion. Furthermore, this explanation is logical given the mechanical disadvantage hip flexor muscles are placed at when the hip approaches peak flexion, and since the hip flexor muscles are relaxed and can be compressed during passive hip flexion (40). Although the literature reports decreased assisted maximal hip flexion, there is no significant decrease in self-generated hip flexion in participants with FAI compared to matched controls.

Considering the lack of expected differences in peak hip flexion between the two groups, it is surprising that the FAI group had decreased total sagittal hip mobility. This decreased level of sagittal hip ROM in participants with FAI was primarily a result of the impingement group having less (though not significant) hip extension ($p = 0.054$) than the control group. No previous studies on passive hip mobility in patients with FAI report a decrease in hip extension. The proposed pathomechanism of cam impingement (20-21), indicates hip mobility limitations are caused by contact between the femur and acetabular labrum. However, hip extension rotates the anterosuperior head-neck ridge away from the acetabular edge, avoiding contact with the acetabulum(40) indicating that it would not be affected by FAI. Furthermore, hip extension is solely limited by soft tissue such as the iliofemoral ligament (40, 42-43), rather than bony contact. The decreased sagittal hip ROM in the FAI group ($p = 0.031$), primarily resulting from hip extension ($p = 0.054$), indicates that the anatomical abnormality may influence the muscles and ligaments supporting the hip joint as well as the documented effect on bone and cartilage. Both the tendon of the iliopsoas muscle and the iliofemoral ligament become very tight during maximal hip extension, and may cause damage to the anterosuperior hip joint capsule and the development of herniation pits on the proximal femur (43-44) which are associated with cam FAI (20). A bulge on the anterosuperior femoral head-neck junction could increase the distance these tissues travel to their distal attachments, causing this tension to occur earlier, and limiting extension. Our findings give no insight on the exact modality of limited hip sagittal ROM in FAI participants, but indicate that it is likely influenced by soft tissue.

In summary, participants diagnosed with cam FAI have significantly lower self-generated dynamic hip internal rotation at 90º of hip flexion and peak hip abduction compared to a matched control group in agreement with our hypotheses. However the postulated reduction in dynamic peak hip flexion in the FAI group as compared to the control group was not supported by our results. We also found that participants with cam FAI have a significantly lower dynamic flexed external rotation, and flexed total transverse ROM. Although not widely acknowledged, there is also supporting evidence of these findings in the passive hip mobility literature (19). Finally, despite the lack of differences in peak hip flexion, the FAI group had attenuated total sagittal hip ROM compared to the control. This unexpected finding was primarily a result of a large but non-significant decrease in peak hip extension in the FAI group. The differences in dynamic flexed external rotation and total sagittal ROM were likely a result of an abnormal soft tissue restriction in the impingement group. The effect of soft tissue on hip mobility in cam FAI should be investigated in future research.

ACKNOWLEDGEMENTS

One or more authors (ML & PB) have received funding from the Canadian Institutes of Health Research.

The authors thank Anna Fazekas Conway, research assistant of the adult reconstruction division of the orthopedic surgery department at the Ottawa Hospital.

REFERENCES

1. Standaert CJ, Manner PA, Herring SA. Expert

opinion and controversies in musculoskeletal and sports medicine: femoroacetabular impingement. Arch Phys Med Rehabil 2008;89:890-3.
2. Beaule PE, Le Duff MJ, Zaragoza E. Quality of life following femoral head-neck osteochondroplasty for femoroacetabular impingement. J Bone Joint Surg Am 2007;89:773-9.
3. Wisniewski SJ, Grogg B. Femoroacetabular impingement: an overlooked cause of hip pain. Am J Phys Med Rehabil 2006;85:546-9.
4. Ganz R, Parvizi J, Beck M, Leunig M, Notzli H, Siebenrock KA. Femoroacetabular impingement: a cause for osteoarthritis of the hip. Clin Orthop Relat Res 2003:112-20.
5. Harris WH. Etiology of osteoarthritis of the hip. Clin Orthop Relat Res 1986:20-33.
6. Laude F, Boyer T, Nogier A. Anterior femoroacetabular impingement. Joint Bone Spine 2007;74:127-32.
7. Leunig M, Casillas MM, Hamlet M, Hersche O, Notzli H, Slongo T, Ganz R. Slipped capital femoral epiphysis: early mechanical damage to the acetabular cartilage by a prominent femoral metaphysis. Acta Orthop Scand 2000;71:370-5.
8. Tanzer M, Noiseux N. Osseous abnormalities and early osteoarthritis: the role of hip impingement. Clin Orthop Relat Res 2004:170-7.
9. Wagner S, Hofstetter W, Chiquet M, Mainil-Varlet P, Stauffer E, Ganz R, Siebenrock KA. Early osteoarthritic changes of human femoral head cartilage subsequent to femoro-acetabular impingement. Osteoarthritis Cartilage. 2003;11:508-18.
10. Beck M, Leunig M, Parvizi J, Boutier V, Wyss D, Ganz R. Anterior femoroacetabular impingement: part II. Midterm results of surgical treatment. Clin Orthop Relat Res 2004:67-73.
11. Guanche CA, Bare AA. Arthroscopic treatment of femoroacetabular impingement. Arthroscopy. 2006;22:95-106.
12. Lavigne M, Parvizi J, Beck M, Siebenrock KA, Ganz R, Leunig M. Anterior femoroacetabular impingement: part I. Techniques of joint preserving surgery. Clin Orthop Relat Res 2004:61-6.
13. Mardones RM, Gonzalez C, Chen Q, Zobitz M, Kaufman KR, Trousdale RT. Surgical treatment of femoroacetabular impingement: evaluation of the effect of the size of the resection. J Bone Joint Surg Am 2005;87:273-9.
14. Murphy S, Tannast M, Kim YJ, Buly R, Millis MB. Debridement of the adult hip for femoroacetabular impingement: indications and preliminary clinical results. Clin Orthop Relat Res 2004:178-81.
15. Myers SR, Eijer H, Ganz R. Anterior femoroacetabular impingement after periacetabular osteotomy. Clin Orthop Relat Res 1999:93-9.
16. Philippon MJ, Stubbs AJ, Schenker ML, Maxwell RB, Ganz R, Leunig M. Arthroscopic management of femoroacetabular impingement: osteoplasty technique and literature review. Am J Sports Med 2007;35:1571-80.
17. Zebala LP, Schoenecker PL, Clohisy JC. Anterior femoroacetabular impingement: a diverse disease with evolving treatment options. Iowa Orthop J 2007;27:71-81.
18. Beck M, Kalhor M, Leunig M, Ganz R. Hip morphology influences the pattern of damage to the acetabular cartilage: femoroacetabular impingement as a cause of early osteoarthritis of the hip. J Bone Joint Surg Br 2005;87:1012-8.
19. Ito K, Leunig M, Ganz R. Histopathologic features of the acetabular labrum in femoroacetabular impingement. Clin Orthop Relat Re. 2004:262-71.
20. Leunig M, Beck M, Kalhor M, Kim YJ, Werlen S, Ganz R. Fibrocystic changes at anterosuperior femoral neck: prevalence in hips with femoroacetabular impingement. Radiology 2005;236:237-46.
21. Ito K, Minka MA, 2nd, Leunig M, Werlen S, Ganz R. Femoroacetabular impingement and the cam-effect. A MRI-based quantitative anatomical study of the femoral head-neck offset. J Bone Joint Surg Br 2001;83:171-6.
22. Wyss TF, Clark JM, Weishaupt D, Notzli HP. Correlation between internal rotation and bony anatomy in the hip. Clin Orthop Relat Res 2007;460: 152-8.
23. Notzli HP, Wyss TF, Stoecklin CH, Schmid MR, Treiber K, Hodler J. The contour of the femoral head-neck junction as a predictor for the risk of anterior impingement. J Bone Joint Surg Br 2002;84: 556-60.
24. Kubiak-Langer M, Tannast M, Murphy SB,

Siebenrock KA, Langlotz F. Range of Motion in Anterior Femoroacetabular Impingement. Clin Orthop Relat Res 2007;458:117-24.
25. Tannast M, Kubiak-Langer M, Langlotz F, Puls M, Murphy SB, Siebenrock KA. Noninvasive three-dimensional assessment of femoroacetabular impingement. J Orthop Res 2007;25:122-31.
26. Eijer H, Myers SR, Ganz R. Anterior femoroacetabular impingement after femoral neck fractures. J Orthop Trauma 2001;15:475-81.
27. Reynolds D, Lucas J, Klaue K. Retroversion of the acetabulum. A cause of hip pain. J Bone Joint Surg Br 1999;81:281-8.
28. Philippon MJ, Maxwell RB, Johnston TL, Schenker M, Briggs KK. Clinical presentation of femoroacetabular impingement. Knee Surg Sports Traumatol Arthrosc 2007;15:1041-7.
29. Crawford JR, Villar RN. Current concepts in the management of femoroacetabular impingement. J Bone Joint Surg Br 2005;87:1459-62.
30. Siebenrock KA, Kalbermatten DF, Ganz R. Effect of pelvic tilt on acetabular retroversion: a study of pelves from cadavers. Clin Orthop Relat Res 2003: 241-8.
31. Meyer DC, Beck M, Ellis T, Ganz R, Leunig M. Comparison of six radiographic projections to assess femoral head/neck asphericity. Clin Orthop Relat Res 2006;445:181-5.
32. Faul F, Erdfelder E, Lang AG, Buchner A. G*Power 3: a flexible statistical power analysis program for the social, behavioral, and biomedical sciences. Behav Res Methods 2007;39:175-91.
33. Bellamy N, Buchanan WW, Goldsmith CH, Campbell J, Stitt LW. Validation study of WOMAC: a health status instrument for measuring clinically important patient relevant outcomes to antirheumatic drug therapy in patients with osteoarthritis of the hip or knee. J Rheumatol 1988;15:1833-40.
34. Kadaba MP, Ramakrishnan HK, Wootten ME. Measurement of lower extremity kinematics during level walking. J Orthop Res 1990;8:383-92.
35. Kadaba MP, Ramakrishnan HK, Wootten ME, Gainey J, Gorton G, Cochran GV. Repeatability of kinematic, kinetic, and electromyographic data in normal adult gait. J Orthop Res. 1989;7:849-60.
36. Davis RB, Ounpuu S, Tyburski D, Gage JR. A gait analysis data collection and reduction technique. Human Movement Science 1991;10:575-87.
37. Della Croce U, Leardini A, Chiari L, Cappozzo A. Human movement analysis using stereophotogrammetry. Part 4: assessment of anatomical landmark misplacement and its effects on joint kinematics. Gait Posture 2005;21:226-37.
38. Leardini A, Chiari L, Della Croce U, Cappozzo A. Human movement analysis using stereophotogrammetry. Part 3. Soft tissue artifact assessment and compensation. Gait Posture 2005;21: 212-25.
39. Reinschmidt C, van den Bogert AJ, Nigg BM, Lundberg A, Murphy N. Effect of skin movement on the analysis of skeletal knee joint motion during running. J Biomech 1997;30:729-32.
40. Calais-Germain B. Anatomy of Movement. Seattle, WA, USA: Eastland Press; 1993.
41. Rab GT. The geometry of slipped capital femoral epiphysis: implications for movement, impingement, and corrective osteotomy. J Pediatr Orthop 1999;19: 419-24.
42. Bucholz RW, Wheeless G. Irreducible posterior fracture--dislocations of the hip. The role of the iliofemoral ligament and the rectus femoris muscle. Clin Orthop Relat Res 1982:118-22.
43. Daenen B, Preidler KW, Padmanabhan S, Brossmann J, Tyson R, Goodwin DW, Bergman G, Resnick D. Symptomatic herniation pits of the femoral neck: anatomic and clinical study. AJR Am J Roentgenol 1997;168:149-53.
44. Hewitt J, Guilak F, Glisson R, Vail TP. Regional material properties of the human hip joint capsule ligaments. J Orthop Res 2001;19:359-64.

CLINICAL STUDY

THE SURGICAL TREATMENT OF OSTEOCHONDRITIS DISSECANS OF THE TALUS AUTOLOGOUS CHONDROCYTE IMPLANTATION VERSUS DRILLING

M. HANDL, P. KOS, J. ADLER[1], F. VARGA[2], E. STASTNY, R. FREI and J. NEUWIRTH[3]

Orthopaedic Clinic; 2nd Faculty of Medicine, Charles University, Prague;[1]Tissue Bank, University Hospital Brno Bohunice; [2]Department of Biophysics, [3]Clinic of Imaging Methods, 2nd Faculty of Medicine, Charles University, Prague, Czech Republic

Received August 6, 2008- Accepted January 15, 2009

Osteochondral lesions, like osteochondritis dissecans (OCD) tali, are difficult to treat because the hyaline articular cartilage has a poor healing capacity. This study has focused on comparing both methods of treating OCD of the talus - autologous chondrocyte transplantation (ACI) and drilling. Between 2003 and 2006 a prospective, randomised cohort study was performed with patients where the options for the treatment were ACI in group A (7 pts - mean age 30.7 yrs), and arthroscopic drilling in group B (10 pts - mean age, 27.5 yrs) Clinical evaluations included Anderson, Berndt and Harty, Mazur and Weber scores and the AOFAS ankle-hindfoot scale. MRI examination in all cases was evaluated pre- and postoperatively in 2w, 2m, 6m and 1 to 3 yrs intervals. Comparing pre-surgical status (clinical scores), no significant difference was found between groups A and B (t-test results - Mazur: p = 0.39; Weber: p = 0.78; AOFAS: p = 0,04). Comparing both preop and postop (at least 1 year f-u) status in both groups, clinical results improved significantly in respect of all scores. The AOFAS score at the most recent follow-up was excellent; 91.7 ± 2.4 points in group A, 93.1 ± 2.1 points group B. MRI evaluation showed a good integration of ACI in Group A; in the case of Group B the MRI finally showed fully filled defects by fibrocartilagineous tissue. Clinical scores and MRI confirmation of ACI ingrowth in the Group A supports this method´s advantage over drilling from the point of view of future OA changes. The authors believe that autologous chondral grafting should be considered for the patient with a symptomatic osteochondral defect of the talus.

This study compared two methods of treating osteochondritis dissecans (OCD) of the talus – either by autologous chondrocyte transplantation (ACI) or by drilling (microfracturing).

The increasing use of ankle arthroscopy has drawn the attention of many orthopedic surgeons to osteochondral lesions in the ankle joint (1). The diagnoses include post-traumatic defects, osteochondritis dissecans (OCD), avascular necrosis (AVN) and osteoarthritis (OA), but even now it is difficult to treat the articular defect due to the hyaline articular cartilage's poor healing capacity. The main reason for this is a lack of blood vessels and nerves as well as its isolation from systemic regulation (2).

OCD is among the more common osteochondral lesions. OCD often causes a partial or total separation of either the chondral or osteochondral fragments. In the beginning symptoms may be slow to appear

Key words: talus, osteochondritis dissecans, cartilage repair, autologous chondrocyte implantation, magnetic resonance imaging

Mailing address: Dr. Milan Handl,
Orthopaedic Clinic, 2nd Faculty of Medicine,
University Hospital Motol, V Úvalu 84,
150 18 Prague 5, Czech Republic
Tel: ++420224 438 856
Fax: ++420224 432 82.
e-mail: milan.handl@lfmotol.cuni.cz

1973-6401 (2009)

without evident pain, swelling, effusions, instability or limited range-of-motion (3).

Surgical options for the treatment of symptomatic osteochondral lesions of the talus are varied and depend on the findings - size, stage and appearance of the lesion (4-5). Many reports have stated that nonoperative treatment has poorer results compared to surgical intervention (6).

Arthroscopic drilling, internal fixation of detached fragments, excision of the lesion, autologous bone or osteochondral grafting (mosaicplasty) and finally autologous chondrocyte implantation are among the various surgical procedures which are performed all over the world (7-10).

Kirschner-wire drilling (microfracturing of subchondral bone) have been commonly used, especially in lesions less than 1 cm^2. The main intention is to gain pluripotent mesenchymal stem cells for the formation of a new hyaline-like cartilage. Unfortunately the results have often led to a fibrocartilaginous repair tissue, which is commonly considered to have poorer biomechanical properties (11-13).

Osteochondral transfer, mosaicplasty and autologous chondrocyte implantation (ACI) are techniques designed to restore hyaline cartilage. Mosaicplasty has been reported to have good results, despite pain at the donor site (12). The technique of culturing autologous chondrocytes is particularly suitable for larger osteochondral lesions. This method uses cell expansion in a monolayer culture, finally formed into a 3-D chondrograft. ACI was pioneered by Brittberg and Peterson to treat full-thickness cartilage defects in the knee and has also had encouraging results in the ankle joint (13). In 2002 Koulalis reported eight patients with OCD of the talus who were treated by ACI (14).

This study reports the use of ACI for the treatment of full-thickness, large (>1 cm^2) defects of the talar dome, originally diagnosed as OCD, and compares it to simple arthroscopic techniques.

ACI is a two-stage procedure. Harvesting the rice-seed-size hyaline cartilage sample is performed during the first diagnostic arthroscopy. Chondrocytes are isolated, enzymatically split, and finally cultured and analyzed for their proliferation. The second stage involves implantating the chondrocytes in the form of a solid autograft fixed by fibrin glue. In some cases, the chondrocytes can be integrated into an artificially engineered scaffold.

Disorders of the joint cartilage are originally diagnosed by radiography, MRI or CT scans, and subsequently visualized and confirmed by the arthroscopic examination. The most popular evaluation system for osteochondral defects of the talus is that described by Berndt and Harty in 1959 (15), while the articular surface can be arthroscopically visualized according to the Outerbridge scale (16).

The efficacy of drilling versus ACI in the treatment of OCD lesions of the talar dome was evaluated by Magnetic resonance imaging (MRI) and arthroscopy, which are two excellent tools for assessing morphological osteochondral changes in the ankle joint. The findings were clinically confirmed by evaluation, according to the Ankle-Hindfoot scale of the American Orthopaedic Foot and Ankle Society (AOFAS score) (17-20).

The purpose of the study was to verify advantage of ACI, which means to prefer hyaline-like cartilage replacement and healing over the other common procedures based on fibrocartilagenous healing. The authors suggest making full use of ACI instead of formerly used procedures. They believe that, from the longterm point of view, the use of hyaline-like cartilage tissue can be more suitable in the prevention of future osteoarthritic changes.

METHODS

A series of patients was treated for OCD of the talar dome between 2003 and 2006. The criteria for the diagnosis were: pain, swelling, effusion, instability, limited range-of-motion and a positive X-ray finding (Berndt -Harty stage III to stage IV). No case had history of trauma and no patient presented a III or IV BH scale.

The patients were prospectively and randomly divided. The options for treatment were ACI in group A, the final follow-up was performed in 7 patients (2 lost at f-u due to failing to attend the periodical visit), and arthroscopic drilling in group B, with 10 pts. The final evaluation was done in both groups. There were 4 right and 3 left ankles in group A, with the defect localized medially in 6 and in 1 laterally on the talar dome. In group B there were 3

right and 7 left ankles, with the defect localized on the medial in 9 and in 1 on the lateral side. In group A there were 3 male and 4 female patients, age at the time of surgery ranged between 14 and 57 years (mean age 30.7 yrs). In Group B there were 7 men and 3 women, aged between 13 and 52 years (mean age, 27.5 yrs). The mean size of the talar dome defects in both groups was 18mm x 10mm (10mm x 7mm to 25mm x 12mm) measured in both directions, anterior/posterior and medial/lateral. The mean time to follow-up was 28.4 months (14 to 39).

The lesions of the talus had been evaluated using standard radiography, MRI and arthroscopy. Clinical pre- and postoperative results of the functional outcome were obtained using Mazur, Weber scores and the AOFAS ankle-hindfoot scale, and radiologically by the Anderson and Berndt-Harty scales. In all cases MRI examination was evaluated pre- and postoperatively at 2 weeks, 2 months, 6 months and at 1 to 3-yr intervals.

Physical examination showed no swelling or deformity in the ankle joints. The preoperative mean range of motion was stiff, limited to 10º at dorsal flexion and 20º at plantar flexion respectively. No significant instabilities were observed when compared to the uninjured contralateral ankle joint. On X-ray, typical radiolucent areas were found, mostly in the medial area of the talar dome.

Indications for surgery included a symptomatic focal talar lesion due to OCD of at least 1 cm in length or diameter, and a rectangular area of at least 80 mm^2 located at the weight-bearing zone of the talar dome (Berndt -Harty stage III to stage IV).

Surgical technique

Arthroscopy of the ankle: standard anterolateral and anteromedial portals under tourniquet control as the routine first diagnostic surgery in both methods. Arthroscopic examinations revealed stage III to IV defects according to the Outerbridge scale (16), which confirmed the preoperative findings according to the Berndt-Harty X-ray scale (Fig. 1) in all cases, with a detaching unstable or completely destroyed large osteochondral fragment, mostly on the medial edge of the talar dome.

The decision for subsequent therapy was based upon these diagnostic findings. In the case of ACI, rice-seed sized cartilage samples had to be harvested using a 5-mm gouge. In our study, in each ankle joint the chondrocytes were always obtained from a non- to low-weight-bearing area at the anterior edge of the talar dome. We preferred this technique to the others because of the ease with which it can be performed (21). The mean weight of the cartilage harvested was about 250 mg. The biopsy material was transported to a laboratory where the chondrocytes were cultured, a process which took about 28 to 42 days.

The autologous chondrocyte implantation of the hyaline-like cartilage was the second step of this procedure. Open surgery under general anaesthesia in the supine position was performed using the same approach as in the first arthroscopy, but lengthened up to 4-5cm to sufficiently expose the talar dome defect (Fig. 2). No oblique medial malleolar osteotomy for the medial talar dome was used in any case.

The ACI procedure routinely continued by preparing the defect bottom of the chondral lesion by debridedment, adjacent to the normal surrounding cartilage and subchondral bone. All the necrotic tissue was removed and thin drilling of the subchondral bone surface was included as a standard part of the procedure. Finally the hyaline-like chondrograft was implanted and firmly attached by fibrin glue (22-23).

Arthroscopic drilling was performed using a Kirschner wire 1.2mm in diameter. The drill holes were located at about 2-3 mm intervals while approaching the subchondral bone to a depth of about 1 to 1.5 cm.

Culturing autologous chondrocytes

After the hyaline cartilage biopsies had been harvested and transported to the laboratory, the cartilage samples were cleaned and cut into small pieces under the laminar hood air flow. The fragments of cartilage were treated with 0.2% trypsin and 0.2% collagenase to digest the matrix and to isolate chondrocytes.

The released chondrocytes were propagated by the conventional monolayer technique. The chondrocytes, suspended in Ham´s F12 medium supplemented with 12% fetal bovine serum and Gentamycin (50 ug/1 ml), were inoculated into the flasks and cultured in a CO^2 ambient at 37°C. A cell monolayer was formed during the successful primoculturing. Thus the required number of cells (5

million cells per 1 ml) was obtained via subculturing the primocultures. The proliferation of chondrocytes was monitored using inverted microscopy. Culturing the chondrocytes generally took about 3-4 weeks.

The 3D (three–dimensional) carrier was based on fibrin glue which was the substance where the cultured chondrocytes were finally used to form a solid chondrograft. It was possible to adapt the size and thickness of such a chondrograft for final implantation, according to the cavity's dimensions. The graft was fixed with fibrin glue and there was no need for additional fixation (e.g. periosteal patch etc.)

Postoperative Rehabilitation

All subjects in this comparative study were operated according to the same protocol. The patients were all immobilized for 2 weeks after surgery with a ninety-degree short leg cast (below the knee). Afterwards passive 0 to 20 degrees of plantar flexion and 10 degrees of dorsal flexion were allowed every two weeks until the full range of motion was achieved. Partial weight-bearing was allowed after 6 weeks, full weight-bearing was allowed 8 weeks after surgery. A full exercise program could commence after 3 months and unrestricted sports activity 6 months after the surgery.

Evaluation

The clinical outcome was evaluated using a combination of scoring scales, and clinical examination taken both pre- and post-operatively at two, six months and annually thereafter. The scoring assessments were completed by patients before clinical examination. The MRI evaluation was done by two blinded and independent examiners, radiologists who had no contact with the surgical group.

MRI was obtained using an MR scanner E-scan EQ equipped with a permanent 0.2T magnet and coil dedicated to ankle joint examination. The gradient strength was 20mT/m and the minimal rise time 0.8msec. The standardized MR imaging protocol consisted of three sequences: HR T1 SE (TR 850, TE 26), HR GE STIR (TR 1640, TE 25) and HR GE T1 (TR 700, TE 16).

The MRI description included the integration of the graft with the adjacent native cartilage, the graft surface and its congruence, and the signal discrepancy between the graft and native cartilage. In subchondral bone, the presence of signal changes typical of bone oedema were also evaluated. In the case of drilling, the recovery of the fibrocartilagineous tissue were compared to the surrounding area. Characteristics of the newly formed tissue were observed and compared to the native hyaline cartilage.

RESULTS

All the treated patients were examined prior to surgery and then according to the protocol in the follow-up period.

Considering the Berndt - Harty score prior to surgery, in group A, 1 patient showed degree 2, 3 patients degree 3 and 3 patients degree 4. In group B, 5 patients showed degree 2, 3 patients degree 3 and 2 patients degree 4.

Using to the Anderson scale, similar results were revealed. In group A, 1 patient showed degree IIA, 3 patients degree III and 3 patients degree IV. In group B, 5 patients showed degree IIA, 3 patients degree III and 2 patients degree IV.

Functional outcome results were obtained for the ankle using the American Orthopaedics Foot and Ankle Society (AOFAS) ankle-hindfoot score, employing an algorithm (outcome collection instrument version 2.0) with a score range from 0 to 100 (score of 90 to 100, excellent; 80 to 89, good; 65 to 79, fair; <65, poor).

Comparing pre-surgical status according to individual clinical scores, no significant difference was found between groups A and B (t-test results - Mazur: $p = 0.39$; Weber: $p = 0.78$; AOFAS: $p = 0.04$). All mentioned pre-surgical results confirmed the random division of patients to groups A and B.

Patient status was checked 2 weeks, 2 months, 6 months, 1, 2 and 3 years after the surgery. The results of the three above-mentioned clinical scores were evaluated at each follow-up and compared for groups A and B (t-test). None of the tests revealed significant differences in patient condition in any time period following the surgical treatment ($p > 0.1$), except AOFAS 6 months after surgery ($p < 0.05$). Average score values for all performed tests are shown in Table 1.

Table 1 - *Mean score values and their standard deviations (in brackets) of individual clinical tests performed at different intervals of the follow-up period. (For the Mazur and AOFAS tests the overall score value was considered, for Weber average values of individual test components were compared.)*

	prior	after 2 months	after 6 months	after 12 months	after 24 months
Mazur (group A)	27.6 (11.7)	43.9 (9.3)	71.7 (9.4)	82.9 (8.3)	83.3 (9.8)
Mazur (group B)	31.8 (8.3)	39.4 (6.8)	71.1 (8.0)	86.1 (9.5)	88.4 (7.1)
Weber (group A)	2.76 (0.67)	2.43 (0.45)	1.33 (0.72)	0.69 (0.47)	0.60 (0.48)
Weber (group B)	2.67 (0.8)	2.33 (0.55)	1.02 (0.61)	0.43 (0.40)	0.41 (0.35)
AOFAS (group A)	26.9 (9.5)	37.9 (7.7)	65.6 (13.1)	84.3 (13.4)	86.3 (12.4)
AOFAS (group B)	37.8 (10.3)	40.3 (8.6)	78.9 (12.1)	90.2 (11.2)	92.1 (9.7)

Fig. 1. *Stage IV defect according to the Berndt-Harty X-ray scale. Completely destroyed large osteochondral fragment on the medial edge of the talar dome.*

Fig. 2. *The autologous chondrocyte implantation of the hyaline-like cartilage using the same approach as in the first arthroscopy, but lengthened up to 4-5cm to sufficiently expose the talar dome defect.*

According to the results presented there was no observable difference in average patient convalescence and status enhancement between the two compared surgical approaches (Fig. 3 and Fig. 4).

MRI results

Group A – ACI

MRI of the ankle at follow-up showed filling of the defects, with a congruent homogeneous joint surface. Only in 1 patient was the exact definition of the edges of the graft observed at 2 weeks and 2 months postoperatively: the MRI signal difference between the chondrograft (more intense) and the native cartilage was possible to distinguish in the GE STIR sequence. The signal discrepancy was not detectable in the rest of the patients. The graft congruence with the surrounding cartilage

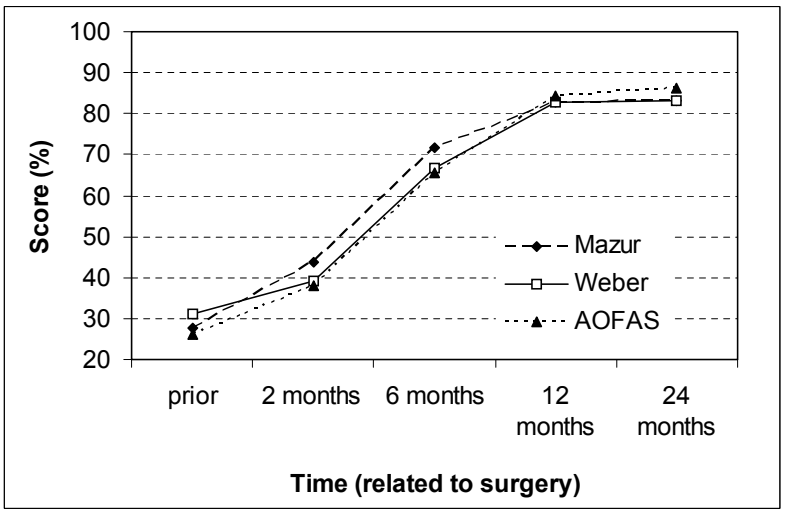

Fig. 3. *Group A – ACI. Trends of individual clinical test score mean values (in percentual scale) at different time intervals following autologous chondrocyte implantation.*

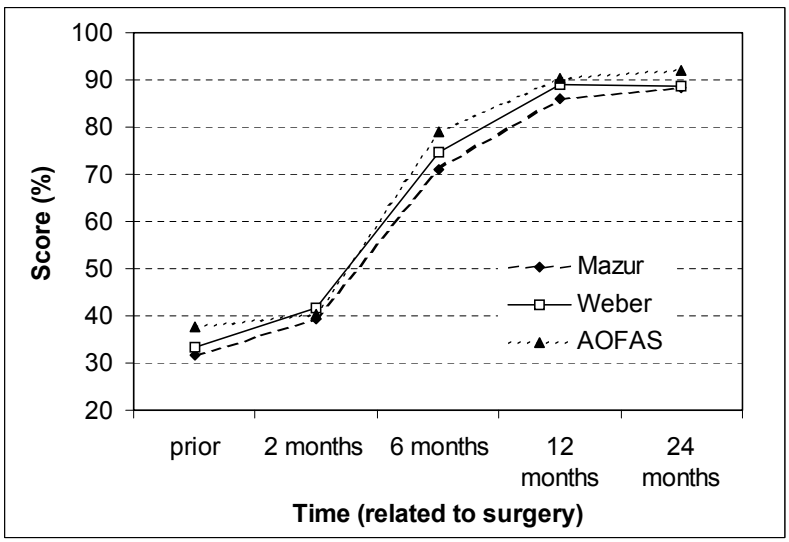

Fig. 4. *Group B – Drilling. Trends of individual clinical test score mean values (in percentual scale) at different time intervals following arthroscopic drilling.*

was satisfactory in all the cases (Fig. 5-6a,b). In 3 patients, when postoperative MRI was evaluated after 2 weeks and 2 months, the graft surface was slightly above the level of the surrounding cartilage. A higher talar subchondral bone signal intensity (on GE STIR sequency) representing bone oedema was evaluated under the chondral defect in all the cases. This bone oedema was still present 1 year postoperatively, but with a tendency to regression.

Group B – Drilling

The MRI signal difference between the fibrocartilagenous tissue and the native surrounding cartilage was possible to distinguish mainly in the GE STIR sequency. The new surface congruence with the surrounding cartilage was satisfactory in all the cases (Fig. 7-8a,b), mostly just lower than the level of the surrounding cartilage. A higher talar subchondral bone signal intensity (on GE STIR

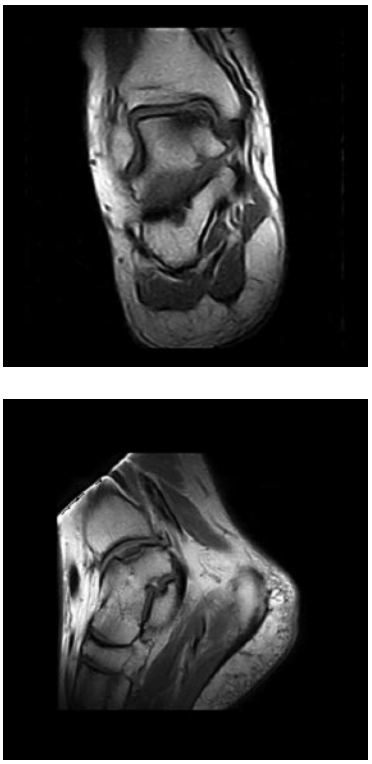

Fig. 5. A), B) *Osteochondritis dissecans with a loose in situ fragment. T1 spin-echo images show an osteochondral defect at the medial part of the talar dome. Figures are of the same patient, matched in anatomical location*.

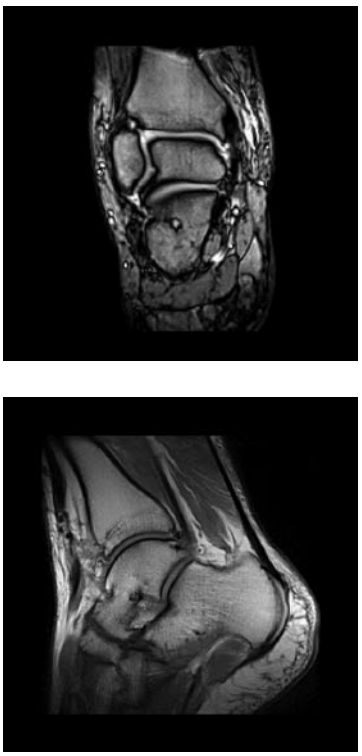

Fig. 6. A), B) *Follow-up MRI study (after 2 years): Coronal 3D gradient-echo (a) and sagittal (b) MR images after autologous chondrocyte implantation show successful repair of the medial part of the talar dome. Figures are of the same patient, matched in anatomical location.*

sequency) representing bone oedema was evaluated under the chondral defect in all cases after 1 year postoperatively.

DISCUSSION

Accurate diagnosis of chondral or subchondral lesions can be difficult. For this reason standard radiographic examination, MRI and ankle arthroscopy are commonly used. Although standard radiography cannot show chondral conditions, it can reveal the quality of the subchondral bone especially in OCD. Thus MRI is an appropriate tool for identifying both cartilage and subchondral bone quality and their possible changes.

The treatment of osteochondral lesions of the talar dome remains controversial. Until now, no treatment has been regarded as a "gold standard" for regenerating hyaline cartilage (24).

Subchondral bone grafting can be performed either antegradely or retrogradely, in the latter case to prevent damage to the articular hyaline cartilage surface (25-26). Bone implantation is advantageous in patients with subchondral cysts, where there is a need to fill the subchondral area. The presence of such a cyst can indicate necrosis of the bone, similar to osteochondritis dissecans or bone infarction (27).

In a different technique reported by Ochi et al., a tissue-engineered cartilage formed by cultured chondrocytes in three-dimensional matrices for cartilage repair was used, this approach uses tissue transplantation over cell transplantation (28-30).

Arthroscopic procedures have reportedly produced results with a good or excellent outcome in approximately 80% of the cases. While these techniques are less invasive than other surgical methods and require only a short period of hospitalization, they have disadvantages. Drilling can damage the intact cartilage of the lesion

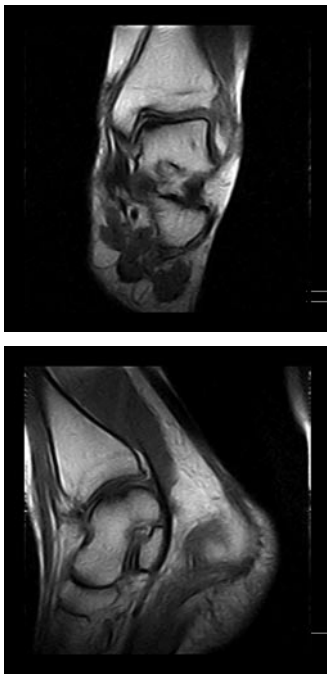

Fig. 7. A), B) *T1 spin-echo MR images demonstrate an articular defect and abnormal low-signal intensity in the anteromedial aspect of the talus, consistent with osteochondritis dissecans. Figures are of the same patient, matched in anatomical location.*

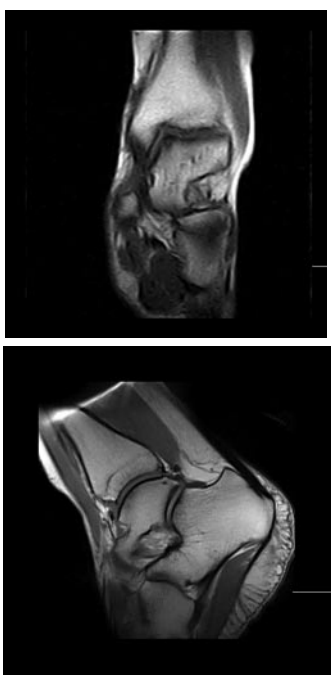

Fig. 8. A), B) *T1 spin-echo MR images obtained 2 years after arthroscopic drilling show repair tissue filling an osteochondral defect with a congruent articular surface. Figures are of the same patient, matched in anatomical location.*

and malleolus. Sometimes there is the need to perform a larger arthrotomy and possible malleolar osteotomy in osteochondral grafting. Osteotomies, particularly on the medial side, can cause morbidity if complicated by nonunion or malunion (31-32). ACI enables repairing which is well confined to the surrounding articular surface (23,33).

According to all scores, clinical results improved significantly when comparing preoperative and postoperative (at least 1 year f-u) status in both groups. MRI evaluation showed that ACI appeared to generate a good repair tissue in Group A. This suggests that filling the defect via a hyaline-like cartilage may be considered and preferred over the fibrocartilage.

This study still presents some limitations. The viability of the chondrograft is one of the main points to be verified. Another weak point is the limited number of patients observed. To date it has been difficult to find a study comparing two methods with more than ten patients (34). Thus, the variability of human potential may also affect the sample. Indeed the large number of variables plays an important role, and this will be hard to fully address in the near future. Certainly, further studies with larger numbers of patients and a longer follow-up will be necessary.

CONCLUSIONS

According to all tests and examinations performed, a very favourable healing process and subsequent recovery was revealed in the two methods compared. No significant difference in clinical test results was observed between patients who underwent drilling or ACI treatment.

The authors believe that the autologous chondrocyte implantation using the tissue-engineered technique - hyaline-like cartilage - can be a good treatment option for patients suffering from osteochondral lesions like OCD.

In case of ACI, MRI has confirmed that this method enables the restoration of a congruency of the cartilage surface, as well as the clinically demonstrated complete pain relief and full joint motion. On the other hand, the drilling procedures remain much less demanding in time and economical terms. Furthermore they require only one operation.

The question of improving the prevention of osteoarthritic changes/degeneration remains partially unresolved and requires further study.

FINANCIAL SUPPORT AND ACKNOWLEDGEMENTS

Sponsored by a grant from the Grant Agency of Charles University, Prague GAUK No. 46/2005 and IGA Ministry of Health, Czech Republic NR 8122 – 3/2004

REFERENCES

1. Agung M, Ochi M, Adachi N, Uchio Y, Takao M, Kawasaki K. Osteochondritis Dissecans of the Talus Treated by the Transplantation of Tissue-Engineered Cartilage. Arthroscopy 2004;20(10):1075-80.
2. Gautier E, Kolker D, Jakob RP. Treatment of cartilage defects of the talus by autologous osteochondral grafts. J Bone Joint Surg Br 2002;84(2):237-44.
3. Schenck RC, Goodnight JM. Osteochondritis dissecans. J Bone Joint Surg Am 1996;78(3):439-56.
4. Clanton TO, DeLee JC. Osteochondritis dissecans: history, pathophysiology and current treatment concepts. Clin Orthop Relat Res 1982;167:50-64.
5. Tol JL, Struijs PA, Bossuyt PM, Verhagen RA, van Dijk CN. Treatment strategies in osteochondral defects of the talar dome: a systematic review. Foot Ankle Int 2000;21(2):119-26.
6. Canale ST, Belding RH. Osteochondral lesions of the talus. J Bone Joint Surg Am 1980;62(1):97-102.
7. Greenspoon J, Rosman M. Medial osteochondritis of the talus in children: Review and new surgical treatment. J Pediatr Orthop 1987 7(6):705-8.
8. Draper SD, Fallat LM. Autogenous bone grafting for the treatment of talar dome lesions. J Foot Ankle Surg 2000 Jan-Feb; 39(1):15-23.
9. Whittaker JP, Smith G, Makwana N, Roberts S, et al. Early results of autologous chondrocyte implantation in the talus. J Bone Joint Surg Br 2005;87(2):179-83.
10. Nadiv DO, Myerson MS. Approach alternatives for treatment of osteochondral lesions of the talus. Foot Ankle Clin 2002;7(3):635-49.
11. Hangody L, Kish G, Modis L, Szerb I, Gaspar L, Dioszequi Z, Kendik Z. Mosaicplasty for the treatment of osteochondritis dissecans of the talus: two to seven year results in 36 patients. Foot Ankle Int 2001;22(7):552-8.
12. Gautier E, Kolker D, Jakob RP. Treatment of cartilage defects of the talus by autologous osteochondral grafts. J Bone Joint Surg Br 2002;84(2):237-44.
13. Petersen L, Brittberg M, Lindahl A. Autologous chondrocyte transplantation of the ankle. Foot Ankle Clin 2003;8(2):291-303.
14. Koulalis D, Schultz W, Heyden M. Autologous chondrocyte transplantation for osteochondritis dissecans of the talus. Clin Orthop Relat Res 2002;(395):186-92.
15. Berndt AL, Harty M. Transchondral fractures (osteochondritis dissecans) of the talus. J Bone Joint Surg Am 1959;41-A:988-1020.
16. Outerbridge RE. The etiology of chondromalacia patellae. J Bone Joint Surg Br 1961; 43-B:752-7.
17. Kitaoka HB, Alexander IJ, Adelaar RS, Nunley JA, Myerson MS, Sanders M. Clinical rating systems for the ankle-hindfoot, midfoot, hallux, and lesser toes. Foot Ankle Int 1994;15(7):349-53.
18. De Smet AA, Fisher DR, Burnstein MI, Graf BK, Lange RH. Value of MR imaging in staging osteochondral lesions of the talus (osteochondritis dissecans): Results in 14 patients. Am J Roentgenol 1990;154(3):555-8.
19. Deutsch AL, Mink JH, Kerr R. MRI of the foot and ankle. Raven Press New York, 1992.
20. Fricová-Poulová M, Neuwirth J, Handl M, Lisý J, Trč21. T. Vývoj morfologických znaků a signálu autologních chondrocytárních implantátů při zobrazení magnetickou rezonancí - prospektivní studie. Čes Radiol 2006; 2:108-12.
22. Matricali GA, Dereymaeker GPE, Luyten FP. The Posteromedial Rim of the Talar Dome as the Site for Harvesting Cartilage in the Ankle: An Anatomic Study. Arthroscopy 2006;22(11):1241-5.
23. Handl M, Trč24. T, Frei F, Hanus M, Šťastný E, Fricová-Poulová M, Neuwirth J, Adler J, Havranová D, Varga F. Treatment of Deep Chondral Defects of the Joints by Transplantation of Cultured Autologous Chondrocytes: Report of Operations Performed over a Period of 30 Months (2003-2005). Revista de ortopedia y traumatología 2006;14(3):1-17.
25. Handl M, Trč26. T, Hanus M, Šťastný E, Fricová-

Poulová M, Neuwirth J, Adler J, Havranová D, Varga F. Autologous chondrocyte implantation in the treatment of cartilage lesions of ankle joint. Acta Chir Orthop Traumatol Cech 2007;74(1):29-36.

27. Martinek V, Ottl G, Imhoff AB. Chondral and osteochondral lesions of the upper ankle joint. Clinical aspects, diagnosis and therapy. Unfallchirurg 1998;101(6):468-75.
28. Kolker D, Murray M, Wilson M. Osteochondral defects of the talus treated with autologous bone grafting. J Bone Joint Surg Br 2004;86(4):521-6.
29. Lee CK, Mercurio C. Operative treatment of osteochondritis dissecans in situ by retrograde drilling and cancellous bone graft. Clin Orthop Relat Res 1981;158:129-36.
30. Thompson J, Loomer R. Osteochondral lesions of the talus in a sports medicine clinic a new radiograph technique and surgical approach. Am J Sports Med 1984;12(6):460-3.
31. Katsube K, Ochi M, Uchio Y, Maniwa S, Matsusaki M, Tobita M, Iwasa J. Repair of articular cartilage defects with cultured chondrocytes in Atelocollagen gel. Comparison with cultured chondrocytes in suspension. Arch Orthop Trauma Surg 2000;120(3-4):121-7.
32. Agung M, Ochi M, Adachi N, Uchio Y, Takao M, Kawasaki K. Osteochondritis Dissecans of the Talus Treated by the Transplantation of Tissue-Engineered Cartilage. Arthroscopy 2004;20(10):1075-80.
33. Ochi M, Adachi N, Nobuto H, Yanada S, Ito Y, Agung M. Articular cartilage repair using tissue engeneering technique-novel approach with minimally invasive procedure. Artif Organs 2004;28(1):28-32.
34. Robinson DE, Winson G, Harries WJ, Kelly AJ. Arthoscopic treatment of osteochondral laesions of the talus. J Bone Joint Surg Br 2003:85(7):989-93.
35. Vališ P, Repko M, Krbec M, Chaloupka R, Šprláková A, Adler J, Nýdrle M. Treatment of the cartilage defect of the ankle by a solid chondrograft. Acta Chir Orthop Traumatol Cech 2005;72(1):52-6.
36. Guillen P, Abelow SP, Jaen TF. Arthroscopic Matrix/Membranous Autologous Chondrocyte Implantation for the Treatment of Large Chondral Defects of the Ankle (SS-89). Arthroscopy 2005;21(6)Supp:e43.
37. Gobbi A, Francisco RA, Lubowitz JH, Allegra F, Canata G. Osteochondral Lesions of the Talus: Randomized Controlled Trial Comparing Chondroplasty, Microfracture, and Osteochondral Autograft Transplantation. Arthroscopy 2006;22(10):1085-92.

BASIC SCIENCE

FIBROCHONDROGENIC DIFFERENTIATION OF HUMAN MESENCHYMAL STEM CELLS

P. VERDONK, R. VERDONK, F. ALMQVIST, E. M. VEYS[1] and G. VERBRUGGEN[1]

Department of Orthopaedic Surgery; [1]Department of Rheumatology, Ghent University, Ghent, Belgium

Received August 25, 2008 – Accepted December 29, 2009

In this *in vitro* study, the authors investigated the fibrochondrogenic differentiation potential of human bone marrow derived mesenchymal stem cells (hBMSC) after expansion in autologous serum. In a second setup, the combination of hBMSC with a meniscus-shaped type I collagen scaffold was evaluated. hBMSC were isolated from adult human bone marrow aspirates and expanded in monolayer condition using DMEM supplemented with 10% autologous serum. hBMSC were subsequently either spun down to form a micropellet or loaded on a biodegradable type I collagen scaffold. Fibrochondrogenic differentiation was initiated by serum-free culture conditions and the addition of TGFβ1, dexamethasone, Ascorbic Acid-2-Phosphate and ITS premix to the medium. Immunohistochemical analysis revealed a specific time-dependent pattern of expression of the different extracellular matrix components (type I and II collagen, aggrecan). At week 3 the extracellular matrix composition resembled closely the composition of native meniscus tissue. Depending on the method used to load the hBMSC on the scaffold, these cells were either located superficially or more evenly distributed within the scaffold. In summary, hBMSC expanded in autologous serum have a meniscus cell-like differentiation potential. hBMSC can be combined with a biodegradable meniscus-shaped scaffold. This cell-scaffold combination can be implanted easily into the meniscus defect thereby delivering autologous hBMSC with meniscus repair potential to this defect.

The meniscus plays an important role in the complex biomechanics of the knee joint. It has function in load bearing, load transmission, shock absorption, joint stability, joint lubrication and joint congruity. Loss of this important anatomical structure results in higher peak stresses on the cartilage and eventually leads to cartilage degeneration and osteoarthritis, as observed by Fairbank over fifty years ago (1).

The human meniscus is also known to have a poor healing potential, partly due to the absence of vasculature: blood vessels are present only in the outer 10-30% of the meniscal body (2). Lesions located in this area can be surgically sutured with a high success ratio (3). The more frequent lesions situated in the avascular part, however, show no or only limited tendency to heal and should hence be resected (4). A partial instead of total meniscectomy is proposed, knowing that cartilage degeneration is proportional to the amount of meniscus that was removed (5). Still, partial meniscectomy results in approximately 4% articular cartilage volume loss per year (6).

Substantial research has already been performed

Key words: meniscus, scaffold, regeneration, repair, knee

Mailing address: Peter Verdonk
Department of Orthopaedic Surgery, Poli 5,
De Pintelaan 185
B9000 Gent, Belgium
Tel: ++32 92402264
Fax: ++32 92404975
e-mail: pverdonk@yahoo.com

1973-6401 (2009)

to substitute the resected meniscus in case of a total or partial meniscectomy, in order to prevent or delay cartilage degeneration, improve biomechanics and relieve pain. Possible surgical approaches include the use of autologous or allogenic tissues and scaffolds: e.g. tendon (7), pediculated Hoffa fat pad (8), periosteal tissue (9), perichondral tissue (10), small intestine submucosa (10), meniscal allografts (11-14), meniscus scaffolds based on native polymers (collagen and hyaluronic acid) (15) or purely synthetic scaffolds such as poly-lactic acid, poly-glucuronic acid and poly-urethane (16). Other than meniscal allografts, a poly-urethane scaffold (Actifit®, Orteq Bioengineering, London, UK) and a collagen type I based meniscus scaffold (CMI®, Regen Biologics, Franklin Lakes, NJ, USA), none of these materials have advanced to human clinical use. These surgical approaches are based on the concept of a timely colonization of the acellular scaffold or allograft tissue by host cells which are probably derived from the synovium and joint capsule (17,18). The phenotype of these host-derived scaffold-colonizing cells ultimately determines the biochemical composition and biomechanical behaviour of these repopulated scaffolds or tissues. Another important variable in this approach is the time needed for colonization of the scaffold or tissue: since these scaffolds or tissues are biodegradable, the colonization and healing by host cells should be faster than the degradation process, for the regeneration or healing of the meniscus substitute to be successful. Hence, an increase of the initial cell number at the defect site and thereby a decrease of the time needed for colonization can be accomplished by seeding cells with a proven meniscus repair potential on or in a biodegradable scaffold prior to implantation.

In this *in vitro* study, the authors investigated the combination of human bone marrow derived mesenchymal stem cells (hBMSC) with a type I collagen scaffold for the repair of meniscus defects. hBMSC are multipotent cells capable to differentiate into multiple mesenchymal cell lineages such as myoblasts, chondrocytes, adipocytes and osteoblasts (19). These cells can be easily isolated from human bone marrow and expanded without loosing their multipotent characteristics in monolayer conditions (19). Therefore, after hBMSC expansion, the use of these autologous cells for tissue engineering purposes appears reasonable.

Bovine serum is the usual supplement to the medium for hBMSC expansion. However, bovine serum proteins attach to the cell membrane and could thus elicit unfavorable immune responses in the host. In addition, the transmission of bovine diseases remains to be an issue. Autologous serum could replace serum of bovine origin for cell expansion, thus eliminating these concerns.

Therefore, the fibrochondrogenic (or meniscus cell-like) differentiation potential of hBMSC after expansion in autologous serum was investigated *in vitro*. In a second setup, hBMSC were seeded on a type I collagen scaffold. Different cell-seeding protocols were investigated. Again, the cell differentiation potential and the colonisation behaviour were investigated.

MATERIALS AND METHODS

Preparation and culture of human bone marrow derived mesenchymal stem cells (hBMSC)

Human bone marrow was obtained from 6 patients undergoing spinal surgery. Patients were otherwise healthy. Fifteen to 20 ml of bone marrow was harvested from the posterior iliac crest in a syringe (Becton Dickinson biopsy needle for bone marrow) containing 20.000U of heparin and was processed immediately. The study protocol was approved by the local ethics committee and an informed consent was obtained from every patient.

The bone marrow sample was diluted with one volume of phosphate buffered saline (PBS, Gibco Invitrogen Corp, Merelbeke, Belgium). Four milliter aliquots of bone marrow suspension were applied on 4 ml aliquots of Ficoll Paque PLUS density gradient medium (Amersham Bioscience, Freiburg, Germany). After centrifugation (1500 rpm, 20 min), interfaces were collected and washed once with medium: Dulbecco's Modified Eagle's Medium (DMEM, Gibco Invitrogen Corp) supplemented with antibiotics (penicillin 10U/ml, streptomycin 10mg/ml, fungizone 0.025 mg/ml) and 0.002M L-glutamine (Gibco Invitrogen Corp). The pellet was resuspended and the cells were seeded on plastic dishes (Nunc, Roskilde, Denmark) at an initial seeding density of 200.000 to 400.000 cells/cm^2. Non-adherent cells were removed from the culture by subsequent medium changes. Culture medium consisted of DMEM supplemented with 10% autologous serum. Autologous serum was prepared under sterile conditions from approximately 40 ml of autologous blood collected by a venipuncture immediately prior to the general anaesthesia.

hBMSC were selected based on their capacity to adhere and proliferate under the specified conditions. Colony forming units were generally observed after 4 to 5 days. Cells were expanded in monolayer conditions for up to 2 weeks before the first subculture. Cultures were trypsinized (Trypsin/EDTA solution, Gibco Invitrogen Corp) at 80% confluence and replated at a seeding density of 2000 to 5000 cells/cm^2 from then on. Cell proliferation was quantified with a Bürker chamber at the time of replating. All cells used in this study had undergone no more than 2 passages and had an undifferentiated morphotype.

Flowcytometry

Flowcytometry was performed on a FACScan (Becton Dickinson, Erembodegen, Belgium) to observe homogeneity of the hBMSC. All markers were used according to the manufacturer's instructions. Monoclonal antibodies (mAb) used were: FITC-CD34 (clone 581, IgG1), FITC-CD44 (clone G44-26, IgG2b), FITC-CD45 (clone HI30, IgG1), PE-CD73 (clone AD2, IgG1) all from Becton Dickinson Pharmingen (Erembodegem, Belgium) and FITC-CD105 (clone SN6, IgG1) from Serotec (Oxford, UK).

CD34 is expressed on early lymphohematopoietic stem and progenitor cells, small-vessel endothelial cells, embryonic fibroblasts, and some cells in fetal and adult nervous tissue (20). CD44 serves as a recyclable receptor for hyaluronan and is widely expressed on the surface of most cell types, including articular cartilage chondrocytes and bone marrow derived mesenchymal stem cells.(20) CD45 is expressed on all hematopoietic cells.(20) CD105 or endoglin modulates the cellular response to TGFβ1 and is expressed on many cell types including endothelial cells, articular chondrocytes, bone marrow derived mesenchymal stem cells, monocytes, etc.(20) CD73 reacts with ecto-5'-nucleotidase, a 70 kDa, glycosyl phosphatidylinositol (GPI)-anchored glycoprotein. CD73 is expressed on subsets of T and B lymphocytes, follicular dendritic cells, epithelial cells and endothelial cells.(20)

Appropriate negative controls were used according to the instructions of the manufacturer (IgG1FITC, IgG1PE).

Fibrochondrogenic differentiation assay of hBMSC expanded in medium supplemented with 10% autologous serum

Expanded hBMSC from 3 donors were washed twice in phosphate buffered saline (PBS, Gibco Invitrogen Corp) and resuspended at a final cell concentration of 500.000 cells/ml in differentiation medium consisting of DMEM supplemented with rhTGFβ_1 (final concentration 10ng/ml, R&D systems, Minneapolis, MN, USA), dexamethasone (final concentration 100ng/ml, Sigma-Aldrich, Bornem, Belgium), Ascorbic Acid 2 phosphate (final concentration 50µg/ml, Sigma-Aldrich) and ITS premix (Becton-Dickinson, prepared according to the instructions of the manufacturer) (19). This cell suspension was added to a round bottom polypropylene tube (Eppendorf AG, Hamburg, Germany) and pelleted down for 6 min at 800 rpm. The differentiation medium was changed twice a week. These culture conditions yielded reproducible cell condensations or so-called micropellets. These micropellets were cultured for up to 3 weeks. This differentiation protocol has previously been described to induce so-called chondrogenic differentiation (19,21). All tests were performed in triplicate to ensure reproducibility.

Composition and permeability of the collagen scaffold

Techniques for the formulation and fabrication of the collagen meniscus implant have been reported in detail previously (22). Briefly, the collagen meniscus implants are fabricated from type I collagen derived from U.S.-origin bovine Achilles tendons. After the tendon tissue is trimmed and minced, the type I collagen fibers are purified by various chemical treatments to remove noncollagenous materials and lipids. Next, the purified collagen fibers are swelled in hyaluronic acid and chondroitine sulphate, and then homogenized. The swollen collagen fibers plus the glycoaminoglycans are coprecipitated by the addition of ammonium hydroxide. The precipitated fibers are dehydrated, lyophilized and chemically crosslinked. Terminal sterilisation is performed by γ irradiation. Pore sizes range from 50 to 500 µm.

To visualize the permeability of the collagen scaffold, different cell-seeding protocols were pretested using 250 µl of India ink. India ink, traditionally used for drawing, is a dispersion of carbon black (dye) in water (solvent). Carbon black particle size varies roughly between 10 and 400 nm. India ink was applied in the identical way as for cell-seeding from (1) the dorsal side (D) of the scaffold (Fig. 1A), (2) the lateral sides (L) (Fig. 1B) or (3) injected into the scaffold from the dorsal side (I) (Fig. 1C). For both D and L seeding, the India ink was applied with a tipped pipette in aliquot of 50 µl while the scaffold was gently squeezed and relaxed to enhance ink adsorption, comparable to a sponge. For I, aliquots of 50 µl where injected into the scaffold from the posterior side at different levels. The scaffold (thickness 5 mm) was subsequently dried and cut in two both axially and transversely to observe staining of the centre of the scaffold. Macroscopic pictures were taken for later analysis.

hBMSC seeding on collagen scaffold

At the end of the second passage, monolayer cultured

cells from 3 donors were trypsinized, washed and resuspended in Hank's balanced salt solution (HBSS, Gibco Invitrogen Corp) at a density of 10 million cells per ml. Two and a half million cells suspended in 250 µl were seeded on the type I collagen scaffold (CMI®, Regen Biologics, Franklin Lakes, NJ, USA) (thickness of the scaffold 3 mm) according to the previously described seeding protocols (D+L, I). To allow the cells to attach to the scaffold, the cell-scaffold combination was transferred to the incubator for 4 hours. Differentiation medium was added after these 4 hours. Medium was changed three times a week. Cell-seeded-scaffolds were cultured for three weeks. All tests were performed in triplicate to ensure reproducibility.

Immunohistology

Immunohistological analysis of the extracellular matrix was performed to determine the cellular phenotype during differentiation. Immunohistology was performed on frozen sections of micropellets (Jung tissue freezing medium, Leica Instruments, Nusslock, Germany) and paraffffine embedded samples of the scaffold-cell combination cultured for 1, 2 or 3 weeks. Monoclonal antibodies (mAb) raised against meniscus specific proteins included mouse anti-human aggrecan (23) (clone 969D4D11, IgG_1, Biosource, Nivelles, Belgium), type I (clone I-8H5, IgG_{2a}, ICN Biomedicals Inc, Aurora, Ohio, USA) and type II (clone II-4CII, IgG_1, ICN Biomedicals Inc) collagen (24). Mouse IgG_1 and IgG_{2a} (Becton Dickinson) were used as isotype – matched negative controls.

The anti-human aggrecan mAb was shown to react specifically with the G1-domain of the invariable hyaluronan-binding region of the human aggrecan molecule. No cross-reactivity with other known matrix components has been detected (23-25). Anti-human type I and type II collagen mAbs were raised in BALB/c mice after immunization with human placental type I collagen and human costal cartilage type II collagen, respectively. On western blots anti-type I collagen was shown to react specifically with the alpha chain and the triple helix molecular form of type I collagen. The anti- type II collagen mAb reacted specifically with the alpha2 (II) chain of human type II collagen (25).

Toluidine blue staining was performed to visualize the proteoglycan content in the extracellular matrix.

Immunohistology for type I and type II collagen on frozen or paraffin embedded sections was performed as describe previously (26). Briefly, a number of sections were pretreated with chondroitinase ABC (40 mU/ml, 30 min, 37°C, Sigma-Aldrich) in order to enhance collagen epitope presentation. The sections were subsequently incubated for 1 hour at room temperature with 10 % human serum to reduce aspecific reactivity. After washing, the appropriate mAb was applied for 1 hour. Subsequently, the sections were incubated with a secondary biotinylated anti-mouse antibody for 15 minutes, followed by 15 minutes with a streptavidine-peroxidase complex (LSAB+ kit, DAKO, Glostrup, Denmark). The color reaction was developed using 3-amino-9-ethylcarbazole (AEC) substrate (DAKO) as chromogen. Finally, the sections were counterstained with haematoxylin.

RESULTS

Flow Cytometry

Cell membrane analysis performed at the end of the second passage revealed a homogenous population positive for CD44, CD105 and CD73 and negative for CD34 and CD45, indicating the absence of hematopoietic stem cells in the culture. CD44, CD105 and CD73 are considered as unspecific hBMSC membrane markers.

Fibrochondrogenic differentiation assay on hBMSC expanded in medium supplemented with 10% autologous serum

hBMSC from bone marrow samples of three consecutive patients were expanded in culture medium supplemented with 10% autologous serum and subjected to the differentiation assay. Cell condensations were reproducibly observed after 1 day in every assay. Immunohistochemical analysis revealed a specific time-dependent pattern of expression of the different extracellular matrix components. Fig. 2 depicts the immunohistological results for the fibrochondrogenic assay of hBMSC derived from a 28 years old patient. Comparable results were obtained for all three patients (aged 28, 42 and 35). Type I collagen was observed early on (week 1, Fig. 2A) and remained present throughout the culture period (Fig. 2B and C). Type I collagen immunoreactivity was also observed throughout the full diameter of the micropellet. This was in contrast with the expression of type II collagen (Fig. 2D and F) and aggrecan (Fig. 2G and I). Both extracellular matrix components were clearly observed at week 2 and week 3 but were absent or only slightly present at week 1. The expression of both components was first observed close to the periphery of the micropellet and progressed to the center of the micropellet over time.

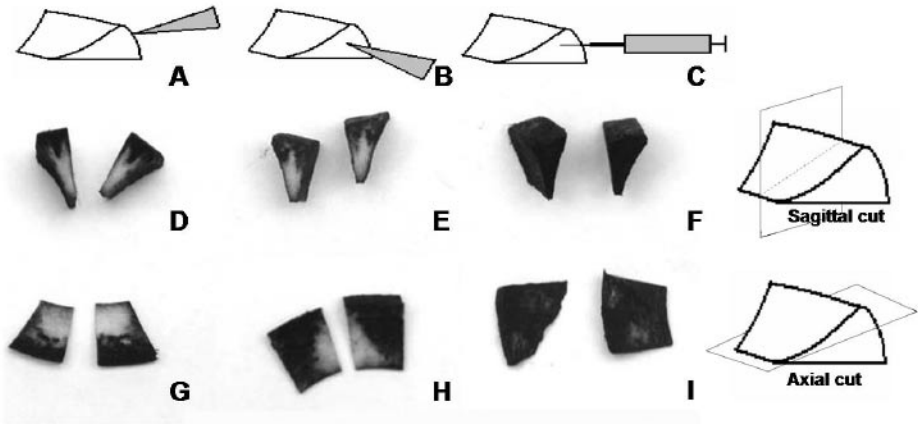

Fig. 1. *Overview of the different techniques used to load the India Ink or the cells on the scaffold. (**A,D,G**) application from the dorsal side of the scaffold with a tipped pipette; (**B,E,H**) application from the lateral sides with a tipped pipette; (**C,F,I**) injection from the dorsal side. The India Ink-loaded scaffolds were subsequently dried and cut sagitally (**D-F**) and axially (**G-I**) to visualize staining of the core of the scaffold.*

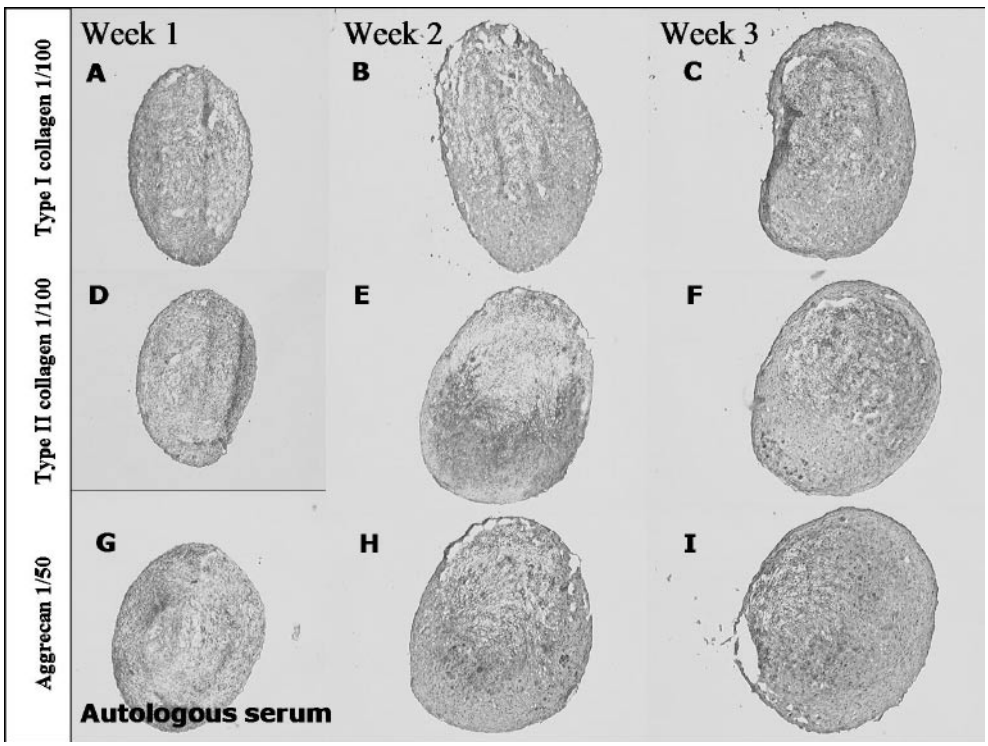

Fig. 2. *Immunohistological results of the fibrochondrogenic differentiation assay of hBMSC expanded in medium supplemented with 10% autologous serum of a male patient (28 years of age). **(A-C)** Type I collagen; **(D-F)** Type II collagen; **(G-I)** Aggrecan. **(A,D,G)** Week 1**; (B,E,H)** Week 2; **(C,F,I)** Week 3. Type I collagen is already expressed at week 1 (A), while type II and aggrecan expression becomes clear at week 2 **(E,H).** At week 3 type I collagen, type II collagen and aggrecan can be visualized throughout the entire micropellet diameter **(C,F,I).** With increasing culture time, a clear increase of the micropellet diameter can also be observed.*

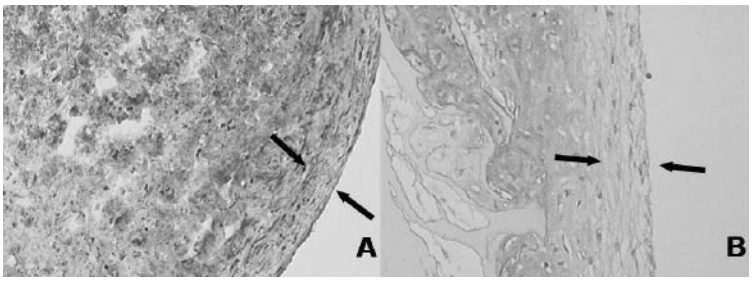

Fig. 3. *A peripheral fibroblast-like cell layer with a thickness of 3-5 cells can be observed in both* ***(A)*** *the micropellet culture system and* ***(B)*** *the cell-scaffold culture. This layer does not stain for type II collagen and aggrecan.*

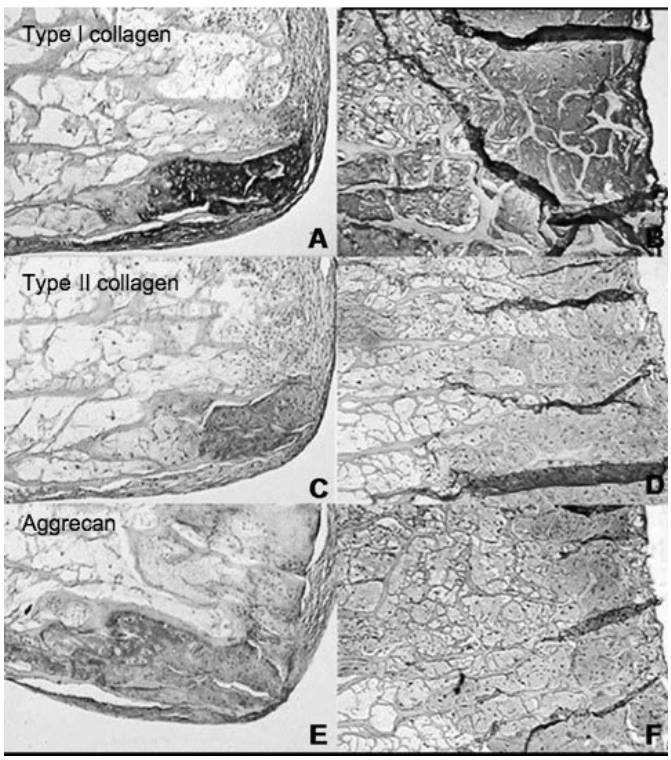

Fig. 4. *Immunohistological results of the hBMSC-seeded biodegradable scaffold after 3 weeks of culture. Staining for type I collagen* ***(A,B),*** *type II collagen* ***(C,D)*** *and aggrecan (E,F). Fibrochondrocyte-like cells are mainly situated at the periphery of the scaffold when the hBMSC were loaded from the dorsal and lateral sides* ***(A,C,E)****. Injection of hBMSC from the dorsal side resulted in fibrochondrocyte-like cells distributed more evenly throughout the scaffold (****B,D,F****).*

Overall, the diameter of the micropellets as well as the distance between cells increased over time indicating an accumulation of extracellular matrix. Cells inside the micropellet became more rounded and were situated in lacunae. A layer of more fibroblast-like cells could be visualized at the periphery of the micropellet (Fig. 3A). This cell-layer was 3-5 cells in thickness and did not stain for type II collagen and aggrecan .

Permeability of the collagen scaffold

A clear difference in the staining pattern could be observed between the different seeding protocols. Application of the India ink from the dorsal side

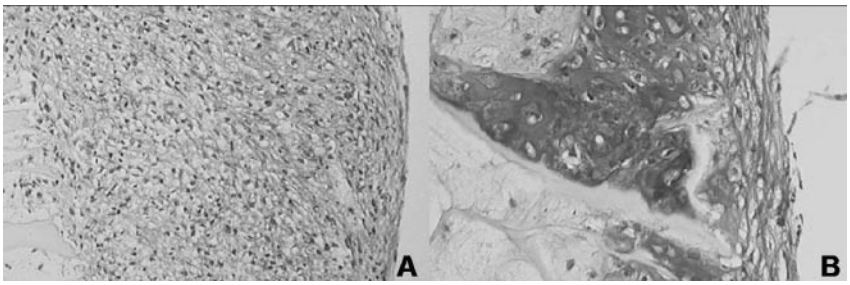

Fig. 5. *Toluidine blue staining of hBMSC-seeded biodegradable scaffold. (**A**) Week 1: high cellular density with only minimal extracellular matrix, negative for toluidine blue. (**B**) Week 2: abundant extracellular matrix, staining positive for toluidine blue. Again a superficial fibroblast-like cell layer can be visualized, which does not stain for toluidine blue.*

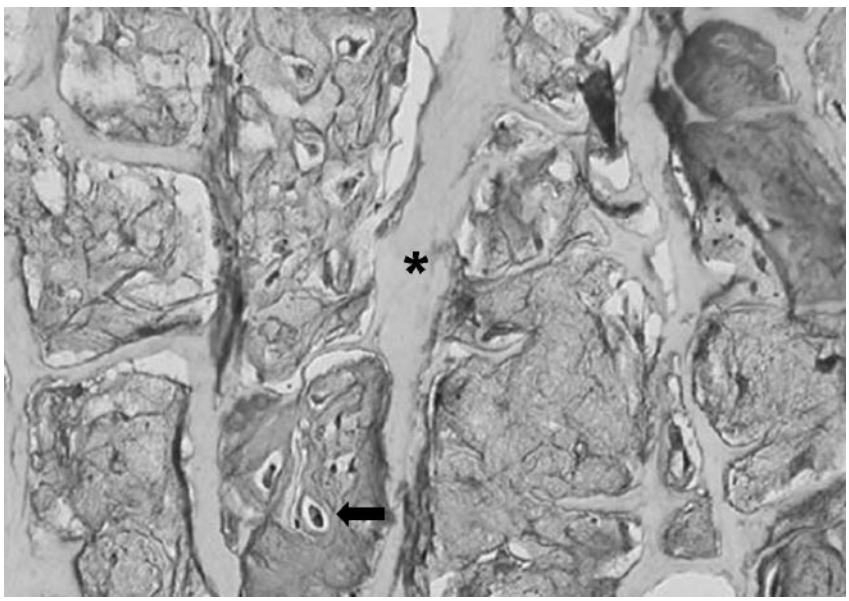

Fig. 6. *Type I collagen stain of hBMSC-loaded biodegradable scaffold (injection, week 3). The cells are situated in lacunae and surrounded by an abundant extracellular matrix, comparable to native meniscus tissue (arrow). Laminar remnants of the scaffold are visible (asterix). Note the 'interdigitation' of the extracellular matrix and the scaffold, proof of ingrowth.*

(Fig. 1A) or from the lateral sides (Fig. 1B) resulted in a staining of the periphery of the scaffold only. The core of the scaffold did not stain as is clearly shown in Fig. 1 (dorsal: Fig. 1D,G; lateral: Fig. 1E,H). This is in contrast with staining by injection of the India ink; both the periphery and the core of the scaffold stained completely (Fig. 1F,I,).

hBMSC seeded on a collagen scaffold

a. seeding from dorsal and lateral (D+L) side

hBMSC attach and encapsulate the type I collagen scaffold (Fig. 4A, C,E). Histological observations comparable to hBMSC cultured as a micropellet were made for the cell-seeded scaffold. Multiple cell layers were observed at the surface of the scaffold. A slow ingrowth of these cells into the scaffold was present. The most superficial two to three cell layers are more fibroblastic in appearance (Fig. 3B), while the deeper cell layers produce an abundant extracellular matrix consisting of type I collagen (Fig. 4A), type II collagen (Fig. 4C) and aggrecan (Fig. 4E) at week 3 of culture. These cells in the deeper layers were situated in lacunae, as seen in native meniscus tissue. Toluidine blue

staining became positive at week 2, indicating the accumulation of proteoglycans in the extracellular matrix (Fig. 5B).

A slow colonisation of the scaffold by hBMSC was observed over the culture period. This colonisation started at the surface of the scaffold and was more pronounced at the corners of the scaffold. A complete colonisation of the scaffold, however, was never observed after 3 weeks.

b. seeding by injection (I)

Concerning time of expression and staining intensity for the different extracellular matrix compounds (type I collagen, type II collagen and aggrecan) after seeding by injection (I), the histological observations were completely comparable with the observations made using previously described seeding (D + L) protocols (Fig. 4B, D, F). A clear difference however was noted on the depth of penetration of the cells into the scaffold. Cells could be observed almost completely throughout the scaffold, both at the periphery and the core. The cells were situated in between the lamellar structure of the scaffold (Fig. 6).

DISCUSSION

Lesions of the inner two-thirds of the meniscus have no healing potential because of the absence of vasculature (2). It is common practice to excise these lesions because they cause a mechanical conflict inside the knee joint. Unfortunately, compartimental cartilage degeneration and osteoarthritis is frequently observed after meniscectomy (5-6). Therefore, repair or regeneration of meniscal tissue has been considered as a therapeutic option for irreparable meniscus damage. It would safeguard the underlying cartilage from degeneration and improve biomechanics of the knee joint.

The acellular type I collagen scaffold has shown repair and regeneration potential of meniscus-like tissue in the clinical situation (15, 27). Reproducible, full restoration of meniscal tissue however has rarely been achieved (15, 27). There are several explanations for this incomplete restoration including: (1) slow repopulation of the scaffold by recipient cells derived from the synovium and joint capsule; (2) combined with an uncertain fibrochondrogenic differentiation potential of these cells. Evidence for fibrocartilagenous or meniscus-like tissue regeneration by host cells derived from the synovial tissue and capsule has been provided in animal experiments (16, 28). Human data on this subject are however scarce and not conclusive. Deep-frozen –and therefore acellular- meniscal allografts are partially repopulated by a mainly fibroblast-like cell type of probable synovial origin (18). Histological analysis of specimen obtained 6 months after CMI implantation showed remnants of the scaffold and connective tissue with newly-formed vessels and fibroblast-like cells (29).

The authors therefore choose to further investigate the combination of this commercially available type I collagen meniscus implant (CMI) scaffold in combination with autologous cells. This combination of a biodegradable scaffold and autologous cells with a reproducible repair potential could increase the initial number of cells present in the scaffold at the time of transplantation and thus decrease the time needed for repopulation.

Several autologous cell-types have been considered for this application. Meniscus cells can be isolated from the resected torn meniscus or from a biopsy of healthy tissue. In both cases the number of cells is usually small and the quality of the cell phenotype possibly compromised by in vitro expansion (30-31). A biopsy would imply additional damage to functional tissue. Autologous articular chondrocytes have shown repair potential of meniscus tears in a pig model and have shown regenerative potential in combination with a hyaluronic scaffold in an ovine model (32-33). Potential drawbacks are however the biochemical composition of the extracellular matrix and again the need for an additional invasive biopsy. Mesenchymal stem cells have generated a great deal of interest in the field of regenerative medicine and tissue engineering because of their ability to proliferate in monolayer conditions without losing their differentiation potential towards several connective tissue lineages including bone, fat, cartilage and muscle (19).

Human bone marrow provides a convenient source of mesenchymal stem cells (19). Other sources including synovial tissue, periost, muscle and adipose tissue have been described and tested extensively (34-37). Of these, synovial tissue

and bone marrow showed superior chondrogenic potential and proliferation (37). For this study, human bone marrow derived mesenchymal stem cells (hBMSC) were used because of the ease with which these cells can be isolated and expanded while retaining their differentiation potential.

The potential clinical applicability of autologous cells in combination with a scaffold depends not only on the cells source and type, but also on the cell expansion conditions. Usually, serum of bovine origin is used to expand human cells and more specifically hBMSC. The use of bovine serum for cell expansion for transplantation purposes, however, is disadvantageous. The concerns of disease transmission and unfavourable immune responses can be solved if autologous human serum provides adequate differentiation potential to hBMSC.

In this study, we have provided proof that hBMSC expanded in monolayer conditions with culture medium supplemented with 10% autologous serum demonstrate, in a reproducible way, a cellular phenotype characterized by the presence of type I collagen, type II collagen and aggrecan in the extracellular matrix, when subsequently cultured in serum-free conditions and stimulated by TGF beta 1 and dexamethasone. These three compounds are typical for the extracellular matrix build-up by fibrochondrocytes from the native human meniscus (38). Therefore, we define this cellular differentiation pattern to be fibrochondrogenic or meniscus cell-like. Previous studies have defined this differentiation pattern as chondrogenic (19,21). We strongly disagree with this definition as type I collagen is not an extracellular matrix compound of human hyaline articular cartilage. With regards to isolation, expansion and osteogenic differentiation of hBMSC, others have demonstrated that 10% autologous serum is comparable to 10% fetal bovine serum (39-41).

We have also demonstrated that hBMSC attached and were able to undergo fibrochondrogenic differentiation when seeded onto the type I collagen scaffold or injected into it. Injection of the cells resulted in a significantly higher number of cells present within the scaffold compared to superficial seeding. Therefore, for the clinical application of a cell-scaffold construct injection would result in a higher number of cells at the site of injury and thus a decrease in the time needed to completely repopulate the scaffold. Fibrochondrogenic differentiated hBMSC showed a limited capacity to repopulate the scaffold when seeded superficially. The India Ink results substantiated these findings: small black carbon particles were excluded from the core of the scaffold probably as a result of the relatively watertight laminar structure of the scaffold when the ink was applied dorsally or laterally. This could also partially explain the incomplete repopulation of acellular scaffolds and grafts observed in the clinical situation today.

Although full characterisation based on membrane markers of hBMSC is still in progress, it is generally accepted that these cells are CD44+CD105+CD34-. Previous studies performed at our institution have shown that phenotypically stable meniscus fibrochondrocytes cultured in alginate are CD44+CD105+CD34-, comparable to the expression pattern of monolayer cultured hBMSC (41). A specific cell population of the normal human meniscus is however CD34+ and is located in the superficial layers of the normal human meniscus (38). Although the exact biological function of this specific cell population is still under investigation, its presence and location appears to be essential in the normal tissue. hBMSC therefore have potential in human meniscus tissue engineering applications, although other cell types may be necessary to obtain a fully functional tissue. Preclinical data have already shown the feasibility of the application of bone marrow derived mesenchymal stem cells for meniscus regeneration in animal models (42-43). These cells appeared to have homed to the site of injury and to have induced a regenerative response. The potential advantages of a cell-scaffold combination are: (1) the manual delivery of the cell-scaffold construct to the injury site thereby eliminating the process of homing of hBMSC towards the injury site and (2) the predefined 3-dimensional shape of the scaffold supporting fibrochondrogenic differentiation (44-45).

CONCLUSION

hBMSC expanded in autologous serum have a fibrochondrogenic differentiation potential. hBMSC can also be combined with a biodegradable meniscus-

shaped scaffold. This cell-scaffold combination can be implanted easily into the meniscus defect thereby delivering autologous hBMSC with meniscus repair potential to this defect. This could increase repair potential of the defect, which allows faster repair and regeneration with meniscus-like tissue and thus shortens the rehabilitation period.

ACKNOWLEDGEMENTS

Dr. Peter Verdonk was a research assistant of the Fund for Scientific Research-Flanders (Belgium) (F.W.O. -Vlaanderen).

REFERENCES

1. Fairbank TJ. Knee joint changes after meniscetomy. J Bone Joint Surg Br 1948; 30B:664-70.
2. Arnoczky SP, Warren RF. Microvasculature of the human meniscus. Am J Sports Med 1982; 10:90-5.
3. Steenbrugge F, Verdonk R, Verstraete K. Long-term assessment of arthroscopic meniscus repair: a 13-year follow-up study. Knee 2002; 9:181-7.
4. Burks RT, Metcalf MH, Metcalf RW. Fifteen-year follow-up of arthroscopic partial meniscectomy. Arthroscopy 1997; 13:673-9.
5. Chatain F, Adeleine P, Chambat P, Neyret P; Societe Francaise d'Arthroscopie. A comparative study of medial versus lateral arthroscopic partial meniscectomy on stable knees: 10-year minimum follow-up. Arthroscopy 2003; 19:842-9.
6. Cicuttini FM, Forbes A, Yuanyuan W, Rush G, Stuckey SL. Rate of knee cartilage loss after partial meniscectomy. J Rheumatol 2002; 29:1954-6.
7. Kohn D, Wirth CJ, Reiss G, Plitz W, Maschek H, Erhardt W, Wulker N. Medial meniscus replacement by a tendon autograft. Experiments in sheep. J Bone Joint Surg Br 1992;74:910-7.
8. Milachowski KA, Kohn D, Wirth CJ. Meniscus replacement using Hoffa's infrapatellar fat bodies--initial clinical results. Unfallchirurgie 1990;16:190-5.
9. Walsh CJ, Goodman D, Caplan AI, Goldberg VM. Meniscus regeneration in a rabbit partial meniscectomy model. Tissue Eng 1999;5:327-37.
10. Bruns J, Kahrs J, Kampen J, Behrens P, Plitz W. Autologous perichondral tissue for meniscal replacement. J Bone Joint Surg Br 1998;80:918-23.
11. Gastel JA, Muirhead WR, Lifrak JT, Fadale PD, Hulstyn MJ, Labrador DP. Meniscal tissue regeneration using a collagenous biomaterial derived from porcine small intestine submucosa. Arthroscopy 2001;17:151-9.
12. Peters G, Wirth CJ. The current state of meniscal allograft transplantation and replacement. Knee 2003;10:19-31.
13. Noyes FR, Barber-Westin SD. Meniscus transplantation: indications, techniques, clinical outcomes. Instr Course Lect 2005; 54:341-53.
14. Verdonk PC, Demurie A, Almqvist KF, Veys EM, Verbruggen G, Verdonk R. Transplantation of viable meniscal allograft. Survivorship analysis and clinical outcome of one hundred cases. J Bone Joint Surg Am 2005;87:715-24.
15. Rodkey WG, DeHaven KE, Montgomery WH 3rd, Baker CL Jr, Beck CL Jr, Hormel SE, Steadman JR, Cole BJ, Briggs KK. Comparison of the collagen meniscus implant with partial meniscectomy. A prospective randomized trial. J Bone Joint Surg Am 2008 Jul;90(7):1413-26.
16. Welsing RT, van Tienen TG, Ramrattan N, Heijkants R, Schouten AJ, Veth RP, Buma P. Effect on tissue differentiation and articular cartilage degradation of a polymeer meniscus implant: A 2-year follow-up study in dogs. Am J Sports Med 2008 Oct;36(10): 1978-89.
17. Arnoczky SP, DiCarlo EF, O'Brien SJ, Warren RF. Cellular repopulation of deep-frozen meniscal autografts: an experimental study in the dog. Arthroscopy 1992;8:428-36.
18. Rodeo SA, Seneviratne A, Suzuki K, Felker K, Wickiewicz TL, Warren RF. Histological analysis of human meniscal allografts. A preliminary report. J Bone Joint Surg Am 2000;82:1071-82.
19. Pittenger MF, Mackay AM, Beck SC, et al. Multilineage potential of adult human mesenchymal stem cells. Science 1999;284:143-7.
20. Proteins review on the web. http://www.ncbi.nlm.nih.gov/PROW/.
21. Johnstone B, Hering TM, Caplan AI, Goldberg VM, Yoo JU. In vitro chondrogenesis of bone marrow-derived mesenchymal progenitor cells. Exp Cell Res 1998;238:265-72.
22. Rodkey WG, Steadman JR, Li ST. A clinical study

of collagen meniscus implants to restore the injured meniscus. Clin Orthop 1999;367S:S281-92.
23. Gysen P, Franchimont P. Radioimmunoassay of proteoglycans. J Immunoassay 1984;5:221-43.
24. Heinegard D, Oldberg A. Structure and biology of cartilage and bone matrix noncollagenous macromolecules. FASEB J 1989;3:2042-51.
25. Kumagai J, Sarkar K, Uhthoff HK, Okawara Y, Ooshima A. Immunohistochemical distribution of type I, II and III collagens in the rabbit supraspinatus tendon insertion. J Anat 1994;185:279-84.
26. Barry F, Boynton RE, Liu B, Murphy JM. Chondrogenic differentiation of mesenchymal stem cells from bone marrow: differentiation-dependent gene expression of matrix components. Exp Cell Res 2001;268:189-200.
27. Steadman JR, Rodkey WG. Tissue-engineered collagen meniscus implants: 5- to 6-year feasibility study results. Arthroscopy 2005;21:515-25.
28. Stone KR, Rodkey WG, Webber RJ, McKinney L, Steadman JR. Future directions. Collagen-based prostheses for meniscal regeneration. Clin Orthop Relat Res 1990;252:129-35.
29. Reguzzoni M, Manelli A, Ronga M, Raspanti M, Grassi FA. Histology and ultrastructure of a tissue-engineered collagen meniscus before and after implantation. J Biomed Mater Res B Appl Biomater 2005;74(2):808-16.
30. Nakata K, Shino K, Hamada M, Mae T, Miyama T, Shinjo H, Horibe S, Tada K, Ochi T, Yoshikawa H. Human meniscus cell: characterization of the primary culture and use for tissue engineering. Clin Orthop 2001;391S:S208-18.
31. Baker BM, Nathan AS, Huffman GR, Mauck RL. Tissue engineering with meniscus cells derived from surgical debris. Osteoarthritis Cartilage 2008 Oct 9, [Epub ahead of print].
32. Peretti GM, Gill TJ, Xu JW, Randolph MA, Morse KR, Zaleske DJ. Cell-based therapy for meniscal repair: a large animal study. Am J Sports Med 2004;32(1):146-58.
33. Kon E, Chiari C, Marcacci M, Delcogliano M, Salter DM, Martin I, Ambrosio L, Fini M, Tschon M, Tognana E, Plasenzotti R, Nehrer S. Tissue engineering for total meniscal substitution: animal study in sheep model. Tissue Eng Part A 2008;14(6): 1067-80.
34. De Bari C, Dell'Accio F, Tylzanowski P, Luyten FP. Multipotent mesenchymal stem cells from adult human synovial membrane. Arthritis Rheum 2001; 44:1928-42.
35. Park J, Gelse K, Frank S, von der Mark K, Aigner T, Schneider H. Transgene-activated mesenchymal cells for articular cartilage repair: a comparison of primary bone marrow-, perichondrium/periosteum- and fat-derived cells. J Gene Med 2005 Sep 2; [Epub ahead of print].
36. Gimble J, Guilak F. Adipose-derived adult stem cells: isolation, characterization, and differentiation potential. Cytotherapy 2003; 5:362-9.
37. Sakaguchi Y, Sekiya I, Yagishita K, Muneta T. Comparison of human stem cells derived from various mesenchymal tissues: superiority of synovium as a cell source. Arthritis Rheum 2005; 52: 2521-9.
38. Verdonk PC, Forsyth RG, Wang J, Almqvist KF, Verdonk R, Veys EM, Verbruggen G. Characterisation of human knee meniscus cell phenotype. Osteoarthritis Cartilage 2005;13:548-60.
39. Kobayashi T, Watanabe H, Yanagawa T, Tsutsumi S, Kayakabe M, Shinozaki T, Higuchi H, Takagishi K. Motility and growth of human bone-marrow mesenchymal stem cells during ex vivo expansion in autologous serum. J Bone Joint Surg Br 2005;87: 1426-33.
40. Shahdadfar A, Fronsdal K, Haug T, Reinholt FP, Brinchmann JE. In Vitro Expansion of Human Mesenchymal Stem Cells: Choice of Serum is a Determinant of Cell Proliferation, Differentiation, Gene Expression and Transcriptome Stability. Stem Cells 2005; 23:1357-66.
41. Stute N, Holtz K, Bubenheim M, Lange C, Blake F, Zander AR. Autologous serum for isolation and expansion of human mesenchymal stem cells for clinical use. Exp Hematol 2004; 32:1212-25.
42. Angele P, Johnstone B, Kujat R, Zellner J, Nerlich M, Goldberg V, Yoo J. Stem cell based tissue engineering for meniscus repair. J Biomed Mater Res A 2008 May;85(2):445-55.
43. Caplan AI. Adult mesenchymal stem cells for tissue engineering versus regenerative medicine. J Cell Physiol 2007 Nov;213(2):341-7. Review.